STRUCTURE-FUNCTION ANALYSIS OF THE *HELICOBACTER PYLORI* VacA p55 DOMAIN

By

Susan E. Ivie

Dissertation
Submitted to the Faculty of the
Graduate School of Vanderbilt University
in partial fulfillment of the requirements
for the degree of
DOCTOR OF PHILOSOPHY
in
Microbiology and Immunology

December, 2009

Nashville, Tennessee

Approved:

Professor Timothy L. Cover

Professor Mark R. Denison

Professor Dana B. Lacy

Professor Andrew J. Link

Professor Richard M. Peek Jr.

Professor Eric P. Skaar

ACKNOWLEDGEMENTS

I am especially thankful to my mentor, Dr. Timothy Cover, for his guidance throughout my graduate studies. I thank him for his patience and support, and for allowing me to pursue my graduate work in his lab. I appreciate his positive outlook and an always-present upbeat attitude. He creates such a peaceful and friendly environment in which to work. I would also like to extend my gratitude to all of the members of the Cover laboratory for teaching me and for their scientific advice and suggestions. I thank Dr. Mark McClain for his support and for always being available to answer my many questions. His advice and expertise was invaluable. Mark was truly an important part of my training. I thank Dr. Holly Algood firstly for her friendship, but also for scientific help. Holly was always there to encourage me, lift me up when my spirits were down, and rejoice with me.

I would also like to thank the members of my thesis committee: Andrew Link (chair), Timothy Cover (mentor), Mark Denison, Borden Lacy, Richard Peek, and Eric Skaar. I appreciate all of their enthusiasm, helpful advice, and constructive criticism for my project. I thank each of them for always being supportive of me and my project. I also would like to acknowledge the support provided by the faculty members and staff of the Department of Microbiology and Immunology.

The work presented in this dissertation was financially supported by the National Institutes of Health, RO1 AI039657, "Structure-Function Analysis of *H. pylori* VacA".

During graduate school, there were definitely some times that were not easy. Throughout it all, I reminded myself of Jeremiah 29:11 that reads "For I know the plans I have for you, declares the Lord, plans to prosper you and not to harm you, plans to give you

hope and a future". God's strength, and His promise that there is a wonderful purpose for my life, has guided me through the good times and the not as good times. I cannot even begin to express my gratitude to my family and friends for their support during this journey. For my family's constant love, encouragement, prayers, and confidence in me, I am forever grateful. I would also like to thank several friends, especially Valerie Busler, Alison Hartwell, Molly Mertz, Alisha Russell, Mark Slagle, and Michael Wright for always reminding me of the important things in life, their constant friendship and prayers, and for always believing in me.

TABLE OF CONTENTS

LIST OF TABLES

LIST OF FIGURES

CHAPTER I

BACKGROUND

Introduction

Humans consume many microorganisms each day, but most cannot successfully colonize the human stomach due to its highly acidic environment of pH 1-2. An exception to this rule is an organism known as *Helicobacter pylori*, which has an extraordinary ability to colonize the human gastric mucosa. This bacterium was first visualized in the late 19th century by European pathologists, but because it could not be isolated, it was ultimately forgotten for almost a century. By 1979, pathologists were again recognizing these bacteria in gastric biopsy specimens; however, it was not until 1982 that the bacterium was first isolated (63), forever changing the view that the human stomach is an inhospitable acidic environment in which bacteria cannot grow. In the Background section, the microbiology and epidemiology of *H. pylori* will briefly be discussed in addition to *H. pylori*-associated diseases. Furthermore, our current understanding of a secreted virulence factor, VacA, will be discussed.

Microbiological characteristics

The gram-negative bacterium *H. pylori* was named because of its spiral or helical shape (62). Although usually spiral shaped, *H. pylori* can appear rod shaped or even coccoid shaped after extended *in vitro* culture or treatment with antibiotics (52). Additionally, each organism has four to six unipolar sheathed flagella, which are essential for bacterial motility and allow movement through the mucus layer overlying gastric epithelial cells (21). These

organisms grow in a microaerophilic, or reduced oxygen, environment, and have an additional need for CO_2. *H. pylori* is urease positive, allowing short-term survival in the acidic gastric lumen. Furthermore, *H. pylori* is both catalase and oxidase positive, which are characteristics used to aid in its identification (52).

Epidemiology and *H. pylori*-associated diseases

H. pylori is present in human stomachs throughout the world, but its prevalence varies greatly among countries. Infection is strongly correlated with socioeconomic status, with prevalence ranging from 70-90% in developing countries, compared to 25-50% in developed countries. Initial colonization occurs predominantly in childhood, and once acquired, the infection persists for the lifetime of the host, unless eradicated with antimicrobial therapy (21). Although a definitive transmission pathway has yet to be defined, two commonly described routes of how *H. pylori* travels to the stomach of one person from that of another are fecal-oral transmission and oral-oral transmission. It is well established that intrafamilial spread plays a major role in transmission (87).

Several diseases that are commonly associated with *H. pylori* colonization include duodenal and gastric ulcers, gastric cancer, and gastric MALT lymphoma (21). Although all infected individuals develop gastritis, very few actually go on to develop more severe disease. It is estimated that *H. pylori*-infected patients have a 10-20% risk of developing ulcer disease and a 1-2% risk of developing gastric cancer (52). It is striking that such a small fraction of individuals carrying *H. pylori* develop illness. The risk of development of disease is known to be dependent on three factors: bacterial virulence, host genetic susceptibility, and environmental factors (2). In 1994, *H. pylori* was classified as a type I, or

definite, carcinogen and gastric cancer is known as one of the leading causes of cancer-related deaths worldwide (101).

H. pylori colonization and virulence factors

H. pylori populations are extremely diverse because of point mutations, substitutions, and insertions and deletions in their genomes (5, 36). Additionally, gastric colonization with more than one distinct strain of *H. pylori* is common, leading to both chromosomal rearrangements and recombination among strains (5, 42). This extraordinary diversity has made it difficult to identify bacterial factors that are associated with disease; however, several putative virulence factors have been described. Two very well characterized virulence factors of *H. pylori* are the *cag* pathogenicity island (*cag* PAI) and the vacuolating cytotoxin A (*vacA*) (8, 57). *H. pylori* strains can be distinguished by the presence or absence of the *cag* PAI, a region of chromosomal DNA made up of approximately 30 genes (86). One gene, *cagA*, is used as a marker of the *cag* PAI. Genes within the *cag* PAI encode proteins that assemble into a type IV secretion system, which can translocate the effector protein CagA into epithelial cells. *cagA*+ strains are more commonly associated with severe gastritis, peptic ulcer disease, and gastric cancer compared to *cagA*- strains (86). The vacuolating cytotoxin A is the focus of this thesis and will be discussed in more detail in the next section. In brief, all *H. pylori* strains carry a *vacA* gene, but there is considerable variation in *vacA* gene sequences among different strains, and several allelic types are associated with an increased risk of disease (52).

In addition to the above factors that contribute to disease, several colonization factors have also been described. These factors contribute to the mechanisms by which *H. pylori*

can survive and grow in the harsh environment of the stomach. All strains of *H. pylori* express urease and flagella, two factors that are required for colonization and survival in the stomach (4). Urease is an enzyme that breaks down urea to form ammonia and carbon dioxide, leading to an increase in pH, and ultimately buffering the acid microenvironment (71). Flagella enable *H. pylori* to penetrate and colonize the gastric mucus layer (77). A number of adhesins and outer membrane proteins are also expressed by *H. pylori* (2); however, their role in colonization has not yet been rigorously assessed in animal models.

Vacuolating cytotoxin A structure and allelic variation

The *vacA* gene encodes for an approximately 140 kDa precursor protein, which undergoes proteolytic processing to yield a 33 amino acid amino-terminal signal sequence, an 88 kDa mature secreted toxin, a ~12 kDa secreted peptide, and an approximately 33 kDa carboxy-terminal domain that remains associated with the bacteria (6, 14, 76, 106). The carboxy-terminal domain exhibits homology to the carboxy-terminal domain of IgA protease of *Neisseria gonorrhoeae* (95), a prototype autotransporter protein (39, 88). In agreement with this, VacA is known to be secreted by a type Va, or autotransporter, mechanism, meaning that it directs its own transport across the bacterial outer membrane (26). The amino-terminal signal sequence is cleaved during translocation across the inner membrane via the Sec pathway and the carboxy-terminal fragment inserts into the outer membrane, forming a β-barrel pore through which the passenger domain is exported. It is not clear whether the mature VacA toxin is cleaved from the autotransporter domain by autoproteolysis or an unidentified protease, but no protease activity has been shown for VacA. The 33 kDa autotransporter domain remains localized in the bacterial cell (26). After

removal of the amino-terminal signal sequence and carboxy-terminal autotransporter domain, the mature 88 kDa VacA is secreted into the culture medium; however, much of the toxin may remain associated with the surface of the bacteria (41).

A functional *vacA* gene is present in all *H. pylori* strains, although there is considerable sequence heterogeneity within the gene (3, 14). This heterogeneity is one of the factors that ultimately leads to variation in toxin activity observed in culture supernatants from different *H. pylori* strains. There are several distinct families of *vacA* alleles, based on sequence analysis at the 5' end of the gene (encoding the amino-terminal signal sequence; designated s1 and s2), the mid-region of the gene (designated m1 and m2), and an additional region of variation termed the intermediate (i) region (3, 91, 100, 116). All combinations of the s and m regions have been described, although s2/m1 alleles are rare (55). Among infected individuals, *H. pylori* strains harboring the m1 allele are more commonly associated with severe disease outcome than are strains with the m2 allele, including an increased risk for gastric carcinoma. Likewise, *H. pylori* strains with an s1 allele are also likely to develop more severe clinical disease compared to strains with an s2 allele (25). It has been found that VacA causes degeneration of the gastric mucosa and acute inflammation in mice when orally administered (106). These human and mouse data highlight the relevance of this bacterial toxin in disease. *In vitro*, type s2 VacA lacks vacuolating cytotoxicity (3, 54, 66), s1/m1 toxins are associated with the highest levels of vacuolating activity in a broad range of cell types, and type s1/m2 forms produce detectable vacuolation in a more limited range of cell types (82, 111, 121).

VacA cellular effects

One of the first noted effects of VacA was its ability to induce large cytoplasmic vacuoles in cultured mammalian cells (57) (Figure I-1). The vacuoles are able to take up the weak base neutral red, suggesting an acidic lumen, and thus the neutral red uptake assay has become a commonly used assay to quantitate vacuolating activity (13) (Figure I-1). Vacuolation is known to be dependent on the presence of weak bases, such as ammonium chloride, in the extracellular medium (15). Several studies have shown that vacuoles induced by VacA are enriched with the markers Rab7, Lamp1, and Lgp110, each of which is typically associated with late endocytic and lysosomal compartments (58, 73, 83, 84). This suggests that vacuolar membranes may be derived from compartments such as these. Although vacuolation is a prominent effect of VacA *in vitro*, it is not commonly seen *in vivo*, and many other activities of this protein have subsequently been identified.

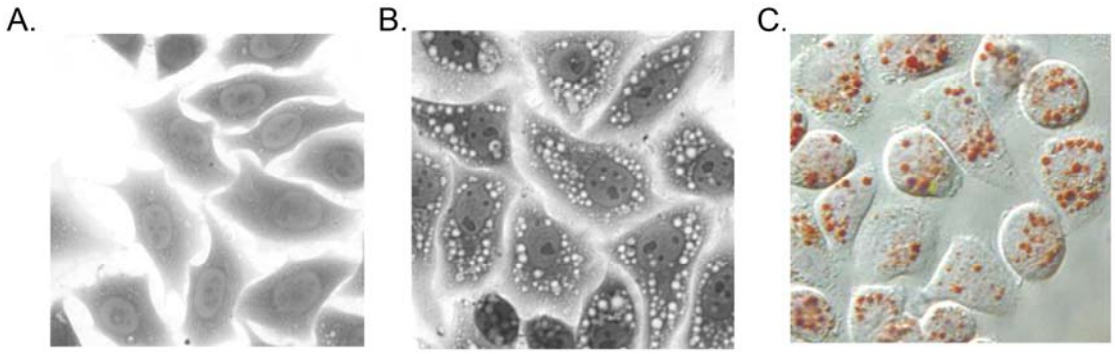

Figure I-1. VacA-induced vacuolation of HeLa cells. The HeLa cell monolayer was left untreated (A) or treated with 5 μg/ml acid-activated VacA at 37ºC (B) in the presence of 5 mM ammonium chloride. In A and B, cells were fixed, stained with crystal violet, and visualized by microscopy. C. HeLa cells were treated with acid-activated VacA in the presence of 5 mM ammonium chloride. The cells were then stained with neutral red dye, washed, and visualized by microscopy. (Figure adapted from (96); neutral red uptake figure obtained from Mark S. McClain, personal communication.)

Other important cellular effects of VacA include depolarization of the membrane potential, alteration of mitochondrial membrane permeability, induction of autophagy, apoptosis, activation of mitogen-activated protein (MAP) kinases, inhibition of antigen presentation, and inhibition of T cell activation and proliferation (9, 18, 107). The exact mechanism by which each of these processes occurs is not fully understood, but many cellular effects of VacA can be attributed to the ability of the toxin to insert into membranes and form anion-selective channels in the host cell membranes (discussed further below) (9). Additionally, VacA targets a variety of cell types, including gastric epithelial cells (27), T cells (33, 102), and mast cells (19, 103).

VacA host-cell intoxication

Binding- The first step in intoxication of host cells is binding of the toxin to the cell surface. On epithelial cells, at least five different putative receptors have been identified. These include the epidermal growth factor receptor (98), heparin sulfate (115), receptor protein tyrosine phosphatases α and β (RPTP α and β) (27, 128, 129), and the plasma membrane sphingolipid known as sphingomyelin (37). VacA has also been found to localize to lipid raft domains on the surface of mammalian cells (34, 85, 96). The most well-characterized interaction is that of VacA and RPTPβ. The interaction of VacA and RPTPβ has been shown to be important in VacA-induced vacuolation (81, 130), activation of signaling pathways (27), and VacA-induced gastric injury in a mouse model (27). The binding of VacA to numerous cell-surface components has made it difficult to identify which interactions are the most relevant for VacA-induced cellular alterations. Additionally, there are conflicting data as to whether the binding of VacA exhibits saturability or specificity (64,

70, 85, 92, 120, 121), two characteristics of a high-affinity ligand-receptor interaction. If indeed VacA binding is not saturable and specific, this suggests that the toxin may be binding to multiple cell surface components or to an abundant, low-affinity receptor.

Ion channel formation- After binding of VacA to the cell surface, the toxin can insert into the plasma membrane to form membrane channels. An important characteristic of these channels is that they are anion selective, leading to the diffusion of ions such as Cl^-, HCO_3^-, and other small molecules across the cell membrane (105, 109). Whole-cell, patch clamp studies have shown that these anion-selective channels lead to a partial depolarization of the membrane potential (105). It is not currently understood if the channel is formed from VacA monomers that have already inserted into the membrane and then assemble to form a pore, or if a membrane-bound pre-pore first forms and then inserts into the membrane.

There is a strong correlation between VacA channel formation and VacA-induced cell vacuolation. Several groups found that VacA mutants that cannot form membrane channels also lack vacuolating activity (66, 69, 108, 118), and it has also been shown that chloride channel inhibitors inhibit cellular vacuolation (43, 105, 110). Additionally, it was found that the amino-terminal hydrophobic region of VacA is long enough to span a membrane, and was experimentally shown to insert into membranes, suggesting it may form part of the VacA channel (65). One model to explain the relationship between VacA channel activity and vacuolation proposes that VacA binds to the cell surface, is internalized, and then forms anion-selective channels in the membranes of late endocytic compartments (108). Channel formation results in the influx of anions into endosomes, stimulating increased proton pumping by the vacuolar ATPase, and accumulation of protonated membrane-permeant weak

bases, such as ammonium chloride. Osmotic swelling then results in vacuole formation (108).

Internalization- Following binding to the cell surface and insertion into the membrane, VacA can undergo internalization into cells via a process that has been termed pinocytosis. The exact mechanism by which VacA is internalized is not fully understood; however, internalization is known to occur at 37ºC but not 4ºC, is inhibited by depleting cells of ATP (70), and is a clathrin-independent process (31, 32, 92). This pinocytic process does not require tyrosine phosphorylation of cellular proteins and does not require RhoA, dynamin, or ADP-ribosylating factor 6 GTPase activities (31). At an early time point, VacA accumulates in early endosomal compartments (also known as GEECs, GPI-anchored proteins-enriched early endosomal compartments) that lack transferrin, caveolin 1, and the EEA1 Rab5 effector, but do contain GPI-anchored proteins (31). VacA can subsequently localize with other endosomal compartments including the large vacuoles that form in response to VacA, as well as the inner mitochondrial membrane (28, 93). Lipid rafts are thought to play an important role in both VacA internalization and intracellular trafficking, but it is not understood how VacA undergoes trafficking to the various intracellular locations (51, 85, 92, 96).

Oligomerization- Individual VacA monomers (approximately 88 kDa in mass) are known to assemble into large oligomeric complexes with a mass of approximately 1,000 kDa (10). Early deep-etch electron microscopy studies reveal that water-soluble VacA oligomers are flower-shaped structures composed of one or two rings, and each ring is composed of six to seven monomers (11, 53, 59) (Figure I-2). These structures are approximately 30 nm in diameter, with a central ring that is approximately 15 nm in diameter (11). When VacA is

exposed to an acidic or alkaline pH, the oligomers disassemble into monomers (11, 72, 128), and this is associated with an increase in VacA activity. It is hypothesized that monomeric forms of VacA associate with the cell membrane, leading to oligomerization and subsequent channel formation in cell membranes (9, 112).

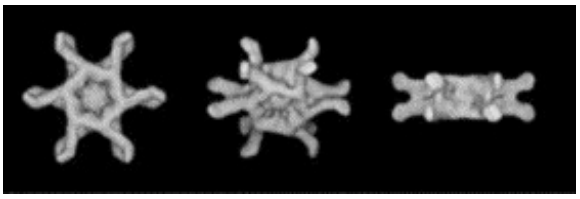

Figure I-2. VacA oligomeric structure. These series of images show a 3D reconstruction of dodecameric wild-type VacA imaged by cryo-negative staining electron microscopy. Each image shows a slight rotation of the oligomer. These images reflect a model with a resolution of approximately 19 Å. Reprinted from (23).

Several studies have shown a correlation between VacA oligomerization and VacA activity (35, 66, 118, 124, 132). In one study by Willhite *et al*, FRET microscopy was used to demonstrate that full-length VacA proteins expressed in transiently transfected cells interact with one another (124). This study was not able to evaluate the exact number of monomers that interact within the cell, but was able to determine that VacA can assemble into an intracellular complex comprising at least two or more monomers (124). This same group also found that when intracellularly expressed, VacA with an inactivating single residue mutation in one monomer (VacA P9A) functionally complemented a second mutant form of a VacA monomer with an inactivating two residue mutation (VacA Δ346-347) (132). This again favors a model in which VacA assembles into a complex of two or more monomers to induce vacuolating activity. Additional evidence correlating oligomerization

and VacA activity is provided by dominant-negative studies (35, 66, 118) which show that an inactive mutant toxin can inhibit the activity of wild-type VacA, presumably from the formation of mixed oligomeric complexes. Further, the formation of these mixed oligomeric complexes, containing wild-type and mutant VacA, has been demonstrated experimentally (66).

VacA structure and function

p33 and p55 VacA domains- The mature 88 kDa VacA toxin can be cleaved at a protease sensitive loop, located primarily between amino acids 311 and 312, into an amino-terminal 33 kDa (p33) and a carboxy-terminal 55 kDa (p55) protein (11, 30, 76, 106). These fragments remain non-covalently associated, and are thought to represent two domains or subunits of VacA (59, 90, 106, 113). Work from our lab has shown that an engineered VacA toxin with an enterokinase cleavage site introduced between p33 and p55, when treated with enterokinase, undergoes complete proteolysis into the p33 and p55 domains (113). The vacuolating activity of enterokinase-treated VacA is indistinguishable from intact VacA. Additionally, enterokinase treated VacA and intact VacA elute in the same high molecular mass fractions. Combined, these data indicates that, upon cleavage, the p33 and p55 fragments remain associated and do not undergo any extensive adverse conformational changes (113).

Previous studies have identified distinct activities for the p33 and p55 VacA domains (Figure I-3). Within the p33 domain, the hydrophobic region between amino acids 1 and 32 plays an important role in the formation of anion-selective channels (65, 69, 118). Amino acid sequences within both the p33 and p55 domains are important for oligomerization of the

toxin (35, 113, 114). Neither the p33 nor the p55 domain alone is sufficient for vacuolating toxin activity when expressed in transiently transfected cells. When expressed intracellularly in transiently transfected cells, the p33 domain along with the first 111 amino acids of the p55 domain is the minimal portion of VacA able to induce cell vacuolation (17, 132, 133). Amino acids within the carboxy-terminus of p55 are thought to play an important role in binding of VacA to cells (30, 82, 90, 119, 120). Very little is known about specific regions within the p55 domain that are important for specific functional activities.

In one recent study, random mutagenesis was used to introduce mutations into the *vacA* gene with the goal of identifying mutant proteins that lacked vacuolating activity (68). In this study, a plasmid expressing recombinant VacA was transformed into a mutator *E. coli* strain, and the mutated plasmids were then transformed into the *E. coli* expression strain ER2566. Until this paper, most work had focused on introducing mutations into the chromosomal *vacA* gene within *H. pylori*, and most of the tested mutant proteins contained large deletions, which could drastically alter VacA structure. Interestingly, of the mutations generated by random mutagenesis that were found to lack vacuolating activity, most mapped to the amino-terminal hydrophobic region of VacA, and no inactivating mutations were identified that mapped to the p55 domain of VacA, suggesting that mutation of individual residues within the p55 domain may not be sufficient to abolish VacA activity (68).

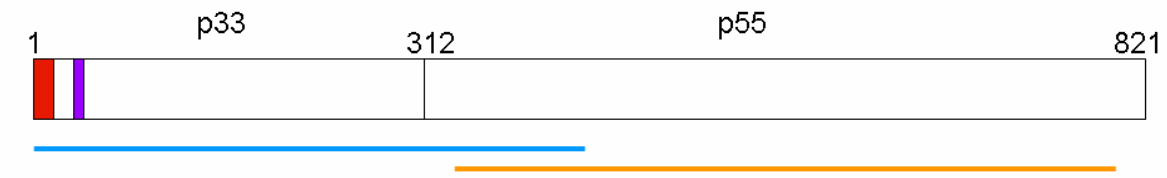

Figure I-3. Functional regions of mature VacA. Mature secreted VacA is comprised of two domains, designated p33 and p55. An amino-terminal hydrophobic region between amino acids 1 and 32 (shown in red) plays an important role in the formation of anion-selective channels. Amino acids in the p33 domain (residues 49-57, shown in purple) are important for oligomerization of the toxin. When expressed intracellularly in transiently transfected cells, the minimal portion of VacA able to induce cell vacuolation is amino acids 1-422 (shown by the light blue line). The crystal structure of the p55 domain has been solved from amino acids 355-811 (shown by the orange line).

Previous work from our lab used yeast 2-hybrid analysis to more clearly understand the process by which VacA assembles into higher ordered structures (113). Specifically, a study by Torres *et al.* investigated the role of p33 and p55 interactions in oligomer formation. The data showed that amino acids 28-196 within the p33 domain and amino acids 313-478 within the p55 domain contribute to the p33-p55 interaction (113). Using yeast two hybrid methods, this study was not able to detect p33-p33 or p55-p55 interactions; interestingly, another study analyzed the properties of a modified p55 fragment (containing all of p55 and 27 amino acids of the p33 domain) secreted by *H. pylori* and found that p55 could form dimers, but not large oligomers (90). Overall, the work by Torres *et al* began to characterize the interactions that mediate assembly of VacA into oligomers. However, this study was not able to distinguish between intramolecular (interactions between p33 and p55 domains within an individual monomer) or intermolecular (interactions between p33 and p55 domains of different 88 kDa monomers) interactions. This study led to another study from our lab in

which recombinantly expressed p33 and p55 were used to gain a better understanding of the functional properties of these two domains (112) (discussed in Chapter II).

p55 crystal structure- Until recently, no high resolution structural data have been available for VacA. This changed when the crystal structure of the VacA p55 domain was determined at a resolution of 2.4 Å (29) (Figure I-4). The crystal structure revealed that the p55 domain folds as a right-handed parallel β-helix. Each coil of the parallel β-helix consists of three parallel β-strands connected by loops of different lengths. Other features of the p55 structure include a small globular domain near the carboxy-terminus that consists of mixed α/β secondary structure elements and the presence of a disulfide bond. In VacA, this closely-spaced pair of cysteines may be important for toxin secretion, as a mutation of either cysteine to serine results in decreased toxin secretion (56).

Analysis of sequence variation among the p55 domain of VacA proteins revealed that there are only two regions of the surface with high sequence conservation (29). One region is located at the amino-terminus of p55, thought to play a role in oligomerization, and the other is located at the carboxy-terminus of the protein and is thought to be important for binding of the toxin to host cells. The authors propose a model in which VacA oligomerization is mediated by contacts between p33 and the amino-terminus of p55 from a neighboring subunit (29). The availability of the VacA p55 crystal structure was instrumental in my thesis project in the lab, allowing me to take a targeted approach to structure-function studies of the toxin.

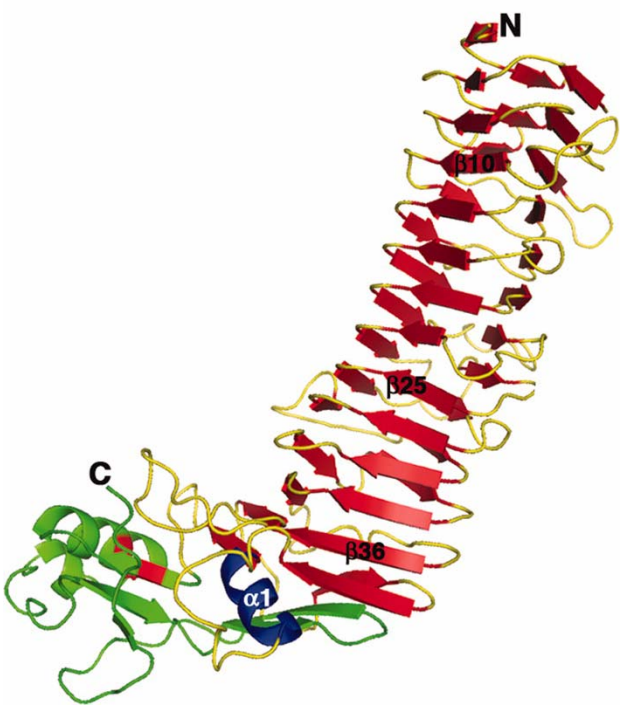

Figure I-4. Crystal structure of the VacA p55 domain. The p55 domain folds as a β-helix, composed of three parallel β sheets (shown in red) connected by loops of varying lengths (shown in yellow). The carboxy-terminus consists of mixed α/β secondary structure elements (shown in green). Reproduced from (29).

Research significance and goals

The VacA toxin produced by *H. pylori* exerts numerous effects on its host, not only targeting the gastric epithelial cell layer, but also targeting the immune system. The biological significance of VacA has been highlighted in animal studies in which orally administered VacA causes degeneration of the gastric mucosa, acute inflammation, and gastric ulcer disease (60, 106). One study has suggested that an isogenic *vacA*-negative *H. pylori* strain is not able to colonize mice as efficiently as the wild-type parental strain (94). Perhaps even more importantly, certain *vacA* genotypes have been correlated with more severe disease outcome in humans (3). Since the discovery of VacA just over 20 years ago, numerous groups have tried to elucidate the mechanism of action of this toxin and its biological role. Although great strides have been made in both of these areas, questions remain such as what functional roles the p33 and p55 domains may play, what specific regions of the toxin are important for oligomerization, and more recently, how the β-helical structure contributes to secretion. Thus, the goals of this thesis were to undertake structure-function studies of VacA to (*i*) characterize subdomains within the p55 domain that are important for oligomerization, and subsequently, host-cell alterations, and (*ii*) study the β-helical portion of p55 to determine the role of individual coils in toxin function. My work describing these areas of study, as well as an additional study, will be divided into three chapters as follows: functional analysis of the p33 and p55 VacA domains in relation to their interaction with host cell membranes (Chapter II), determining a subdomain of p55 important for oligomerization (Chapter III), and analysis of the β-helical region of the VacA p55 domain (Chapter IV). In Chapter V, I will present unpublished work describing efforts to better understand VacA-host cell interactions.

Interaction of p33 and p55 VacA domains with host cell membranes

It is well-established that the mature 88 kDa VacA toxin can undergo partial proteolytic cleavage to yield two fragments known as p33 and p55. Previous work has also suggested that these two fragments represent two domains of VacA, with amino acids near the amino-terminus of p33 being involved in anion channel formation and the p55 domain being involved in VacA binding to mammalian cells (9). The goal of this study was to analyze functional properties of recombinantly expressed p33 and p55. My contribution to this study was to analyze the interaction of the p33 and p55 domains with host cell membranes and their subsequent internalization.

Determine subdomains of p55 important for oligomerization

Many of the cellular effects of VacA result from the formation of oligomeric complexes. Work from our lab began characterizing the role of the p33 and p55 domains in the processes of VacA binding, internalization, and oligomerization (112, 113) and laid the foundation to identify functional domains within VacA that contribute to specific steps in the intoxication process. The minimum portion of VacA required for cell vacuolation comprises a 422 amino acid protein, corresponding to the entire p33 domain and about 111 residues from the amino-terminus of the p55 domain (133). This suggests that the amino-terminal portion of p55 may comprise a subdomain with a functional activity distinct from cell binding. Thus, the goal of this study was to investigate properties of VacA that are conferred by the p55 amino-terminal subdomain. Our data indicate that the assembly of functional oligomeric VacA complexes is dependent on specific sequences within this p55 amino-terminal subdomain.

Study of the β-helical region of the VacA p55 domain

The recent determination of the crystal structure of the p55 domain of VacA revealed that it is a right-handed parallel β-helix (29). In addition to VacA, the structures of two other autotransporter passenger domains (pertactin and hemoglobin protease) have been solved and each also folds as a β-helix (24, 80). A recent study by Junker *et al.* found that more than 97% of predicted autotransporter sequences were predicted to adopt a right-handed parallel β-helix structure (47). Much remains unknown about the properties of β-helical proteins that are responsible for the unique properties of individual autotransporter passenger domains. Therefore, in this study, we set out to identify specific β-helical elements required for secretion and activity of VacA.

Additional studies of VacA host-cell interactions

As discussed in the Background, VacA has numerous effects on epithelial cells. Upon first joining the lab, I undertook several small projects to further understand the role of VacA in MAP kinase signaling and apoptosis, and also tried to identify epithelial cell proteins that were up- or down-regulated as a result of VacA intoxication. Further study of these topics may provide new insights into the actions of this multifunctional toxin and perhaps lead to a better understanding of the pathogenesis of *H. pylori*-associated diseases.

CHAPTER II

FUNCTIONAL PROPERTIES OF THE p33 AND p55 DOMAINS OF THE *HELICOBACTER PYLORI* VACUOLATING CYTOTOXIN

Introduction

The mature secreted 88 kDa vacuolating cytotoxin (VacA) from *H. pylori* can undergo partial proteolytic cleavage to yield two fragments that are 33 kDa (p33) and 55 kDa (p55) in mass. These fragments are thought to represent two domains or subunits of VacA (11, 106, 113, 132). Amino acid sequences within a hydrophobic region near the amino-terminus of the p33 domain have been shown to play a role in the formation of anion-selective membrane channels, and the p55 domain is important for VacA binding to mammalian cells (9). However, detailed analysis of the functional roles of p33 and p55 had not been performed; therefore, the goal of this study was to investigate various functional properties of recombinantly expressed p33 and p55 VacA domains.

The results presented in this chapter were published in the *Journal of Biological Chemistry*; I was the second author on the paper. In the remainder of the Introduction, I will summarize data generated by the co-authors. In the Results section of this chapter, I will present the work that I did.

To begin studying functional properties of the p33 and p55 VacA fragments, each fragment was expressed as a recombinant protein, based on methods previously developed to express full-length VacA (67). Western blot analysis showed that each protein was successfully expressed as a 33 kDa protein (p33) or a 55 kDa protein (p55) (112). It has been shown that recombinantly expressed full-length 88 kDa VacA exhibits vacuolating activity

when added to mammalian cells (67). To investigate if either the p33 or p55 proteins were capable of inducing vacuolation, the recombinant proteins were added to cells individually or in combination. No detectable vacuolating activity was observed when *E. coli* extracts containing the p33 or p55 protein were added individually to HeLa cells. In contrast, when extracts containing the p33 and p55 proteins were mixed and then added to HeLa cells, extensive cell vacuolation was detected (112). These results indicate that the p33 and p55 VacA domains can complement each other for vacuolating activity.

It was hypothesized that the ability of the p33 and p55 proteins to complement each other for vacuolating activity might require the formation of protein complexes comprising these two proteins. Immunoprecipitation experiments were performed to test whether the p33 and p55 domains could physically interact. p33/p55 interactions were detected, whereas p55/p55 and p33/p33 interactions were not detected (112), suggesting that recombinant p33 and p55 proteins are capable of interacting in solution to form p33/p55 protein complexes. Additional immunoprecipitation experiments showed that the p33/p55 complex can potentially be composed of at least three independent subunits, consisting of one p55 and two p33 proteins (112).

Using purified 88 kDa VacA from *H. pylori* culture supernatant, immunoprecipitation methodology was used to investigate if recombinant p33 and p55 fragments could physically interact with wild-type VacA from *H. pylori*. When the p33 and p55 domains were tested independently, neither p33 nor p55 interacted with full-length VacA; however, when a p33/p55 mixture was incubated with full-length VacA, both p33 and p55 interacted with the 88 kDa VacA (112). These data suggest that both p33 and p55 play a role in the process by which VacA assembles into oligomeric structures.

In the next series of experiments, the capacity of the recombinant p33 and p55 proteins to interact with mammalian cells was investigated. The first approach used was western blotting. When either p33 or p55 was added individually to HeLa cells, weak binding was detected. When the p33 and p55 domains were mixed and then added to HeLa cells, the amount of p33 and p55 protein associated with cells was substantially increased compared with the amount detected when these proteins were tested individually (112). In the remainder of this chapter, I will present the work that I did, specifically confocal microscopy data showing binding and internalization of the p33 and p55 domains.

Methods

Plasmid construction- VacA-expressing plasmids were constructed by cloning *vacA* sequences from *H. pylori* strain 60190 into pET-41b (Novagen), using procedures similar to those described previously (67). A *vacA* sequence encoding the VacA p33 domain (amino acids 1-312 of the mature, secreted *H. pylori* VacA toxin) with a 6-His tag at the carboxy-terminus (p33His) was PCR-amplified from the pMM592 plasmid (67) using primers BA9146 and OP6228. The PCR product was digested with SpeI and SalI and ligated into XbaI- and SalI-digested pET-41b (conferring kanamycin resistance; Novagen). We also generated a plasmid that encoded a VacA p33 domain with two tags (c-Myc and 6-His), each at the carboxy-terminus of the protein (p33Myc-His). A *vacA* sequence encoding the p55 domain (amino acids 312-821 of the mature, secreted *H. pylori* VacA toxin) with a c-Myc tag (p55Myc) at the amino-terminus was PCR-amplified from *H. pylori* VT330 genomic DNA using primers OP6229 (5'-CCCACTAGTAAGAGGAGACGCCATGGCAAACGCCGCA CAGG-3') and AND515a (5'-CCCCGTCGACTTAAGCGTAGCTAGCGAAACGCG-3').

Also, a *vacA* sequence encoding the p55 domain with a 6-His tag at the amino-terminus was generated using primers AND7265 (5'-CCCACTAGTAAGAGGAGACGCCATGCATCA CCATCACCATCACAAAAACGACAAACAAGAGAGC-3') and AND515a. PCR products were digested and cloned into pET41b as described above. The use of these primers resulted in a modification of the ribosomal binding site of pET-41b, and encoded a methionine at the amino-terminus of each VacA protein. The entire *vacA* fragment in each plasmid was analyzed by nucleotide sequence analysis in order to verify that no unintended mutations had been introduced.

Expression of recombinant VacA proteins- VacA expression plasmids were transformed into the *E. coli* expression strain JM109 (DE3), and transformants were then inoculated into TB-KAN and grown at 37°C overnight with shaking. These cultures were diluted 1:100 into TB-KAN, and incubated at 37°C until they reached an optical density (OD_{600}) of 0.5. Cultures were then induced with a final IPTG concentration of 0.5 mM and incubated at 25°C for 16-18 hours (p55 proteins) or at 37°C for 2 hours (p33 proteins). *E. coli* extracts containing soluble proteins were generated as described previously with minor modifications (67). Briefly, 50 ml of IPTG-induced cultures were pelleted, washed in 0.9% NaCl, and resuspended in a solution (1 ml) that contained 10 mM Tris (pH 7.5), 100 mM NaCl, 1 mM EDTA, protease inhibitors (Complete Mini; Roche), and 20,000 units of ReadyLyse lysozyme (Epicentre) per ml. Bacterial cells were incubated on ice for 30 min with periodic mixing, after which a solution (3 ml) containing 50 mM Tris (pH 8.0), 2.67 mM $MgCl_2$, and 74 units of Omnicleave Nuclease (Epicentre) per ml was added. Samples were then mixed briefly, subjected to four successive rounds of freezing (in a dry ice-methanol bath) and

thawing at 37°C, and then the insoluble debris was pelleted. The *E. coli* soluble extracts containing the VacA proteins were collected and stored at -20°C until use.

Analysis of VacA binding and internalization into mammalian cells- To analyze interactions of VacA with the surface of cells, *E. coli* soluble extracts containing recombinant VacA proteins were added to HeLa cells grown on cover glasses in 6 well plates for 1 hour at 4^{o}C or 37^{o}C. VacA interactions with mammalian cells were then analyzed by indirect immunofluorescence (58, 96). Briefly, cells were washed with tris-buffered saline (TBS; 10 mM Tris, 150 mM NaCl, pH 7.5) and fixed with 3.7% formaldehyde. Fixed cells were incubated with an anti-c-Myc antibody (1:500) or with an anti-VacA polyclonal antiserum that recognizes the p55 domain, for 1 hour at 25°C. Cells were then washed and incubated with a Cy3-conjugated secondary antibody (1:500) for 1 hour at 25°C. To analyze VacA internalization into host cells, *E. coli* soluble extracts containing single recombinant VacA proteins or mixtures of recombinant VacA proteins were incubated with HeLa cells for 1 hour at 37^{o}C. Afterward, medium containing unbound proteins was removed and the cells were incubated in fresh tissue culture medium (without FBS or ammonium chloride) for 16 hours at 37^{o}C. The cells were then washed with TBS, fixed with 3.7% formaldehyde, and permeabilized with 100% methanol for 30 minutes at -20^{o} C (58). Cells were incubated with the anti-VacA polyclonal antiserum or the anti-c-Myc antibody, followed by a Cy3-conjugated secondary antibody. After immunolabeling, cover glasses were washed with phosphate-buffered saline, mounted on slides with Aqua-Polymount (Polysciences, Warrington, PA), and viewed with a LSM 510 confocal laser scanning inverted microscope (Carl Zeiss).

Results

Analysis of binding of p33 and p55 VacA domains to mammalian cells

As presented in the Introduction of this chapter, western blotting was used as a first approach to investigate p33 and p55 interactions with mammalian cells. As a second approach, we used indirect immunofluorescence methodology. As expected, full-length 88 kDa c-Myc-tagged VacA purified from *H. pylori* bound to the surface of HeLa cells, and the binding could be detected with either an anti-c-Myc antibody or a polyclonal anti-VacA antiserum that recognizes the p55 domain (Figure II-1; panels 1 and 5) (30, 96). In contrast, no immunoreactive signal on the surface of cells was detected with these antibodies following incubation of cells with negative control extracts (Figure II-1; pET, panels 2 and 6). When recombinant p33 and p55 domains were added individually to cells, binding of p33 (either p33Myc-His or p33His) to the surface of cells was detectable (Figure II-1, panel 3 and data not shown), but binding of p55 was not detected (Figure II-1; panel 7). We were able to detect binding of the p55 domain to the surface of cells by immunoblot methodology, but we were unable to detect interaction of the recombinant p55 protein with the surface of HeLa cells using immunofluorescence assays, despite testing two different forms of this protein (p55His or p55Myc) and multiple antibodies, including the anti-VacA polyclonal antiserum. We presume that the relevant epitopes are not accessible to the antibodies under the conditions of the immunofluorescence assay. When the p33 and the p55 proteins were mixed and then added to HeLa cells, both proteins were detected on the surface of HeLa cells (Figure II-1, panels 4 and 8). Thus, binding of p55 to the cell surface was detected by immunofluorescence assay if the p33 and p55 domains were added together to cells, but not

if p55 was added independently to cells. Interestingly, the distribution of p33 on the surface of HeLa cells was punctate when p33 was added alone to cells, whereas it was continuous (non-punctate) when p33 was added to cells together with the p55 domain (Figure II-1; panels 3 and 4). These data indicate that the interactions of p33 and p55 VacA domains with the surface of cells are substantially altered if both domains are present.

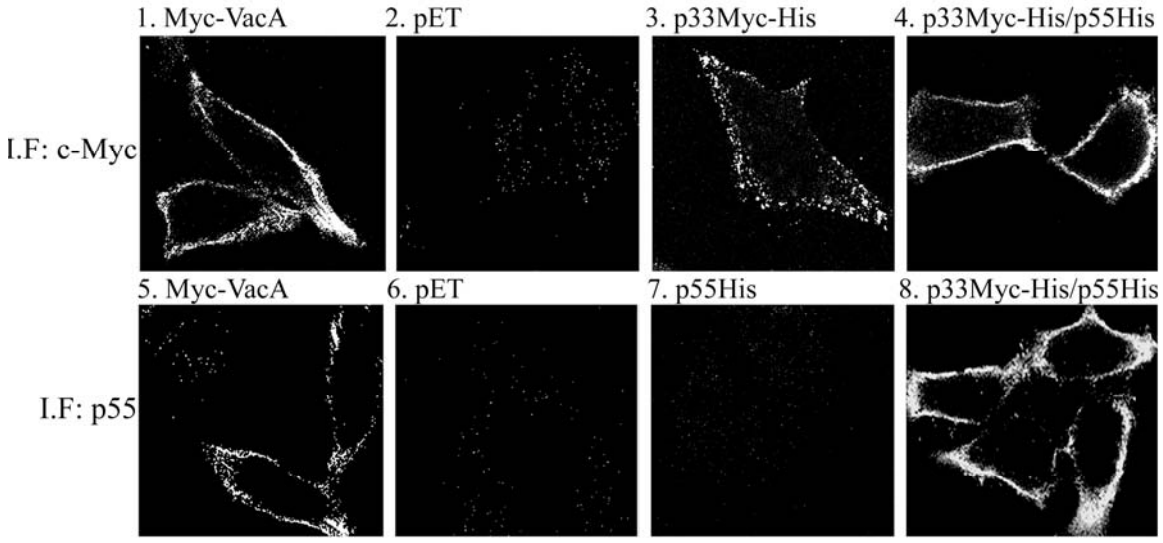

Figure II-1. Binding of p33 and p55 VacA domains to mammalian cells. HeLa cells were intoxicated for 1 hour at 37ºC with acid-activated c-Myc-VacA (Myc-VacA; 5 μg/ml) purified from *H. pylori* culture supernatant (panels 1 and 5), *E. coli* negative control extract without VacA proteins (pET; panels 2 and 6), *E. coli* soluble extracts containing p33Myc-His (panel 3), p55His (panel 7), or the p33Myc-His/p55His mixture (panels 4 and 8). The capacity of the VacA proteins to interact with the cell membrane of host cells was assessed by indirect immunofluorescence (I.F.) using anti-c-Myc (panels 1-4) and an anti-VacA polyclonal antibody that recognizes the p55 domain (panels 5-8).

Intracellular localization of the p33 and p55 VacA domains

We next investigated whether the p33 and p55 proteins were internalized into mammalian cells. HeLa cells were intoxicated with either purified VacA from *H. pylori*, or *E. coli* soluble extracts containing the p33 domain, the p55 domain, or the p33/p55 mixture. Internalized VacA was visualized by indirect immunofluorescence analysis of permeabilized cells. The 88 kDa VacA purified from *H. pylori* was internalized into HeLa cells (Figure II-2, panel 1) as shown previously. Little if any internalization of the p33 or p55 protein was detected when these proteins were added individually to cells (Figure II-2, panels 2 and 3). In contrast, when the p33 and the p55 proteins were mixed and then added to cells, both domains were internalized (Figure II-2, panels 4 and 5). These data indicate that both the p33 and p55 VacA domains are required for toxin internalization into target cells.

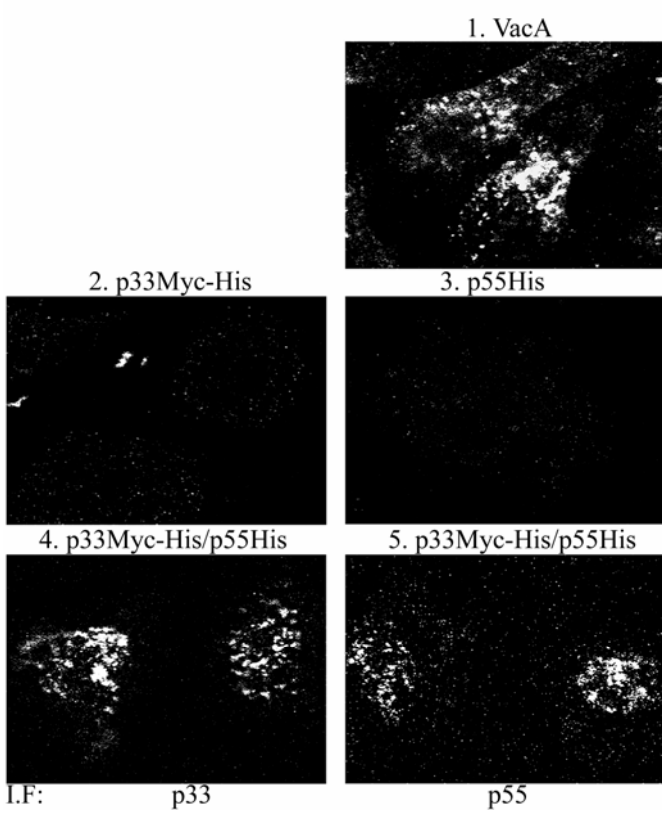

Figure II-2. Internalization of p33 and p55 VacA domains into mammalian cells. Wild-type acid-activated VacA purified from *H. pylori* culture supernatant (panel 1), or *E. coli* soluble extracts containing p33Myc-His (panel 2), p55His (panel 3), or the p33Myc-His/p55His mixture (panels 4 and 5) were added to HeLa cells for 1.5 hours at 37ºC. The cells were then incubated in fresh medium for an additional 16 hours at 37ºC. The ability of VacA to enter into cells was assessed by indirect immunofluorescence (I.F.) of permeabilized cells using an anti-VacA antibody to detect the p55 domain (5E4; panels 1, 3, and 5) and an anti-c-Myc antibody to detect the p33Myc-His protein (panels 2 and 4).

Sequential addition of the p33 and p55 VacA domains

To further investigate the role of p33 and p55 interactions with host cells and to establish which component is important for initial contact with the cell, we sequentially incubated HeLa cells with *E. coli* soluble extract containing p33 followed by extract containing p55 ($p33^1$, $p55^2$), or p55 followed by p33 ($p55^1$, $p33^2$). We investigated the binding of sequentially added VacA domains to the surface of host cells, using indirect immunofluorescence methodology. In these sequential addition experiments, both p33 and p55 domains could be detected on the cell surface, regardless of the order of addition ($p55^1$, $p33^2$ or $p33^1$, $p55^2$) (Figure II-3, panels 2 and 3). In contrast, binding of p55 to cells was not detectable by immunofluorescence in experiments in which p55 was added independently (Figure II-1, panel 7). When the p55 and p33 proteins were added sequentially to cells, both proteins localized on the cell surface in a punctate distribution, regardless of the order of addition (Figure II-3, panels 2 and 3). In contrast, when cells were incubated with the p33/p55 mixture, both proteins localized in a continuous (non-punctate) pattern on the surface of HeLa cells (Figure II-3, panel 1).

We next tested the hypothesis that there might be differences in the internalization of VacA, depending on the order in which VacA domains are added to cells. When the p55 domain was added first to cells followed by the p33 domain ($p55^1$, $p33^2$), a condition that results in cell vacuolation, internalization of the p55 protein was detected ($p55^1$, $p33^2$; Figure II-4). When the p33 protein was added first followed by the p55 protein ($p33^1$, $p55^2$), a condition that fails to cause cell vacuolation, neither p55 nor p33 was detected inside cells ($p33^1$, $p55^2$; Figure II-4). Thus, in these sequential addition experiments, there are marked

differences in the internalization of VacA depending on the order in which VacA domains are added to cells.

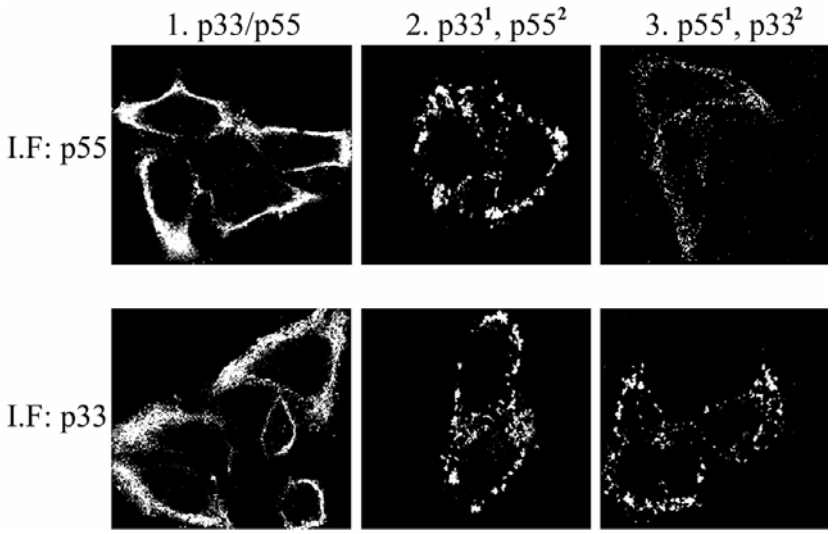

Figure II-3. Sequential addition of p33 and p55 domains to HeLa cells-binding. HeLa cells were intoxicated for 1 hour at 37°C with *E. coli* soluble extract containing a p33/p55 mixture (column 1). Alternatively, p33 was bound first followed by p55 ($p33^1$, $p55^2$; column 2), or p55 was bound first followed by p33 ($p55^1$, $p33^2$; column 3) as described above. The capacity of the VacA proteins to interact with the cell membrane of host cells was assessed by indirect immunofluorescence using an anti-VacA polyclonal antibody to detect p55His (p55; top panels) and an anti-c-Myc antibody to detect the p33Myc-His protein (p33; bottom panels).

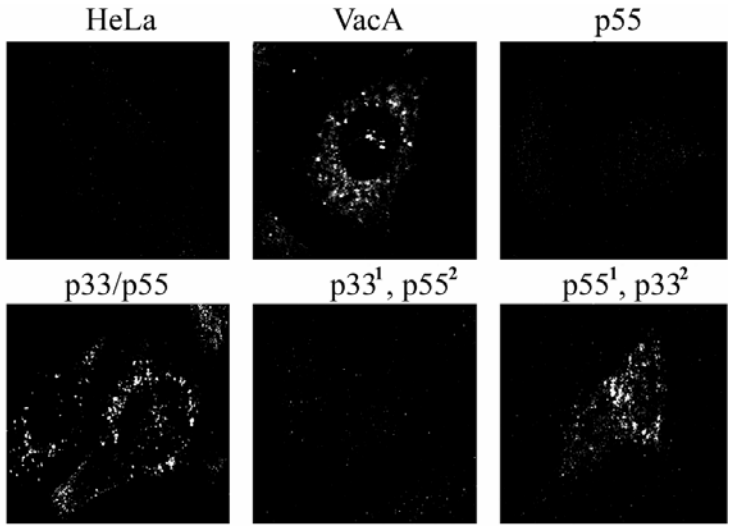

Figure II-4. Sequential addition of p33 and p55 domains to HeLa cells-internalization. HeLa cells were incubated with acid-activated VacA purified from *H. pylori* or *E. coli* soluble extracts containing the indicated recombinant VacA proteins. Then the cells were incubated in fresh culture medium for an additional 16 hours at 37ºC. Entry of VacA into cells was analyzed by indirect immunofluorescence (I.F.) of permeabilized cells using an anti-VacA polyclonal antibody to detect the p55 VacA domain.

Discussion

The *H. pylori* VacA toxin produces a wide array of structural and functional alterations in intoxicated mammalian cells (9, 74). An important goal is to identify functional domains of VacA that contribute to specific steps in the intoxication process. Previous studies have demonstrated that the mature secreted VacA toxin undergoes proteolytic degradation to yield two fragments (p33 and p55) (11, 106, 113), but the relevant structural features of these two putative domains remain poorly characterized. In the current study, we investigated various properties of recombinant p33 and p55 VacA domains.

We demonstrate that VacA interactions with the surface of cells are altered in several ways when both p33 and p55 domains are present, compared to when only a single domain is present. First, in comparison to individual p33 and p55 domains, a p33/p55 mixture binds more avidly to the cell surface. This increased binding is observed for both the p33 and p55 domains. Second, when p55 is added to cells in the absence of p33, the binding of p55 is detectable in immunoblot assays but not in immunofluorescence assays. In contrast, if a mixture of p55 and p33 domains is added to cells, the binding of p55 is detectable in both assays. This suggests that the conformation or orientation of the p55 domain on the surface of cells may be altered in the presence of the p33 domain. Finally, when added individually to cells, the p33 domain localizes in a punctate distribution on the cell surface, but when added to cells along with p55, p33 localizes in a continuous (non-punctate) distribution on the cell surface. Previous studies have reported the existence of multiple cell surface receptors for VacA secreted by *H. pylori*, and accordingly, it seems likely that recombinant p33/p55 complexes may bind to multiple different cell surface components.

In the current study, we demonstrate that when added together, the p33 and p55 proteins are both internalized by host cells, whereas internalization is not detectable when the p33 or p55 domains are added individually to host cells. The failure of p55 to be internalized when added independently to cells is consistent with the results of a previous study, in which a mutant VacA protein consisting mainly of the p55 domain was secreted by *H. pylori* and bound to the surface of host cells but was not internalized (90). One possible scenario is that binding of p33/p55 VacA complexes to a specific site on the cell surface (for example, a specific receptor and/or lipid rafts) promotes VacA oligomerization. The p33/p55 oligomeric complex may then undergo a conformational change to permit membrane insertion of the p33 domain, and that the complex can then be internalized into the cell. The capacity of internalized p33/p55 complexes to induce cell vacuolation is consistent with results of a previous study, which showed that intracellular co-expression of p33 and p55 results in vacuolating cytotoxic activity (133).

Further insight into the functional roles of p33 and p55 domains comes from studies in which these domains are added sequentially to cells. We demonstrate that binding of p55 to the cell surface followed by addition of p33 ($p55^1$, $p33^2$) results in cell vacuolation. This result can be explained by the formation of p55/p33 complexes on the surface of cells. We speculate that the isolated p55 domain is able to bind specific cell-surface components that promote oligomerization, membrane insertion and internalization of VacA. Thus, internalization of VacA into cells may be dependent on an interaction of the p55 domain with specific cell surface components. Several previous studies have provided evidence indicating that amino acid sequences in the p55 domain of p88 VacA contribute to the process of VacA binding to cells (30, 90, 120, 121). In the current study, binding of p33 to the cell surface

followed by addition of p55 ($p33^1$, $p55^2$) did not result in detectable cell vacuolation. We speculate that p33 may not be able to bind certain relevant cell surface components that are required for VacA internalization. Alternatively, sequential addition in this order ($p33^1$, $p55^2$) may not permit the formation of the p33/p55 complexes, or might prevent the formation of p33/p55 complexes in the proper conformation required for internalization.

Importantly, the work in this chapter indicates that both the p33 and p55 VacA domains are capable of interacting with the cell surface and the interaction is higher when the p33 and p55 domains are added together. One way in which this finding could be further explored would be to investigate what cellular components each domain binds to, and if this changes if the domains are added individually or together. Additionally, the data show that if p33 is added first, followed by the p55 domain, there is no internalization or vacuolating activity. In this regard, investigation of what the p55 domain binds to may help to figure out what receptors are required for internalization. This chapter also describes internalization of the p33 and p55 domains when the domains are mixed and added to cells together. Experiments could be done to learn where these domains localize within the cell.

Overall, this study shows that VacA is unique from other pore-forming toxins, in that two independently expressed functional domains can reconstitute cytotoxic activity, suggesting that VacA may have unique structural properties. This functional characterization laid the foundation for my future work in the lab, to not only more closely study the role of p55 in oligomerization, but also to study in more detail the functional characteristics of the p55 domain.

CHAPTER III

A *HELICOBACTER PYLORI* VacA SUBDOMAIN REQUIRED FOR INTRACELLULAR TOXIN ACTIVITY AND ASSEMBLY OF FUNCTIONAL OLIGOMERIC COMPLEXES

Introduction

Helicobacter pylori VacA is a secreted pore-forming toxin that is comprised of two domains, designated p33 and p55. The p55 domain has an important role in binding of VacA to the cell surface. About 111 residues at the amino-terminus of p55 (residues 312-422) are essential for the intracellular activity of VacA (133), which suggests that this region may constitute a subdomain with an activity distinct from cell binding. The goal of the current study was to investigate properties of VacA that are conferred by the p55 amino-terminal subdomain. Thus far, a two-amino-acid deletion mutation (Δ346-347) is the only small alteration within the p55 amino-terminal subdomain that is known to abrogate vacuolating toxin activity (132). Efforts to identify additional small inactivating mutations in the p55 domain using a random mutagenesis approach have not been successful (68). A previous study reported that the VacA Δ346-347 mutant protein lacked vacuolating activity when expressed intracellularly, but the basis for this lack of activity has not yet been investigated (132).

To identify the Δ346-347 mutant protein, a series of six-amino-acid deletion mutations was introduced into a 110-amino-acid region (spanning residues 325-435) at the amino-terminal end of p55 (Steven R. Blanke, personal communication). Plasmids encoding wild-type or mutant VacA proteins were transfected into HeLa cells and cell vacuolation was quantified by neutral red uptake. These experiments revealed that vacuolating activity was

completely ablated by each of the six-amino-acid deletion mutations spanning residues 345-365, 375-400, and 410-415 (Steven R. Blanke, unpublished data). The region spanning residues 345-350 was then narrowed down, and it was published that the Δ346-347 mutant protein lacked vacuolating activity when transfected into host cells (133).

In the current study we sought to investigate the basis for inactivity of the Δ346-347 mutant protein and to compare the properties of VacA Δ346-347 with those of wild-type VacA. We report that the Δ346-347 mutant protein is proteolytically processed and secreted by *H. pylori* in a manner similar to wild-type VacA. However, the Δ346-347 mutant protein does not cause membrane depolarization and is impaired in the ability to assemble into functional oligomeric VacA complexes. These results provide evidence that assembly of VacA into functional oligomeric complexes is dependent on specific sequences, including amino acids 346 and 347, within the p55 amino-terminal subdomain.

Methods

H. pylori strains and purification of VacA from H. pylori broth culture supernatants- The *vacA* gene (Genbank accession number Q48245) from *H. pylori* 60190 (ATCC 49503) served as the parent DNA for construction of all mutants in this study. Throughout this study, we used an amino acid numbering system in which residue 1 refers to alanine-1 of the secreted 88 kDa VacA protein, and the p55 domain corresponds to amino acids 312 to 821. The crystal structure of residues 355 to 811 (within the p55 domain) has recently been determined (29). Wild-type *H. pylori* strain 60190 and strains that express a VacA Δ6-27 mutant protein or a c-Myc-tagged VacA protein have been described previously (Table III-1) (66, 118). An *H. pylori* strain expressing a Δ346-347 mutant protein was constructed as

described below. *H. pylori* strains were grown in sulfite-free Brucella broth containing activated charcoal (38). VacA Δ6-27 and VacA-c-Myc proteins were purified in an oligomeric form from culture supernatants of *H. pylori,* using gel filtration chromatography (11, 66, 118). It was not possible to purify VacA Δ346-347 from *H. pylori* broth culture supernatants by using gel filtration. Therefore, for all experiments designed to compare the activity and properties of wild-type VacA and VacA Δ346-347, these proteins were purified from *H. pylori* culture supernatants using Cellufine Sulfate Matrex beads (Chisso Corporation, Tokyo, Japan) (35), unless otherwise specified. Proteins in *H. pylori* broth culture supernatants were precipitated with ammonium sulfate, the resuspended proteins were dialyzed in sodium phosphate buffer (20mM sodium phosphate, 100mM sodium chloride, pH 7), and the dialyzed samples were then incubated with Matrex beads at room temperature for 30 minutes. VacA was eluted from the beads with sequentially increasing concentrations of NaCl. As a negative control, culture supernatant from a *vacA* null mutant strain (60190 *vacA*::km) was processed in the same manner.

Expression of VacA Δ346-347 in H. pylori- A Δ346-347 mutation (encoding a deletion of VacA amino acids 346 and 347) was introduced into the *H. pylori* chromosomal *vacA* gene by natural transformation and allelic exchange using a *sacB*-based counterselection approach, as described previously (66, 69, 118). Sequence analysis of a PCR product was performed to confirm that the desired mutation had been introduced successfully into the chromosomal *vacA* gene.

Expression of Recombinant VacA Proteins in E. coli- pMM592 is a previously described plasmid that allows expression of an 88 kDa VacA protein in *E. coli* (Table III-1) (67). Plasmids for expression of VacA p33 and p55 fragments have been described previously (112); the encoded p33 proteins contain either a His_6 tag at the carboxy-terminus of the protein (p33 His) or both c-Myc and His_6 tags at the carboxy-terminus of the protein (p33 Myc-His), and p55 contains a His_6 tag at the amino-terminus of the protein (His p55). To construct pMM592 Δ346-347 (pSI200), the *vacA* gene from pET20b-1-741 Δ(346-347)-GFP (132) was digested with EcoRI and KpnI and ligated into EcoRI- and KpnI-digested pMM592. To introduce additional substitution and deletion mutations into the codons for amino acids 346 and 347, we performed inverse PCR, using appropriate primers and pSI200 as template DNA (127). The resulting PCR products were then ligated and transformed into *E. coli* DH5α. To construct a plasmid encoding the p55 domain of VacA with a Δ346-347 mutation, the corresponding region of *vacA* (encoding amino acids 312-821) was amplified using primers AND7265 (5'-CCCACTAGTAAGAGGAGACGCCATGCATCACCATCAC CATCACAAAAACGACAAACAAGAGAGC-3') and AND515a (5'-CCCCGTCGACTTA AGCGTAGCTAGCGAAACGCG-3') (112), which resulted in insertion of a His_6 tag at the amino terminus. The PCR product was digested with SpeI and SalI and ligated into XbaI- and SalI-digested pET41b (Novagen), to yield p55 Δ346-347 (pSI209). In each case, the plasmids were analyzed by sequence analysis to confirm that the desired mutation was present and that no new mutations had been introduced. VacA expression plasmids were transformed into the *E. coli* expression strain ER2566 (New England Biolabs), which encodes an IPTG (isopropyl-β-D-thiogalactopyranoside)-inducible copy of the RNA polymerase gene from bacteriophage T7. VacA-expressing *E. coli* strains were cultured in

Terrific Broth (Invitrogen) supplemented with 25 μg/ml kanamycin (TB-KAN) (67, 112), and extracts containing soluble proteins were generated as described previously (67, 68).

Cell culture analysis of VacA proteins expressed in H. pylori or E. coli- HeLa and AZ-521 cells were grown as described previously (112). In all experiments, preparations of VacA purified from *H. pylori* culture supernatants were acid-activated by the addition of 100 mM hydrochloric acid, lowering the pH to 3, before VacA was added to cells (20, 70). An equivalent volume of a corresponding preparation from a *vacA* null mutant (60190 *vacA*::km) was used as a negative control. For experiments using multiple recombinant VacA proteins, the relative concentrations of recombinant VacA in different *E. coli* soluble extracts were assessed by immunoblotting, and the extracts were then normalized so that the relative concentrations of VacA in different preparations were approximately equivalent (112). In comparison to wild-type VacA, none of the mutant proteins exhibited substantial differences in stability or susceptibility to proteolytic degradation. Signals were generated by the enhanced chemiluminescence reaction (Amersham Biosciences) and detected using x-ray film. Recombinant VacA proteins were added to cells as described previously (112). After incubation, cell vacuolation was examined by inverted light microscopy and quantified by a neutral red uptake assay (13). Neutral red uptake data are presented as A_{540} values (mean ± S.D.). Levels of neutral red uptake produced by negative control samples were subtracted as background.

To test for dominant-negative activity, wild-type VacA (purified by gel filtration) was acid-activated and then mixed with acid-activated preparations of VacA Δ346-347 (purified by Matrex affinity resin), VacA Δ6-27, or a mock sample from a *vacA* null mutant strain.

The mixtures were then neutralized by diluting with neutral pH medium before addition to HeLa cells (118). The samples were incubated with cells for 1 hour at 37°C, removed, and fresh serum-free medium containing 5 mM ammonium chloride was added to cells for 5 hours at 37°C. Cell vacuolation was detected by inverted light microscopy and quantified by a neutral red uptake assay.

Membrane Depolarization- Analysis of membrane potential was performed as described previously (69, 105) except that AZ-521 cells were detached with Accutase. Purified acid-activated VacA, or a mock preparation derived from an *H. pylori vacA* null mutant strain was added to the cells, and changes in the fluorescence were monitored.

Blue Native Gel Electrophoresis- Blue native gel electrophoresis (126) was used to investigate the oligomeric state of VacA proteins. In this technique, protein complexes are separated based on molecular size under non-denaturing conditions. Purified wild-type VacA and VacA Δ346-347 proteins were desalted using Zeba Desalt Spin Columns (Pierce). Approximately 13 μg (5 μl) of each sample was mixed with 1 μl 1% dodecylmaltoside (a non-ionic detergent that is not expected to disrupt protein complexes), then mixed with 2.5 μl 50% glycerol and 5% Coomassie blue G-250 dye stock suspension to give a detergent/dye ratio of 1.0g/g, and electrophoresed on a 4-13% polyacrylamide gel. Lanes were cut out from the gel, boiled in SDS electrophoresis buffer for 10 minutes, and mounted on top of an 8% SDS polyacrylamide gel for second dimension analysis. After transfer to nitrocellulose, the samples were immunoblotted with an anti-VacA polyclonal serum (#958), followed by an

HRP-conjugated secondary antibody. Signals were generated by the enhanced chemiluminescence reaction and detected using x-ray film.

Modified SDS-PAGE methodology- The oligomeric state of VacA proteins was also assessed using a variant of the usual SDS-PAGE methodology. VacA preparations were mixed with 4% SDS lysis buffer (containing 1.5% Tris, 20% glycerol, 4% SDS, 10% 2-mercaptoethanol, and 0.002% Bromphenol Blue), resulting in a final SDS concentration of 2% in each sample. These samples were either boiled or not boiled, electrophoresed on an SDS-polyacrylamide gel (6% separating gel and 4% stacking gel), and analyzed by immunoblotting as described above.

Immunoprecipitation of VacA proteins- Immunoprecipitations were performed as described previously, with minor modifications (66, 112). Briefly, *E. coli* soluble extracts containing either c-Myc- or His_6-tagged VacA fragments (112) were mixed for 1 hour at room temperature. The mixtures tested included the combination of p33 Myc-His with either His p55 or His p55 Δ346-347. Samples were normalized by immunoblotting with an antibody to the His_6 epitope (anti-His, Santa Cruz Biotechnology). After 1 hour, these samples were diluted in 1 ml PBS (pH 7) containing 0.05% Tween 20 and 2% ammonium sulfate. Anti-c-Myc monoclonal antibody (9E10) (3 μg) was added, and the mixture was incubated at 4°C for 2 hours. Protein G-sepharose beads (Amersham Biosciences) were added to the VacA-antibody mixture and incubated for 16-18 hours at 4°C. The immunoprecipitated proteins were separated from the beads by boiling the beads in SDS-PAGE sample buffer and were analyzed by immunoblotting with an anti-His antibody followed by an HRP-conjugated

secondary antibody. To analyze a potential interaction between p33 His, His p55 Δ346-347, and full-length 88kDa VacA, normalized *E. coli* extracts containing the former two proteins were mixed with acid-activated c-Myc-tagged VacA (Myc-VacA) purified from *H. pylori* culture supernatant (2 μg/ml) for 1 hour at 25°C, and the proteins were immunoprecipitated with an anti-c-Myc antibody as described above. Immunoprecipitated proteins were analyzed by immunoblotting with anti-His and anti-c-Myc antibodies, followed by an HRP-conjugated secondary antibody.

Table III-1. *H. pylori* strains and plasmids

***H. pylori* strain or plasmid**	**Description**	**Reference**
***H. pylori* strains**		
60190	ATCC 49503; Encodes wild-type s1/m1 VacA	(14)
VT330	Encodes VacA with c-Myc epitope	(66)
AV452	Encodes VacA Δ6-27	(118)
SI433	Derived from *H. pylori* strain VM025, which contains a *sacB*-kan cassette within *vacA*; SI433 encodes VacA Δ346-347	(118) and this study
60190 *vacA*::km	*vacA* null mutant	(14)
Plasmids		
pMM592	Encodes wild-type VacA, amino acids 1-821	(67)
pSI200	Derived from pMM592; encodes VacA Δ346-347	This study
pSI201	Derived from pSI200; encodes VacA Δ346	This study
pSI202	Derived from pSI200; encodes VacA Δ347	This study
pSI203	Derived from pSI200; encodes VacA G347A	This study
pSI204	Derived from pSI200; encodes VacA G347R	This study
pSI205	Derived from pSI200; encodes VacA D346L/G347V	This study
pSI206	Derived from pSI200; encodes VacA D346E/G347V	This study
pSI207	Derived from pSI200; encodes VacA D346L/G347R	This study
pSI208	Derived from pSI200; encodes VacA D346R/G347R	This study
pSI209	Encodes VacA His p55 Δ346-347	This study
pET41b VacA p55	Encodes VacA His p55	(112)
pET41b VacA p33 MH	Encodes VacA p33 Myc-His	(112)
pET41b VacA p33 H	Encodes VacA p33 His	(112)

Results

Secretion of VacA Δ346-347 by *H. pylori* and analysis of binding and vacuolating activity

To investigate properties of the VacA Δ346-347 protein, we introduced the Δ346-347 mutation into the *H. pylori* chromosomal *vacA* gene by natural transformation and allelic exchange as described in Methods. An 88 kDa VacA protein was detected in broth culture supernatant from the Δ346-347 mutant *H. pylori* strain, which indicated that the 140 kDa precursor protein (9) containing the Δ346-347 mutation underwent proteolytic processing and secretion, similar to wild-type VacA (Figure III-1). We next investigated the interactions of wild-type VacA and VacA Δ346-347 with HeLa cells. Flow cytometry analysis, performed as described previously (1), revealed that both wild-type VacA and VacA Δ346-347 bound to HeLa cells in a dose-dependent manner (data not shown), thereby indicating that VacA Δ346-347 was not defective in binding to HeLa cells. Saturable binding was not assessed in these binding experiments. The capacity of VacA Δ346-347 to be proteolytically processed and secreted by *H. pylori,* as well its retention of cell-binding activity, suggested that this mutant protein was not grossly misfolded. Notably, wild-type VacA caused cell vacuolation, whereas cell vacuolation was not observed when VacA Δ346-347 was added to HeLa cells (Figure III-2A). Similarly, wild-type VacA caused extensive vacuolation of AZ-521 gastric epithelial cells, whereas VacA Δ346-347 did not cause vacuolation of these cells (data not shown).

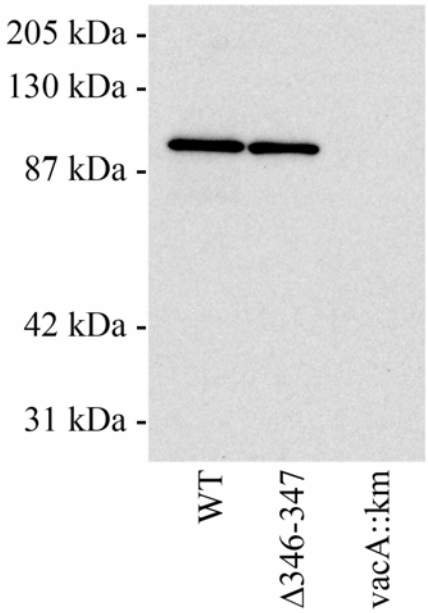

Figure III-1. Secretion of VacA Δ346-347. Wild-type (WT) *H. pylori* strain 60190, an isogenic mutant strain encoding a VacA Δ346-347 protein, and a *vacA* null mutant strain (60190 *vacA*::km) were cultured in *Brucella* broth containing activated charcoal, and proteins in the broth culture supernatants were precipitated with a 50% saturated solution of ammonium sulfate. Proteins were electrophoresed on a 10% SDS-polyacrylamide gel, transferred to a nitrocellulose membrane, and immunoblotted with polyclonal anti-VacA serum. WT VacA and VacA Δ346-347 were each proteolytically processed to yield an 88 kDa protein that was secreted by *H. pylori* into the broth culture supernatant.

Analysis of cellular depolarization

Addition of wild-type VacA to cells results in depolarization of the resting membrane potential, a phenomenon attributed to insertion of VacA into the plasma membrane to form anion-selective channels (96, 105). In the next experiments, we compared the capacity of wild-type VacA and VacA Δ346-347 to cause depolarization of AZ-521 cells. Consistent with previously published results, we found that addition of wild-type VacA to cells induced membrane depolarization (Figure III-2B), and a mock preparation derived from an *H. pylori vacA* null mutant strain did not induce depolarization. When VacA Δ346-347 was added to AZ-521 cells, membrane depolarization was not detected (Figure III-2B). Similar results were obtained using HeLa cells instead of AZ-521 cells (data not shown). The failure of the VacA Δ346-347 mutant protein to depolarize AZ-521 cells suggests that this mutant toxin is defective in membrane channel formation.

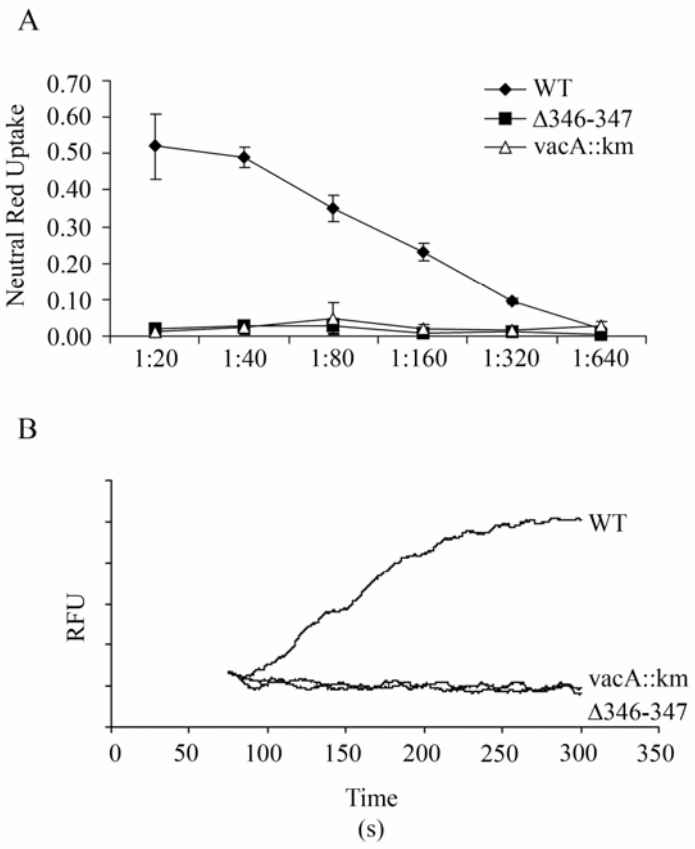

Figure III-2. Functional analysis of VacA Δ346-347 activity. *H. pylori* strains expressing WT VacA or VacA Δ346-347, and a *vacA* null mutant strain (60190 *vacA*::km) were grown in broth culture and VacA proteins were purified as described in Methods. Concentrations of WT VacA and VacA Δ346-347 were normalized based on immunoblot assays, and the preparations were tested for vacuolating activity and membrane depolarization. (A) Analysis of vacuolating activity. For VacA-containing samples, a dilution of 1:20 corresponds to a VacA concentration of approximately 15 μg/ml. An equivalent volume of sample from the *vacA*::km null mutant strain was tested as a control. Acid-activated samples were added to the medium overlying HeLa cells and vacuolating activity was quantified using a neutral red uptake assay. Results represent the mean ± S.D. from triplicate samples. (B) Analysis of depolarization. AZ-521 cells were loaded with oxonol VI (a probe used to monitor membrane potential). After the addition of acid-activated VacA proteins (10 μg/ml) or a control preparation (*vacA*::km), changes in fluorescence were monitored. WT VacA induced membrane depolarization, whereas VacA Δ346-347 and the control *vacA*::km preparation did not. RFU, relative fluorescence units. Results are representative of four experiments.

Oligomerization of VacA Δ346-347

VacA 88 kDa monomers produced by *H. pylori* are known to assemble into large water-soluble flower-shaped structures (11). Assembly of VacA monomers into oligomeric structures is likely to be required for membrane channel formation and membrane depolarization. To test whether VacA Δ346-347 formed oligomers similar to those formed by wild-type VacA, we initially used gel filtration followed by analysis of fractions by immunoblotting using anti-VacA serum. Consistent with previous studies (11, 23), wild-type VacA was detected in fractions corresponding to a molecular mass of about 1000 kDa. When VacA Δ346-347 was analyzed in the same manner, only trace amounts of VacA Δ346-347 were detected in these high molecular mass fractions (data not shown). Trace amounts of VacA Δ346-347 were detected in a broad range of lower molecular mass fractions, without evidence of a well-defined peak. The gel filtration elution properties of VacA Δ346-347 are similar to those reported for a mutant VacA protein containing a deletion of the p33 domain (90) and similar to several mutant VacA proteins containing large deletions within the p33 domain (118). The gel filtration properties of VacA Δ346-347 differ markedly from those of several previously described inactive VacA proteins with mutations in the p33 domain, which formed large oligomeric structures similar to wild-type VacA (68, 69, 118).

We next used gel electrophoresis methods to analyze the oligomeric state of VacA Δ346-347. Efforts to detect wild-type VacA oligomers using native gel electrophoresis were unsuccessful, because VacA did not enter the gel. Therefore, we analyzed the wild-type and mutant VacA proteins using blue native gel electrophoresis (BN-PAGE), as described in Methods. Wild-type VacA was detected as a complex substantially larger than 775 kDa (Figure III-3A, top panel). In this analysis, the molecular mass of VacA Δ346-347 was

substantially lower than that of wild-type VacA (Figure III-3A, bottom panel). VacA Δ346-347 appeared as a horizontal streak instead of a well-circumscribed spot, which suggested that this proteinaceous spot may be comprised of a heterogeneous mixture of oligomeric structures.

As another approach to compare the oligomeric state of VacA Δ346-347 and wild-type VacA, we used a modification of the SDS-PAGE procedure in which samples were suspended in loading buffer containing SDS, and then either boiled or not boiled prior to electrophoresis. As expected, both wild-type VacA and VacA Δ346-347 yielded 88 kDa bands if the proteins were boiled prior to SDS-PAGE (Figure III-3B). In the absence of boiling, wild-type VacA was detected as both a high molecular mass complex (>250 kDa) and an 88 kDa band (Figure III-3B). When unboiled VacA Δ346-347 was analyzed in the same manner, the high molecular mass complex was not detected, but a smaller complex was detected (Figure III-3B). This modified SDS-PAGE assay does not permit an accurate determination of the molecular mass of non-denatured proteins or protein complexes, based on comparison with molecular mass markers. However, the results suggest that VacA Δ346-347 can form a complex with a mass larger than that of the 88 kDa VacA monomer, but smaller than that of wild-type VacA oligomers. Collectively, the gel filtration results, BN-PAGE experiments, and modified SDS-PAGE results all suggest that VacA Δ346-347 and wild-type VacA differ in the ability to assemble into large oligomeric complexes. In addition, it is possible that complexes formed by VacA Δ346-347 are less stable in the presence of detergent than are the complexes formed by wild-type VacA.

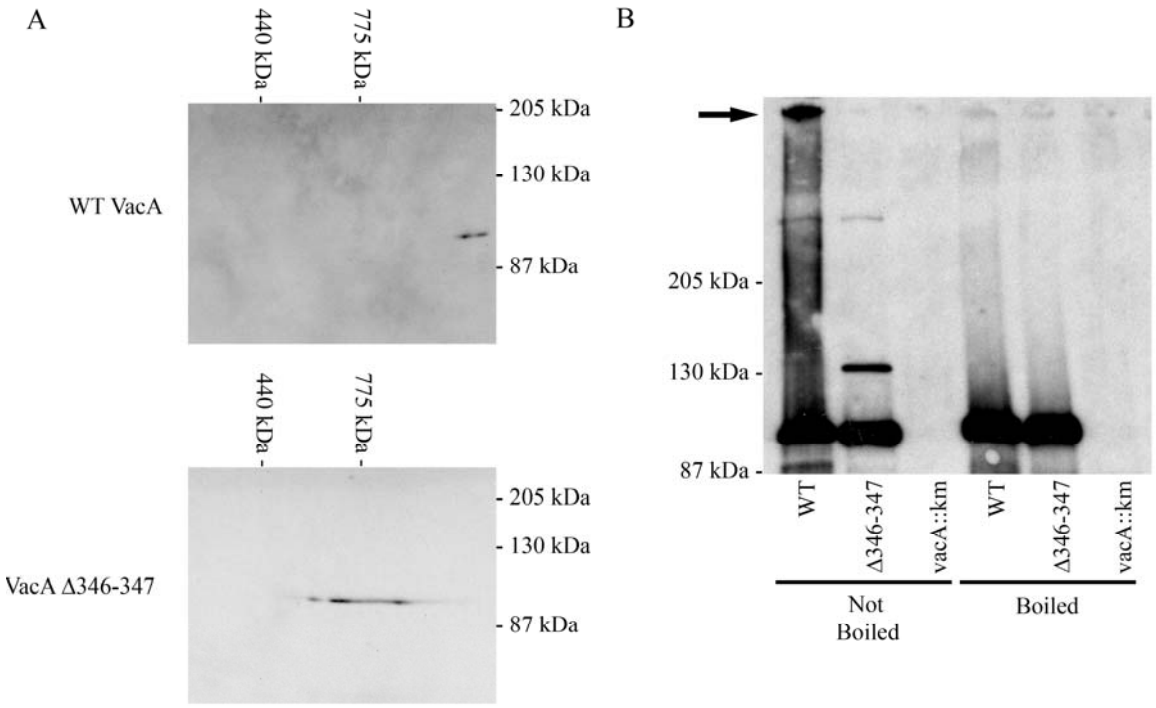

Figure III-3. Analysis of oligomer formation by wild-type VacA and VacA Δ346-347. (A) BN-PAGE. WT VacA (top panel) and VacA Δ346-347 (bottom panel) were purified and then analyzed by BN-PAGE, followed by immunoblotting using an anti-VacA serum. (B) Analysis by modified SDS-PAGE. VacA was precipitated from *H. pylori* broth culture supernatants with ammonium sulfate and VacA protein concentrations were normalized based on immunoblot analysis. Equivalent amounts of precipitated proteins were suspended in an SDS-containing buffer. One set of preparations (lanes 1-3, left) was not boiled, and a duplicate set of preparations (lanes 4-6, right) was boiled prior to SDS-PAGE. Samples were run on a 6% SDS gel followed by immunoblotting with an anti-VacA serum. The arrow indicates a large oligomeric VacA complex.

Interaction between p33 and p55 Δ346-347

When *E. coli* extracts containing VacA p33 and p55 fragments are mixed and added to HeLa cells, extensive cell vacuolation is seen, whereas when added to cells individually, the p33 and p55 proteins do not induce cell vacuolation (112). To further investigate the effect of the Δ346-347 mutation on VacA activity and oligomerization, we expressed an isolated p55 VacA fragment containing the Δ346-347 mutation in *E. coli*. As expected, a mixture of p33 plus wild-type p55 proteins induced vacuolation of HeLa cells (Figure III-4A). When a mixture of p33 plus p55 Δ346-347 was added to HeLa cells, vacuolation was not detected. To determine whether p55 Δ346-347 could physically interact with p33, we performed immunoprecipitation experiments. Different combinations of epitope-tagged recombinant proteins were mixed and immunoprecipitation was performed as described in Methods. As shown in Figure III-4B, p33 and p55 Δ346-347 interacted in solution, similar to the interaction of p33 with wild-type p55. The inclusion of two negative controls excluded non-specific interactions between p55 and the antibody or beads (Figure III-4B). These data indicate that the Δ346-347 mutation does not abrogate interactions between the p33 and p55 VacA domains.

Interactions of p33 and p55 domains with full-length 88 kDa VacA

We have previously shown that a mixture of p33 and p55 VacA fragments can physically interact with wild-type full-length VacA (112, 114). Therefore, we next investigated whether a mixture of p33 and p55 Δ346-347 could interact with 88 kDa VacA. For these experiments, we used a c-Myc-tagged 88 kDa VacA protein (Myc-VacA) purified from *H. pylori* culture supernatant and recombinantly expressed p33 and p55 Δ346-347.

After mixing Myc-VacA with p33 and p55 fragments, proteins were immunoprecipitated with an anti-c-Myc antibody. As expected, when the wild-type p33-p55 mixture was incubated with 88 kDa Myc-VacA, all three proteins were immunoprecipitated (Figure III-4C). Similarly, when the p33-p55 Δ346-347 mixture was incubated with 88 kDa Myc-VacA, both fragments interacted with full-length VacA (Figure III-4C).

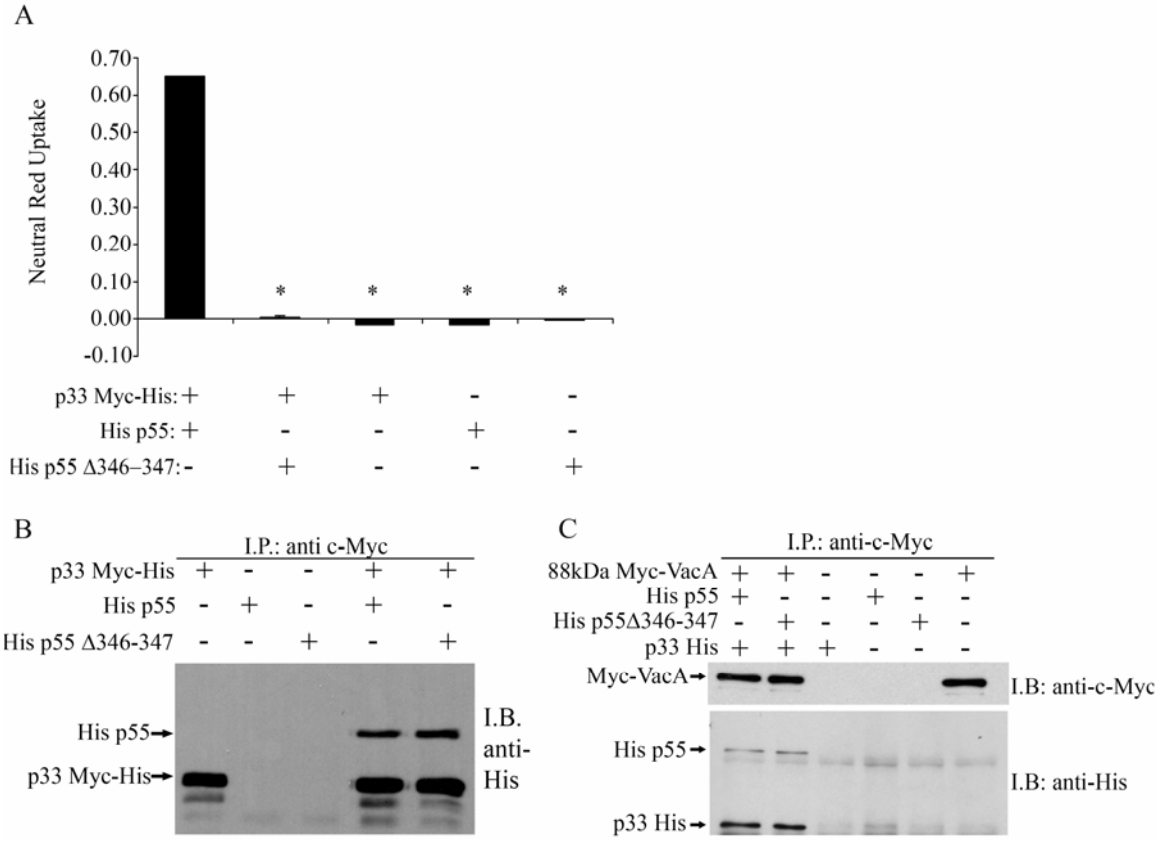

Figure III-4. Analysis of recombinant p33, p55, and p55 Δ346-347 VacA domains. (A) Vacuolating toxin activity. *E. coli* soluble extracts containing the indicated recombinant VacA proteins were normalized and added to HeLa cells as described in Methods. Vacuolating activity was quantified using a neutral red uptake assay. Results represent the mean ± S.D. from triplicate samples. * $p \leq 0.05$ as determined using ANOVA followed by Dunnett's post hoc test as compared to p33 Myc-His combined with His p55. (B) Interaction of p55 Δ346-347 with p33. *E. coli* soluble extracts containing normalized concentrations of p33 Myc-His, His p55, or His p55 Δ346-347 were mixed and proteins were immunoprecipitated (I.P.) with an anti-c-Myc antibody. Immunoprecipitated proteins were electrophoresed on a 10% SDS-polyacrylamide gel, transferred to a nitrocellulose membrane, and immunoblotted (I.B.) with an anti-His antibody. (C) Interaction of p33-p55 Δ346-347 with 88 kDa VacA. *E. coli* extracts containing normalized concentrations of p33 His, His p55, and His p55 Δ346-347 were mixed with acid-activated c-Myc-tagged 88 kDa VacA protein (Myc-VacA). Proteins were immunoprecipitated with an anti-c-Myc antibody and then were immunoblotted with an anti-c-Myc antibody (top panel) or an anti-His antibody (bottom panel).

Inhibition of wild-type VacA cytotoxic activity by VacA Δ346-347

Certain inactive mutant forms of VacA can act as dominant negative inhibitors of wild-type VacA activity (35, 66, 114, 118). Previous studies have suggested that the dominant-negative activity of mutant VacA proteins requires protein-protein interactions between wild-type VacA and the mutant proteins (35, 66, 114, 118). The observation that VacA Δ346-347 can form mixed oligomeric complexes suggested that this mutant toxin might be capable of acting in a dominant negative manner. Therefore, we next investigated whether VacA Δ346-347 could inhibit wild-type VacA activity. As a control, we tested another mutant toxin (VacA Δ6-27) previously shown to act as a dominant negative inhibitor (35, 66, 114, 118). Wild-type VacA and mutant toxins (VacA Δ346-347 or VacA Δ6-27) were mixed together and then the mixtures were added to HeLa cells. As shown in Figure III-5, VacA Δ346-347 inhibited the cell-vacuolating activity of wild-type VacA, even when the concentration of VacA Δ346-347 was lower than that of wild-type VacA. These results indicate that VacA Δ346-347 acts as a dominant-negative inhibitor of wild-type VacA activity.

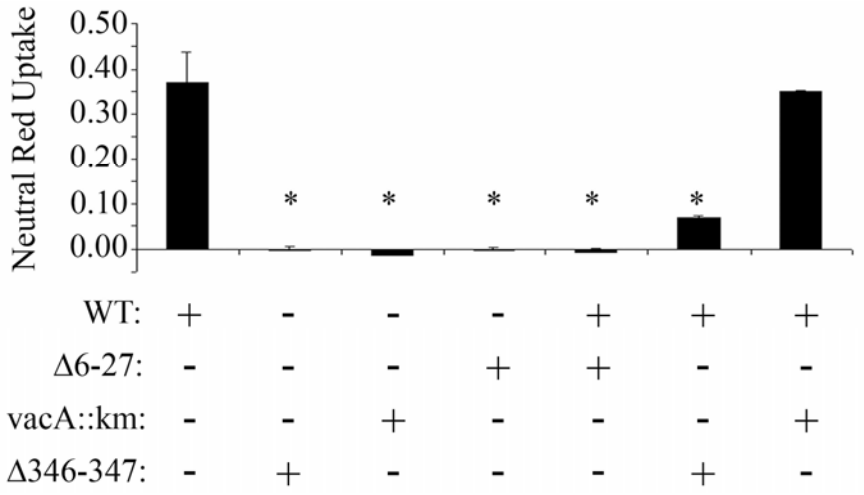

Figure III-5. Inhibition of wild-type VacA cytotoxic activity by VacA Δ346-347. Preparations of acid-activated wild-type VacA (WT; 15 μg/ml) were incubated with 15 μg/ml acid-activated VacA Δ6-27, 8 μg/ml acid-activated VacA Δ346-347, or an equivalent volume of an acidified preparation from a *vacA* null mutant strain (*vacA*::km) as described in Methods, and the mixtures were then added to the medium overlying HeLa cells for 1 hour at 37°C. Toxins were removed and fresh medium containing 5 mM ammonium chloride was added to HeLa cells for 5 hours at 37°C. Vacuolating activity was quantified using a neutral red uptake assay. Results represent the mean ± S.D. from triplicate samples. * $p \leq 0.05$ as determined using ANOVA followed by Dunnett's post hoc test as compared to WT.

Mutational analysis of residues 346 and 347

To undertake a more detailed mutational analysis, we expressed VacA Δ346-347 using a system that allows expression of a functional 88 kDa cytotoxic form of VacA in *E. coli* (67). It has not been possible to purify well-defined dodecameric structures when VacA is expressed in *E. coli* (M. S. McClain and T. L. Cover, unpublished results), but this system nevertheless permits analysis of vacuolating toxic activity (67). Soluble *E. coli* extracts containing VacA Δ346-347 or wild-type VacA were generated as described in Methods. Both recombinant proteins were successfully expressed based on immunoblotting analysis (data not shown). As expected, when extracts containing wild-type VacA were added to cells, extensive cell vacuolation was detected. In contrast, when *E. coli* extracts containing VacA Δ346-347 were added to HeLa cells, no vacuolation was detected (Figure III-6). To further investigate the role of VacA amino acids 346 (aspartic acid) and 347 (glycine) in VacA activity, we introduced several additional mutations into these sites. *E. coli* soluble extracts containing the mutant proteins were added to HeLa cells and vacuolating activity was measured by neutral red uptake. A mutant protein containing a deletion of amino acid 346 caused cell vacuolation similar to that caused by wild-type VacA (Figure III-6). In contrast, when amino acid 347 was deleted, vacuolating activity was not detected (Figure III-6).

The introduction of specific pairs of substitution mutations at position 346 and 347 (D346L/G347R or D346R/G347R) abrogated VacA activity (Figure III-6). In contrast, other pairs of substitution mutations at these positions (D346L/G347V or D346E/G347V) did not abrogate VacA activity. Introduction of the G347R mutation alone (without any change at position 346) resulted in a partial loss of VacA activity. Thus, the loss of activity resulting

from the Δ346-347 mutation was recapitulated by deletion of a single residue (amino acid 347) or by specific pairs of substitution mutations.

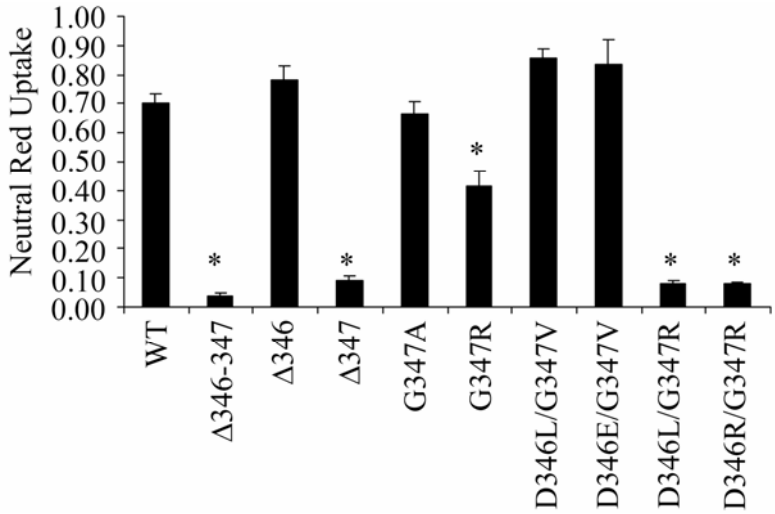

Figure III-6. Mutational analysis of VacA residues 346 and 347. Full-length WT VacA and a panel of VacA proteins containing mutations in residues 346 and/or 347 were expressed in *E. coli*. *E. coli* soluble extracts containing the indicated recombinant proteins were normalized based on immunoblotting so that they contained equivalent concentrations of VacA, and were then added to the medium overlying HeLa cells. Vacuolating activity was quantified using a neutral red uptake assay. Results represent the mean ± S.D. from triplicate samples. * $p \leq 0.05$ as determined using ANOVA followed by Dunnett's post hoc test as compared to WT VacA.

Discussion

In this study, we sought to elucidate properties of VacA that are conferred by an amino-terminal p55 subdomain that is required for vacuolating activity when VacA is intracellularly expressed in transiently transfected cells, but has not been found to be required for binding as have other regions of the p55 domain. A recent analysis of the p55 VacA crystal structure (residues 355 to 811) showed that a substantial portion of the p55 domain comprises a beta-helical fold (29). The crystal structure reveals that the amino-terminal portion of p55 is spatially separated from carboxy-terminal portions of p55, which is consistent with the concept of an amino-terminal subdomain. The analysis in the current study focused on alterations in VacA that result from a small deletion mutation (Δ346-347, corresponding to the deletion of contiguous aspartic acid and glycine residues, respectively). High resolution structural data are not available for the portion of VacA comprising residues 346 and 347 (29), but the presence of adjacent glycine and proline residues at positions 347 and 348, respectively, suggests that this segment will represent part of a loop or turn.

As described in this study, VacA Δ346-347 lacked vacuolating activity when added to the surface of cells, and in contrast to wild-type VacA, VacA Δ346-347 did not cause cell depolarization. The failure of this mutant toxin to induce cell depolarization suggests that it is unable to form membrane channels (69, 105). Multiple biochemical analyses provided evidence that the Δ346-347 mutation disrupts or weakens intermolecular VacA interactions. Defective VacA intermolecular interactions could result in impaired assembly or impaired stability of oligomeric complexes required for membrane channel activity, or could result in an impaired ability of oligomers to undergo a conformational transition necessary for channel formation.

Thus far, very little is known about which amino acid sequences in VacA contribute to protein-protein interactions and oligomerization. Prior to the current study, the smallest mutation known to disrupt VacA oligomerization was a deletion of residues 49-57, located within the p33 domain (35). The current data indicate that residues 346-347 (located within the p55 domain) contribute to VacA oligomerization. Thus, amino acid sequences in both the p33 domain and the p55 domain are required for assembly of VacA into large oligomeric structures. This conclusion is consistent with a model for VacA oligomerization that is based on docking of the p55 crystal structure into a 19 angstrom cryo-EM map of a VacA dodecamer (29) (Figure III-7).

The Δ346-347 mutation could potentially interfere with VacA oligomerization by disrupting p33-55 interactions. It is also theoretically possible that the Δ346-347 mutation may disrupt p55-p55 interactions; however, at present there is not convincing evidence indicating that p55-p55 interactions are required for VacA oligomer formation, and interactions between isolated p55 fragments have not been readily detectable by immunoprecipitation or yeast two-hybrid methods (112, 113). Immunoprecipitation experiments indicated that p55 Δ346-347 can interact in solution with p33 (Figure III-4B), and a mixture of p33 plus p55 Δ346-347 can interact with full-length VacA (Figure III-4C). Thus, the Δ346-347 mutation does not completely abrogate p33-p55 interactions. Our model predicts that the assembly of VacA proteins into large oligomeric structures requires multiple types of p33-p55 interactions, including interaction of a single p55 domain with p33 domains from one or two adjacent molecules (intermolecular interactions) as well as an interaction with p33 from the same molecule (intramolecular interaction) (Figure III-7). These multiple types of p33-p55 interactions presumably are mediated by multiple different contact points

on the surface of p55 (FigureIII-7). Based on this model, the Δ346-347 mutation could interfere with VacA oligomerization, despite failure of this mutation to completely abrogate p33-p55 interactions.

An interesting property of VacA Δ346-347 is its ability to inhibit the activity of wild-type toxin in a dominant-negative manner (Figure III-5). Several dominant negative mutant forms of VacA have been described in previous studies (35, 66, 114, 118), and at least one of these mutants (VacA Δ6-27) is able to block membrane channel formation by wild-type VacA (118). It has been hypothesized that the inhibitory activity of these mutants is dependent on their ability to physically interact with wild-type VacA, thereby forming mixed oligomeric complexes that are defective in functional activity (66, 118). Similarly, the dominant negative phenotype of several *Bacillus anthracis* protective antigen mutants is also due to the formation of mixed oligomeric complexes containing wild-type and mutant proteins (97, 99). In contrast to two previously described dominant negative mutant proteins (VacA Δ6-27 and VacA s2/m1) (66, 118), the mutant protein described in the current study (VacA Δ346-347) failed to assemble into large oligomeric structures. Similarly, a recent study reported that another mutant protein, VacA Δ49-57, failed to cause cell vacuolation and did not form large oligomeric structures, but was able to inhibit the activity of wild-type VacA in a dominant-negative manner (35). One possibility is that the mechanisms of dominant negative inhibition are different for one group of mutants (VacA Δ6-27 and VacA s2/m1) compared to the second group of mutants (VacA Δ346-347 and VacA Δ49-57). Alternatively, it is likely that the latter mutants, although defective in assembly into large oligomeric structures, are still able to physically interact with wild-type VacA. Specifically, the VacA Δ346-347 protein has a defective oligomerization site within the p55 domain, but it

has an intact p33 domain. As shown in Figure III-7, each subunit within a dodecamer makes contact with other subunits via multiple p33-p55 intermolecular interactions. Based on this model, it is predicted that VacA Δ346-347 (via its p33 domain) would be able to interact with wild-type VacA. We speculate that oligomers containing both wild-type and mutant components would be defective in the ability to undergo conformational changes required for channel formation, and therefore, would be defective in vacuolating activity.

In summary, this study provides new insights into properties of VacA that are conferred by the p55 amino-terminal subdomain. Ongoing structure-function studies of VacA should lead to a better understanding of how VacA forms membrane channels and causes alterations in human cells.

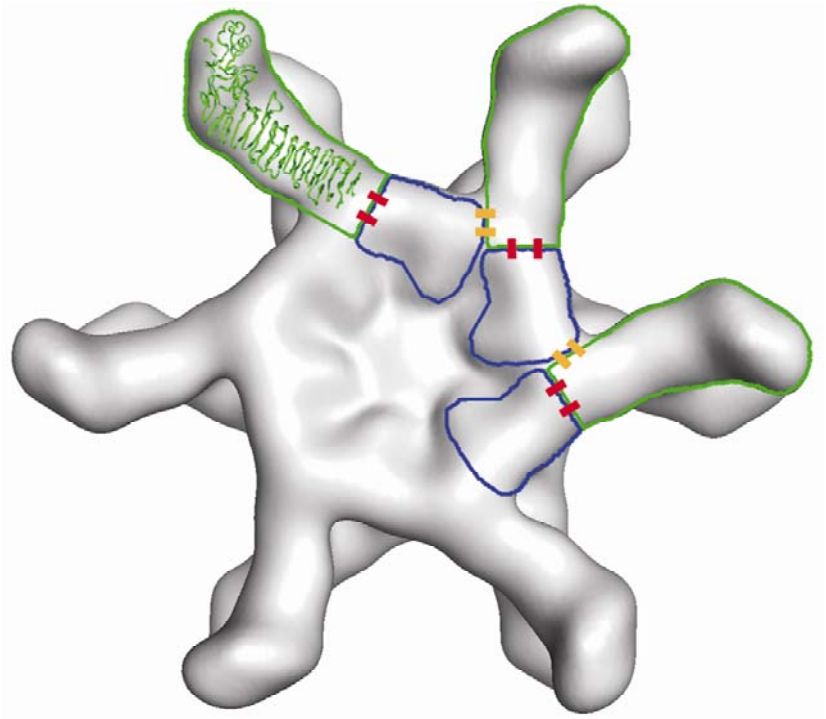

Figure III-7. Model depicting how the Δ346-347 mutation interferes with oligomerization of VacA. The model is based on docking the p55 crystal structure into a 19-Å cryo-EM map of a VacA dodecamer (23, 29). p55 subunits are outlined in green, and p33 subunits are outlined in blue. Intramolecular p33-p55 interactions are depicted as red bars, and intermolecular p33-p55 interactions are depicted as yellow bars. We predict that residues 346 to 347 are located at or near the sites of yellow bars, and thus a Δ346-347 mutation would disrupt intermolecular p33-p55 interactions.

CHAPTER IV

STRUCTURE-FUNCTION ANALYSIS OF A β-HELICAL REGION IN THE *HELICOBACTER PYLORI* VacA p55 DOMAIN

Introduction

Numerous bacterial pathogens secrete virulence factors by a type V (autotransporter) pathway (16). Crystallographic studies of three passenger domains secreted by a classical (type Va) autotransporter pathway revealed that each has a predominantly β-helical structure (24, 29, 80), and it is predicted that nearly all autotransporter passenger domains share a β-helical fold (47). Thus far, there has been relatively little progress in understanding the properties of β-helical proteins that facilitate protein secretion, and very little is known about the structural features that are responsible for the unique properties of individual autotransporter passenger domains.

VacA is synthesized as a 140 kDa precursor protein, which undergoes proteolytic processing to yield a 33-amino acid signal sequence, a mature 88 kDa secreted protein, a ~12 kDa secreted peptide, and a carboxy-terminal domain that remains associated with the bacteria (14, 95, 106). The mature 88 kDa VacA passenger domain can be proteolytically processed into an amino-terminal 33 kDa (p33) fragment and a carboxy-terminal 55 kDa (p55) fragment (76), which are considered to represent two domains or subunits of VacA (106, 112, 113) (Figure IV-1A). Recently the crystal structure of the p55 domain of a VacA protein was determined (29). The most striking feature of this domain is the presence of a right-handed parallel β-helical structure, composed of coiled, parallel β-sheet structures (Figure IV-1B). Each coil of the parallel β-helix consists of three parallel β-strands connected by loops of different lengths. Other features of the p55 structure include a small

globular domain near the carboxy-terminus that consists of mixed α/β secondary structure elements and the presence of a disulfide bond. The β-helical portion of the VacA p55 domain of *H. pylori* strain 60190 consists of about 13 coils (Figure IV-1B) (29).

In the current study, we tested the hypothesis that specific structural elements within the β-helical region of the p55 domain are essential for VacA secretion and vacuolating toxin activity. To test this hypothesis, we generated *H. pylori* mutant strains expressing VacA proteins in which individual coils of the β-helix were deleted, and we then analyzed the secretion and activity of these mutant proteins.

Methods

H. pylori strains and growth conditions. *H. pylori* wild-type strain 60190 (ATCC 49503) was the parent strain used for construction of all mutants in this study. *H. pylori* strains were grown on trypticase soy agar plates containing 5% sheep blood at 37°C in ambient air containing 5% CO_2. *H. pylori* liquid cultures were grown in sulfite-free Brucella broth containing 10% fetal bovine serum (BB-FBS). Throughout this study, we used an amino acid numbering system in which residue 1 refers to alanine 1 of the secreted 88 kDa VacA protein, and the p55 domain corresponds to amino acids 312 to 821 (GenBank accession number Q48245).

Introduction of deletion mutations into the chromosomal vacA gene of H. pylori. To introduce in-frame internal deletion mutations into a plasmid encoding VacA, we performed inverse PCR using pMM592 (encoding wild-type VacA, amino acids 1 to 821) (67) as template DNA, 5'-phosphorylated primers, and Pfu Turbo polymerase (Stratagene). The

resulting PCR products were then ligated and transformed into *E. coli* DH5α. Each plasmid was analyzed by DNA sequencing to verify that the desired deletion was present. To introduce the mutations into the *H. pylori* chromosomal *vacA* gene (66, 69, 117), *H. pylori* strains containing a *sacB*-kanamycin cassette within *vacA* (VM025, VM018, or VM028) (118) were transformed with plasmids containing *vacA* deletion mutations. Sucrose-resistant, kanamycin-sensitive transformants were selected by growth on Brucella broth plates supplemented with 10% FBS and 5.5% sucrose (118). Full-length *vacA* sequences encoding the p33 domain and the p55 domain were PCR-amplified from mutant strains, and the nucleotide sequences of PCR products were analyzed to confirm that the desired mutation had been introduced successfully into the chromosomal *vacA* gene.

Immunoblot analysis of VacA. To detect VacA expression, proteins in individual samples were separated by SDS-polyacrylamide gel electrophoresis, transferred to nitrocellulose membrane, and immunoblotted using a polyclonal rabbit anti-VacA antibody (#958) raised against the secreted 88 kDa passenger domain (96), followed by horseradish peroxidase-labeled rabbit IgG. As a control, samples were immunoblotted with rabbit antiserum to HspB (a GroEL heat shock protein homolog) purified from *H. pylori* broth culture supernatant (7). Signals were generated by the enhanced chemiluminescence reaction and detected using x-ray film.

Concentration and normalization of VacA proteins. H. pylori strains were grown in BB-FBS for 48 hours. Broth culture supernatants were concentrated 30-fold by ultrafiltration with a 30 kDa cutoff membrane. Relative concentrations of VacA in different broth culture

supernatant preparations were determined by antigen-detection ELISA (118). Broth culture supernatants were diluted in carbonate buffer (18mM Na_2CO_3, 34.8mM $NaHCO_3$) and allowed to adhere to an ELISA plate overnight at room temperature. After removal of unbound VacA proteins, wells were blocked with phosphate buffered saline (PBS) containing 3% BSA and 0.05% Tween 20. VacA was detected with rabbit anti-VacA antiserum (#958) and horseradish peroxidase-labeled rabbit IgG followed by TMB substrate (Pierce). To permit normalization of VacA concentrations in different preparations, samples were diluted with culture supernatant from a *vacA* null mutant strain.

Sonication of H. pylori. *H. pylori* grown on blood agar plates were suspended in sonication buffer [20 mM Tris-acetate (pH 7.9), 50 mM potassium acetate, 5 mM Na_2EDTA, 1 mM dithiothreitol (DTT), protease inhibitor cocktail] and sonicated on ice for three 10 second pulses. The lysate was centrifuged at 15,000 rpm and the supernatant collected.

Susceptibility of VacA to proteolysis by trypsin. *H. pylori* grown on blood agar plates were suspended in phosphate buffered saline (PBS), and bacterial suspensions were treated with trypsin (0.05%) for 30 min at 37ºC. After addition of a protease inhibitor cocktail, the bacteria were pelleted, and the pellet washed once with PBS containing protease inhibitor. The pellet was then suspended in SDS lysis buffer, boiled, and analyzed by immunoblot. Sonicated preparations of *H. pylori* were treated with trypsin and analyzed in the same manner.

Analysis of VacA reactivity with a monoclonal antibody. Normalized concentrated culture supernatants were diluted in carbonate buffer and allowed to adhere to an ELISA plate overnight at room temperature. After removal of unbound VacA proteins, wells were blocked with phosphate buffered saline (PBS) containing 3% BSA and 0.05% Tween 20. VacA was detected with mouse anti-VacA (5E4) (117) and horseradish peroxidase-labeled mouse IgG followed by TMB substrate (Pierce).

Cell culture analysis of VacA proteins. HeLa cells were grown as described previously (112). AZ-521 cells, a human gastric adenocarcinoma cell line (Culture Collection of Health Science Research Resources Bank, Japan Health Sciences Foundation) and RK13 cells (ATCC CCL-37), a rabbit kidney cell line, were grown in minimal essential medium supplemented with 10% FBS and 1 mM non-essential amino acids. For vacuolating assays, cells were seeded at 2 X 10^4 cells/well into 96-well plates 24 hours prior to each experiment. The VacA content of different samples was normalized as described above. Serial dilutions of samples were added to serum-free tissue culture medium overlying cells (supplemented with 5 mM ammonium chloride) and incubated for 5-10 hours at 37ºC. An equivalent volume of a corresponding preparation from a *vacA* null mutant was used as a negative control. After incubation, cell vacuolation was examined by inverted light microscopy and quantified by a neutral red uptake assay (13). Neutral red uptake data are presented as A_{540} values (mean ± S.D.). Background levels of neutral red uptake by cells treated with culture supernatant from a *vacA* null mutant were subtracted to yield net neutral red uptake values.

Analysis of binding of mutant VacA proteins. To analyze interactions of VacA with the surface of cells, cells were seeded into 96-well plates 24 hours prior to each experiment so as to obtain sub-confluent cells. The VacA content of different samples was normalized by western blot with an anti-VacA polyclonal antibody. HeLa, RK13, and AZ-521 cells were incubated with the *H. pylori* culture supernatants containing VacA for 1 hour at 4ºC. Cells were quickly washed three times with cold PBS, and then the cells were washed three additional times for 5 minutes each with cold PBS. Cells were lysed directly in the wells of the 96-well plate by adding SDS-containing buffer. The presence of VacA in these cell lysates was detected by immunoblotting.

Results

Expression and secretion of mutant VacA proteins by *H. pylori*

To test the hypothesis that specific β-helical elements within the VacA p55 domain are required for VacA secretion and activity, we introduced an ordered series of eight deletion mutations, each 20 to 28 amino acids in length, into a portion of the *vacA* gene that encodes the p55 domain. These deletion mutations were designed so that each would result in the deletion of a single coil of the β-helix (Figure IV-1A; representative single coils are highlighted in Figure IV-1B). By designing the deletion mutations in this manner, it was predicted that the mutant proteins would exhibit reductions in the length of the β-helical region but would exhibit minimal changes in protein folding in comparison to the wild-type protein. All of the deletion mutations analyzed in this study are located outside of the VacA region (amino acids 1-422) previously found to be required for cell vacuolation when VacA

is expressed in transiently transfected cells (133). Each of the mutations was introduced into the *H. pylori* chromosomal *vacA* gene by natural transformation and allelic exchange as described in Methods.

Each mutant *H. pylori* strain was tested by immunoblot analysis for the capacity to express VacA. We first analyzed expression of the mutant strains grown on blood agar plates. Each mutant strain expressed a VacA protein with a mass of ~85 kDa (corresponding to the VacA passenger domain), which indicated that in each case, the ~140 kDa VacA protoxin underwent proteolytic processing similar to wild-type VacA (data not shown). We next analyzed expression and secretion of VacA when the bacteria were grown in broth culture. Immunoblot analysis of the bacterial cell pellets indicated that, as expected, each of the mutants strains expressed an ~85 kDa protein (Figure IV-2A), but in comparison to wild-type VacA, several of the mutant forms of VacA were expressed at lower levels (Figure IV-2A and B). Immunoblot analysis of the broth culture supernatants indicated that each of the mutant strains secreted or released an ~85 kDa VacA protein. In comparison to secretion of VacA by the wild-type strain, several of the mutant VacA proteins were secreted at moderately reduced levels, and three mutant proteins (VacA Δ559-579, Δ580-607, and Δ608-628) were nearly undetectable in culture supernatant (Figure IV-2C and D). Analysis of the culture supernatants by ELISA yielded similar results (data not shown).

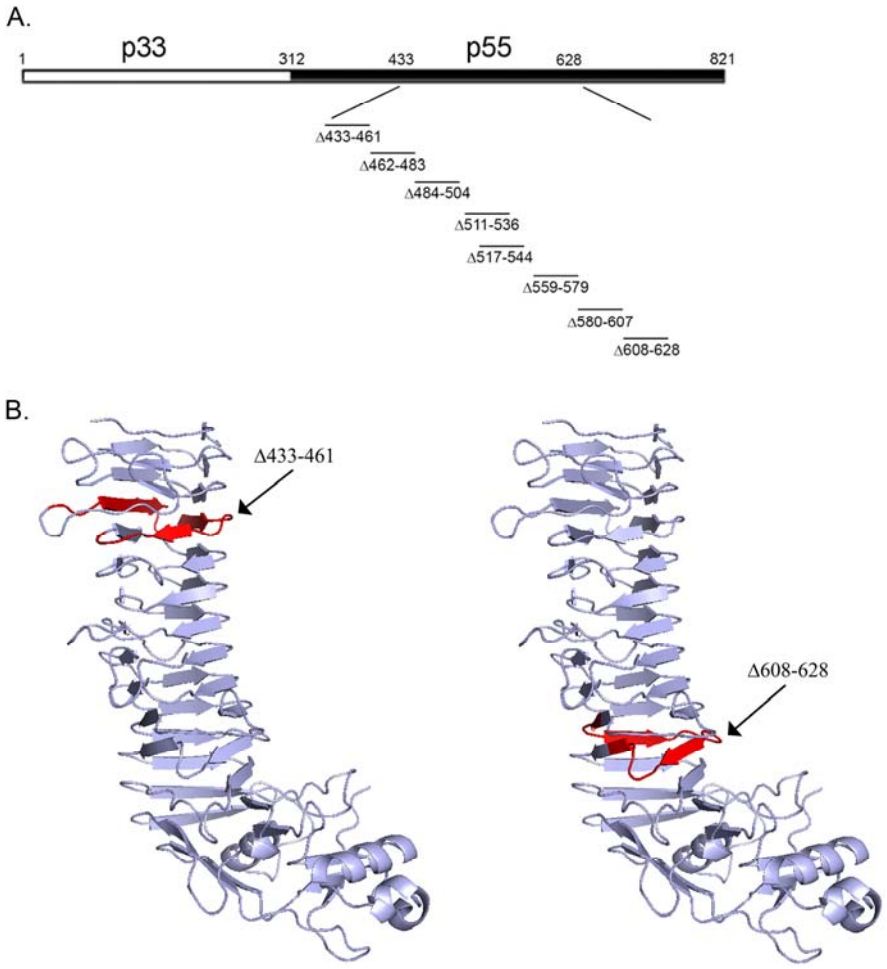

Figure IV-1. Introduction of deletion mutations into the VacA p55 domain. (A) Diagram of the full-length 88 kDa VacA protein secreted by *H. pylori* strain 60190 (14). p33 (amino acids 1 to 311) and p55 (amino acids 312-821) domains are shown. Mutations encoding single coil deletions within the β-helix of the p55 domain were introduced into the *H. pylori* chromosomal *vacA* gene by natural transformation and allelic exchange as described in Methods. The relative position of each single coil deletion is shown. (B) Crystal structure of the p55 VacA domain of *H. pylori* strain 60190 (29). The most amino-terminal deletion (amino acids 433-461) and the most carboxy-terminal deletion (amino acids 608-628) are highlighted in red.

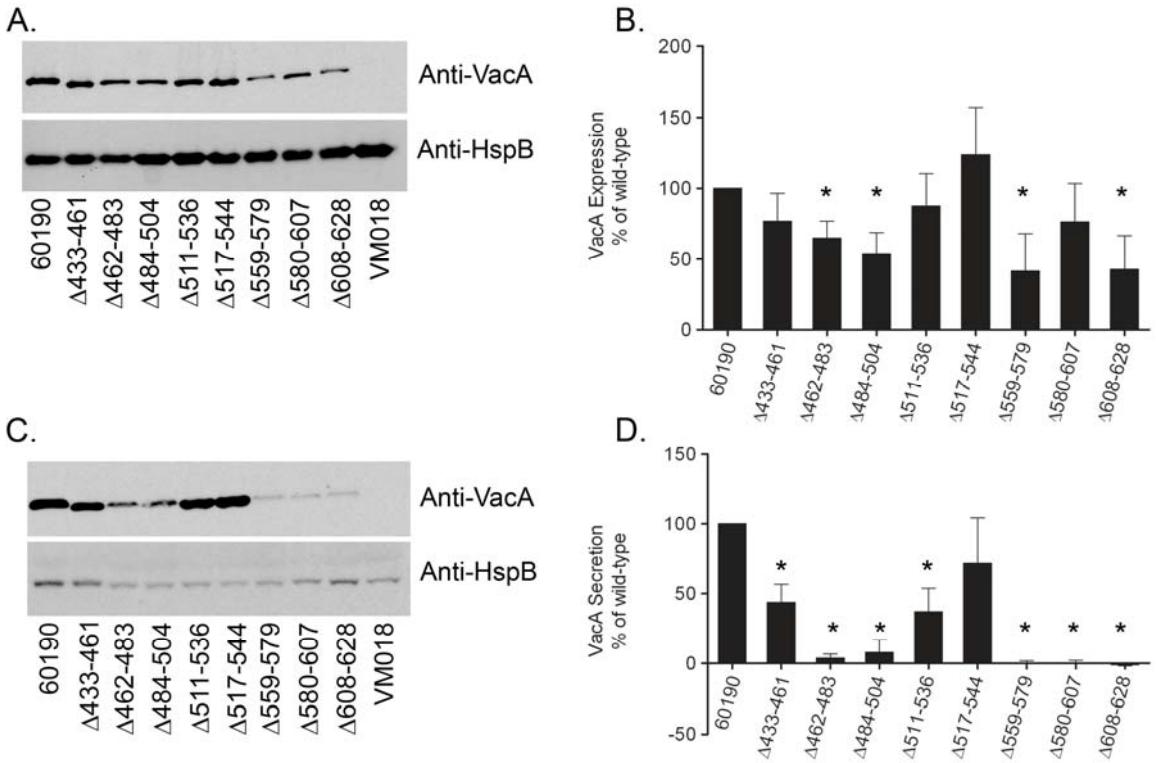

Figure IV-2. Expression and secretion of wild-type and mutant VacA proteins. *H. pylori* wild- type and mutant strains were grown in broth culture. Broth cultures were normalized by optical density (OD 600nm) and then pellets (A) and unconcentrated broth culture supernatants (C) were analyzed by immunoblot assay using polyclonal anti-VacA serum #958. Samples were also immunoblotted with a control antiserum against *H. pylori* heat shock protein (HspB). The intensity of immunoreactive VacA bands was quantified by densitometry (panels B and D). Wild-type VacA and each of the mutant proteins were expressed and proteolytically processed to yield ~85-88 kDa proteins that were secreted into the broth culture supernatant. VM018 is an *H. pylori* strain with a *vacA* null mutation (118). Western blots are representative of three independent experiments; histograms are based on data from three independent experiments. *, $p<0.05$ compared to wild-type VacA, as determined by Student's t-test.

Susceptibility of VacA mutant proteins to proteolytic cleavage by trypsin

Previous studies have shown that the wild-type 88 kDa VacA passenger domain is secreted into the extracellular space and that 88 kDa proteins also remain localized on the surface of *H. pylori* (41). To investigate whether the mutant VacA proteins were localized on the bacterial surface similar to wild-type VacA, the wild-type and mutant *H. pylori* strains were harvested from blood agar plates and treated with trypsin as described in Methods. Wild-type VacA and each of the ~85 kDa mutant proteins were cleaved by trypsin, resulting in several different patterns of proteolytic degradation products (Figure IV-3A). Degradation of each of the ~85 kDa VacA mutant proteins by trypsin provided evidence that each mutant protein was localized on the surface of the bacteria (Figure IV-3A).

The observed variation in the proteolytic digest patterns (Figure IV-3A) could be attributable to differences in the orientation of VacA mutant proteins on the bacterial cell surface in relation to the outer membrane, or alternatively, VacA mutant proteins might differ in susceptibility to proteolytic cleavage. To test the hypothesis that VacA mutant proteins varied in susceptibility to proteolytic cleavage, lysates of *H. pylori* strains were generated by sonication, and the solubilized proteins were treated with trypsin as described in Methods. Trypsin digestion of two of the mutant proteins (Δ511-536 and Δ517-544) yielded proteolytic digest patterns that were identical to each other and similar to that of trypsin-digested wild-type VacA (Figure IV-3B). Trypsin digestion of two other mutant proteins (Δ433-461 and Δ484-504) yielded different digest patterns, but these mutant proteins were not completely degraded (Figure IV-3B). Four mutant proteins (Δ462-483, Δ559-579, Δ580-607, and Δ608-628) were completely degraded by trypsin (Figure IV-3B). In general, the four mutant proteins that exhibited relative resistance to trypsin digestion were secreted at relatively high

levels compared to mutant proteins that were completely degraded by trypsin (compare Figure IV-2 and Figure IV-3). The observed differences among mutant VacA proteins in susceptibility to trypsin-mediated proteolysis suggested that there were differences in the folding of the individual mutant proteins.

To test whether the four mutant proteins exhibiting relative resistance to trypsin-mediated proteolysis (i.e. VacA Δ433-461, Δ484-504, Δ511-536, and Δ517-544) shared common properties with wild-type VacA, we analyzed the reactivity of these proteins with an anti-VacA monoclonal antibody (5E4) that recognizes a conformational epitope (117). Each of the four mutant VacA proteins was recognized by the 5E4 antibody (Figure IV-4), which provided additional evidence that these mutant proteins were folded in a manner similar to that of wild-type VacA.

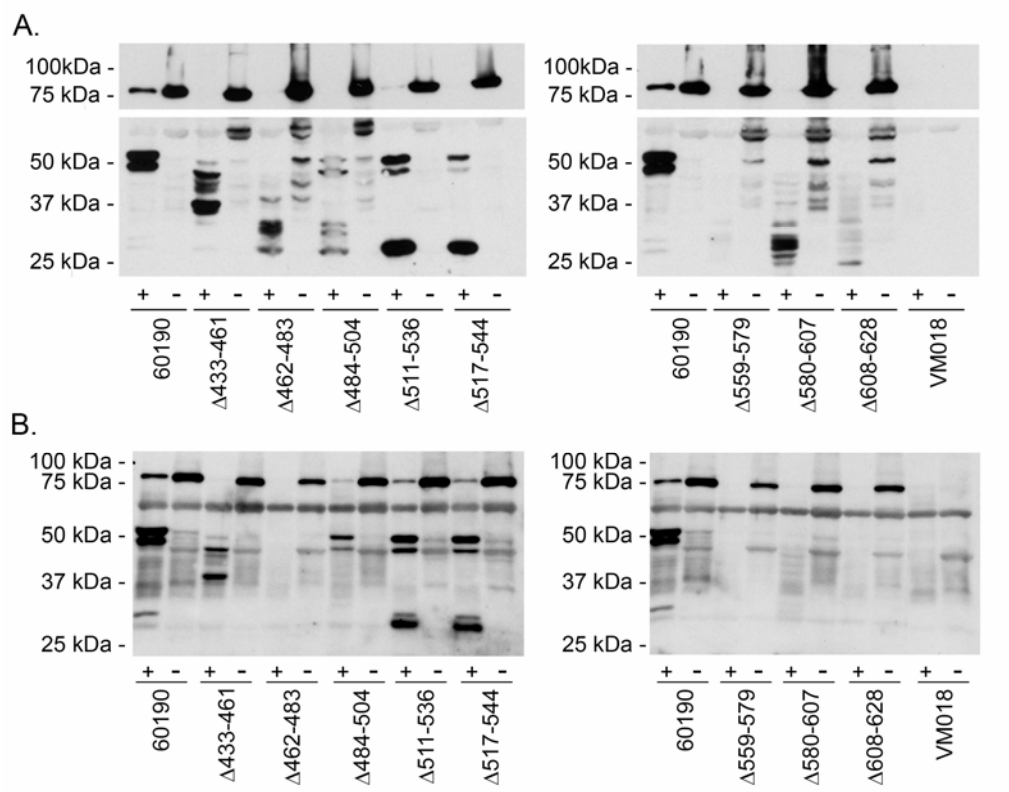

Figure IV-3. Susceptibility of VacA proteins to proteolytic cleavage by trypsin. (A) Intact *H. pylori* strains expressing wild-type or mutant VacA proteins were suspended in PBS and incubated in the presence (+) or absence (-) of trypsin as described in Methods. After centrifugation, bacterial pellets were analyzed by immunoblot analysis using polyclonal anti-VacA serum #958. A short immunoblot exposure is shown for analysis of the full-length VacA bands (85-88 kDa), whereas a longer exposure is shown for analysis of proteolytic digest products. (B) *H. pylori* strains expressing wild-type or mutant VacA proteins were sonicated as described in Methods. After centrifugation, the soluble portion was analyzed further. The total protein concentration of each sample was approximately 7.5 μg/ml, as determined by A_{280} values (data not shown). Samples were incubated in the presence (+) or absence (-) of trypsin and analyzed by immunoblot analysis using polyclonal anti-VacA serum #958.

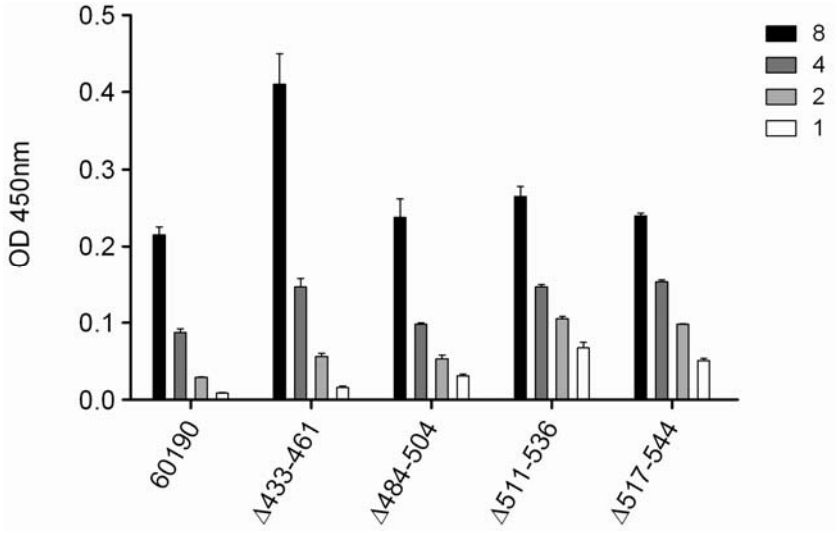

Figure IV-4. Reactivity of VacA mutant proteins with a monoclonal anti-VacA antibody. *H. pylori* strains expressing wild-type or mutant VacA proteins were grown in broth culture and secreted VacA proteins were normalized as described in Methods. Wells of ELISA plates were coated with broth culture supernatants, and reactivity of the proteins with an anti-VacA monoclonal antibody (5E4) that recognizes a conformational epitope was determined by ELISA. Reactivity of a *vacA* null mutant was subtracted as background. Relative VacA concentrations are indicated. Values represent the mean ± SD from triplicate samples.

Analysis of vacuolating activity of mutant VacA proteins

We next investigated whether the mutant VacA proteins retained vacuolating toxin activity. We focused these studies on the four mutant proteins that were secreted at the highest levels and that exhibited evidence of protein folding similar to that of wild-type VacA (i.e. VacA Δ433-461, Δ484-504, Δ511-536, and Δ517-544). Analysis of the vacuolating toxin activity of the remaining VacA mutant proteins was not possible due to prohibitively low concentrations of the secreted mutant proteins and inability to normalize the concentrations of these proteins. *H. pylori* culture supernatants containing wild-type VacA and the four mutant proteins of interest were normalized by ELISA so that the VacA concentrations were similar, as described in Methods. The mutant proteins were initially tested for their ability to induce vacuolation of HeLa cells. Each of the mutant proteins (VacA Δ433-461, Δ484-504, Δ511-536, and Δ517-544) induced vacuolation of HeLa cells (Figure IV-5A), but one of the mutants, VacA Δ433-461, exhibited reduced vacuolating activity compared to wild-type VacA. At the highest concentration of toxin added to cells, the reduction in activity observed for the VacA Δ433-461 mutant protein compared to wild-type VacA was approximately 30%. The same preparations of mutant proteins were then tested for their ability to induce vacuolation of AZ-521 cells (human gastric epithelial cells) and RK13 cells (rabbit kidney cells), two cells lines that have been used commonly for analysis of VacA activity (45, 82, 121). VacA Δ484-504, Δ511-536, and Δ517-544 each caused vacuolation of RK13 and AZ-521 cells, but VacA Δ433-461 lacked detectable vacuolating activity for both RK13 and AZ-521 cells (Figure IV-5B and C). Thus, in contrast to wild-type VacA and the other mutant VacA proteins tested in this analysis, VacA

Δ433-461 caused reduced vacuolation of HeLa cells and did not cause detectable vacuolation of RK13 or AZ-521 cells.

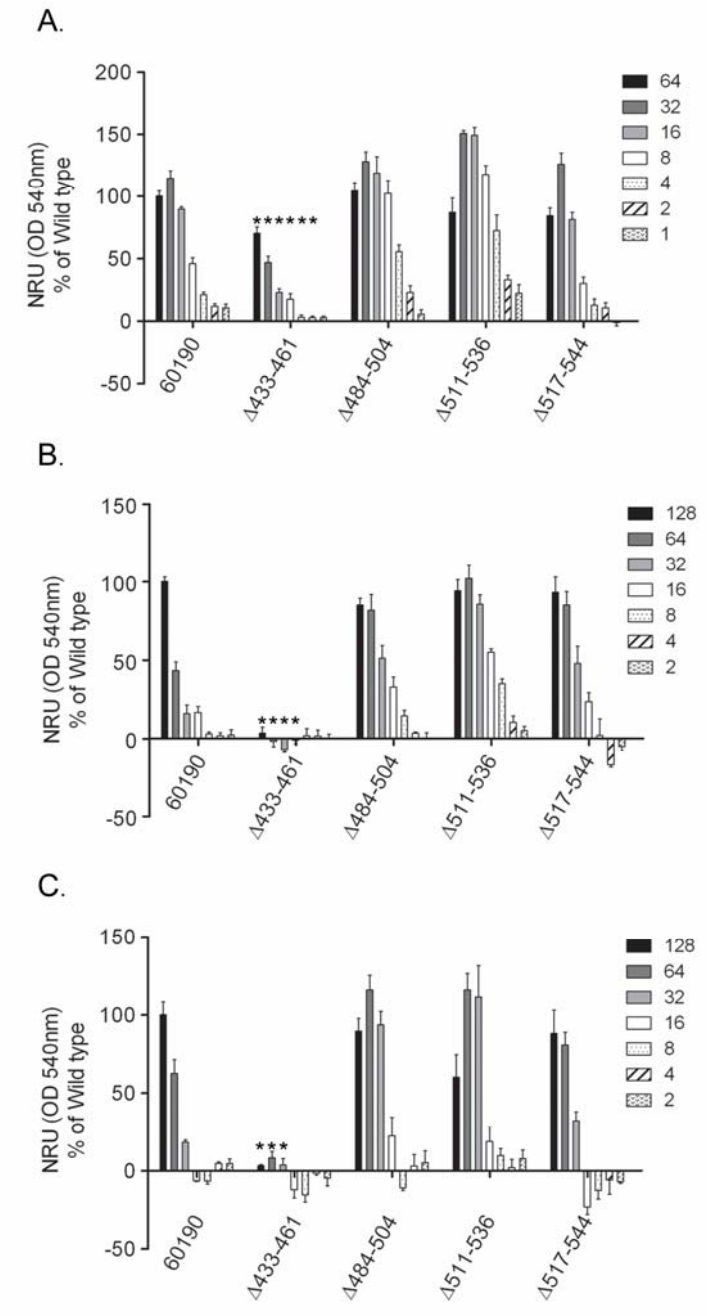

Figure IV-5. Vacuolating cytotoxic activity of mutant proteins. *H. pylori* strains expressing wild- type or mutant VacA proteins were grown in broth culture and secreted VacA proteins were normalized as described in Methods. Serial two-fold dilutions of VacA-containing preparations were added to HeLa cells (A), RK13 cells (B), and AZ-521 cells (C). Vacuolating activity was measured by neutral red uptake. Relative VacA concentrations are indicated. Results represent the mean ± SD from triplicate samples, expressed as a percent of neutral red uptake induced by wild-type VacA. *, $p \leq 0.02$ as determined by Student's t-test compared to wild type VacA. Similar results were observed in three independent experiments.

Analysis of binding of VacA Δ433-461

We hypothesized that the lack of vacuolating activity of VacA Δ433-461 on RK13 and AZ-521 cells might be due the inability of the mutant to bind to these cell types. Therefore, we next investigated the binding of VacA Δ433-461 to HeLa , RK13, and AZ-521 cells. Because the other mutants tested for vacuolating activity were similar in activity to wild-type VacA, we focused the binding studies only on VacA Δ433-461. *H. pylori* culture supernatants containing wild-type VacA and the mutant protein of interest were first normalized by western blot so that the VacA concentrations were similar. VacA Δ433-461 was able to bind to all three cell types at levels similar to wild-type VacA (Figure IV-6), suggesting that this mutant toxin does not exhibit a defect in binding. Interestingly, the total level of binding of wild-type VacA and VacA Δ433-461 is reduced in AZ-521 cells compared to HeLa and RK13 cells (Figure IV-6). When vacuolating assays were performed with the wild-type and mutant toxins, AZ-521 cells were more sensitive to the toxin (i.e. required more-diluted toxins and shorter incubation with the toxin) compared to HeLa cells. When AZ-521 cells were incubated with toxins for eight hours (the normal incubation time for toxin with HeLa cells before doing neutral red uptake), AZ-521 cells were rounded up and did not appear healthy compared to HeLa cells. This increased sensitivity makes the observation of reduced total binding to AZ-521 cells interesting.

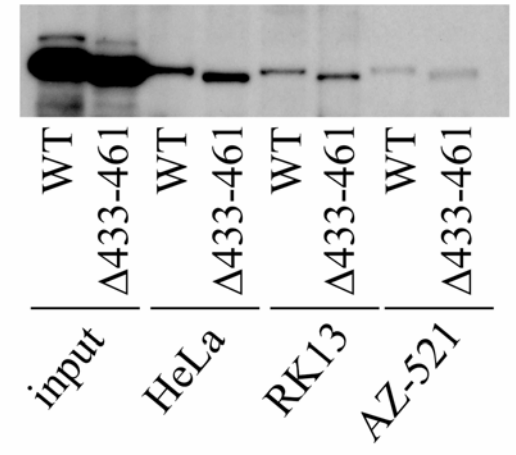

Figure IV-6. Binding of VacA Δ433-461. *H. pylori* strains expressing wild- type or mutant VacA proteins were grown in broth culture and secreted VacA proteins were normalized as described in Methods (*input*). Normalized VacA-containing preparations were added to HeLa, RK13, and AZ-521 cells for 1 hour at 4ºC. The capacity of VacA to interact with cell membranes was assessed by immunoblot analysis using an anti-VacA polyclonal antibody.

Discussion

In this study, we sought to identify regions of the p55 β-helix that are essential for VacA secretion and vacuolating toxin activity. All of the VacA mutant proteins analyzed in this study were designed in a manner that resulted in the deletion of a single coil of the β-helix, based on analysis of the crystal structure of the VacA p55 domain (29). We predicted that all of the mutant VacA proteins would retain a β-helical structure, and that this mutagenesis approach would result in minimal disruptions in protein folding. We found that several individual coils within the p55 domain could be deleted without substantially altering the capacity of the proteins to undergo proteolytic processing and secretion by *H. pylori*. In contrast, we found that the deletion of other coils led to a marked defect in VacA secretion. In addition to the mutant VacA proteins shown in Figure IV-1, we also generated several *H. pylori* mutant strains expressing VacA proteins in which two coils (Δ433-483) or four coils (Δ433-529) of the β-helix were deleted. These mutant strains expressed truncated VacA proteins of the expected size (approximately 82 and 77 kDa, respectively) at levels similar to wild-type VacA, but these mutant proteins were poorly secreted (data not shown). These findings suggest that VacA proteins containing large deletions within the β-helical region of the p55 domain are poorly secreted. Similarly, a previous study reported efforts to introduce large deletions into the region of the *H. pylori* chromosomal *vacA* gene that encodes the VacA p55 domain, but most of the resulting mutant proteins were neither expressed nor secreted by *H. pylori* (118).

In the current study, the three mutant VacA proteins that exhibited the most striking defects in secretion (Δ559-579, Δ580-607, Δ608-628) each contained deletions that are localized near the carboxy-terminus of the β-helix. A notable feature of these mutant

proteins was that in comparison to wild-type VacA, they exhibited increased susceptibility to trypsin proteolytic cleavage. Interestingly, a study of *Bordetella pertussis* BrkA revealed that a β-helical region near the carboxy-terminus of the passenger domain is required for folding of this protein (79). The authors proposed that this domain acts as an intramolecular chaperone to promote folding of the passenger domain concurrent with or following translocation through the outer membrane. Similarly, studies of *B. pertussis* pertactin indicate that the carboxy terminal β-helical region of this protein exhibits enhanced stability and can fold as a stable core structure (46, 47). We speculate that VacA amino acids 559-628 have a similar functional role in promoting protein folding and secretion. Collectively, our current studies of VacA, combined with previous studies of pertactin and BrkA, suggest that autotransporter passenger domains from a variety of bacterial species may be dependent on a carboxy-terminal β-helical region for protein folding and protein secretion.

An additional finding in the current study is that several individual coils within the p55 domain can be deleted without adverse effects on vacuolating toxin activity. VacA Δ484-504, Δ511-536, and Δ517-544 mutant proteins each retained vacuolating activity similar to that of wild-type VacA. The retention of vacuolating activity despite the deletion of entire coils of the β-helix correlates well with results from a previous study, which reported that inactivating point mutations within the portion of *vacA* encoding the p55 domain could not be identified (68). In the current study, one of the VacA mutant proteins (Δ433-461) clearly exhibited a defect in vacuolating activity compared to wild-type VacA. The VacA Δ433-461 mutant retained the capacity to be secreted by *H. pylori*, which suggests that this protein was not substantially altered in folding. Further evidence for intact folding of the VacA Δ433-461 mutant protein was provided by the demonstration that this mutant

protein is recognized by an anti-VacA monoclonal antibody (5E4) that reacts with a conformational epitope and the demonstration that this mutant protein exhibits resistance to trypsin proteolysis. Further studies will need to be performed to determine the precise amino acids within this coil that contribute to vacuolating toxin activity.

In summary, these results reveal that within the VacA β-helix, there are regions of plasticity that tolerate alterations without detrimental effects on protein secretion or activity. We speculate that there are similar regions of plasticity within other autotransporter passenger domains. The current data also provide evidence that a β-helical region near the carboxy-terminus of the VacA passenger domain is required for proper folding and secretion; this feature may be a general property of autotransporter passenger domains. Finally, the current results suggest that VacA amino acids Ser^{433}-Phe^{461} contribute to vacuolating toxin activity. Further study of these topics may lead to a better understanding of the role of the β-helical structure in secretion and activity of autotransporter passenger domains.

CHAPTER V

ADDITIONAL STUDIES OF VACA HOST-CELL INTERACTIONS

Introduction

Upon first joining the lab, I undertook several small pilot projects to investigate effects of VacA on epithelial cells. The known cellular effects of VacA on epithelial cells include alteration of mitochondrial membrane permeability, apoptosis, activation of mitogen-activated protein kinases (MAPK), and depolarization of the membrane potential (9); however, there are still unanswered questions in each of these areas. In this chapter, I will present preliminary data from my projects studying MAPK activation, identification of VacA-induced changes in expression of epithelial cell proteins, apoptosis, intracellular localization, and studies of GFP-tagged VacA domains.

Effects of *H. pylori* on phosphorylation and activation of MAPK pathways

Several studies have shown that VacA can directly induce vacuolation, mitochondrial damage, cytochrome c release, and apoptosis of epithelial cells (28, 48, 50, 57). The mechanisms by which VacA exerts its cytotoxic effects have not been completely elucidated, but evidence suggests that the different effects may occur through different pathways. Because VacA is thought to cause cell death by mitochondrial damage, a study by Nakayama *et al.* hypothesized that VacA could also disrupt other signaling pathways; they therefore examined the effects of VacA on mitogen activated protein kinases (MAPK) (75). The authors found that purified VacA activates two groups of MAPK, both p38 and Erk 1/2, in the AZ-521 gastric epithelial cell line. By treating cells with an inhibitor of p38 kinase

activity, the authors found that vacuolation, decrease in mitochondrial membrane potential, and cytochrome c release still occurred, suggesting that these activities are not related to the p38 signaling pathway (75).

When I began the signaling project, one goal was to determine whether we could reproduce the finding by Nakayama *et al.* that purified VacA stimulated p38 and Erk 1/2 phosphorylation. Other questions that that we wanted to answer included: could the system be characterized in more detail with respect to dose response or kinetics, what is upstream and downstream of p38 and Erk 1/2 phosphorylation (for example specific receptors that VacA must bind to, other kinases, transcription factors), is this effect seen in cell types besides AZ-521, do VacA mutants produce the same effects, and what pathway leads to VacA-induced effects such as vacuolation and cytochrome c release. Ultimately, studies such as these could lead to a better understanding of VacA's mechanism of action.

Effect of purified VacA on activation of Erk 1/2 and p38- We first treated adherent AZ-521 cells with purified acid-activated VacA (10 µg/ml and 20µg/ml) or a control acid-activated buffer not containing VacA for 10, 30, 60, and 120 minutes. Prior to the addition of VacA, cells were serum starved overnight. After incubation with the toxin, cells were lysed with a buffer containing 62.5 mM Tris (pH 6.8), 2% SDS, 10% glycerol, 50 mM DTT, 0.1 % bromphenol blue, 10 mM NaF, 1mM Na_3OV, and complete protease inhibitor cocktail (Pierce). Samples were run on a 4-20% gradient gel, transferred to nitrocellulose, and immunoblotted with anti-phospho-p38, anti-phospho-Erk 1/2, or an antibody against total p38 and Erk 1/2, followed by a horseradish peroxidase (HRP)-conjugated secondary antibody and detected using X-ray film. In contrast to the previous published study, we detected very little p38 or Erk 1/2 phosphorylation above background levels after addition of VacA. We

observed a very small increase in Erk 1/2 phosphorylation at 10 and 30 minutes (Figure V-1). At 10 and 30 minutes, there was a 1.34-fold increase and 1.22-fold increase, respectively, in Erk 1/2 phosphorlyation when acid-activated VacA was added to cells compared to when acid-buffer without VacA was added to cells. These experiments were performed at least twice and with two additional gastric epithelial cell lines, AGS and MKN-28, and HeLa cells with similar results (data not shown). Our background levels of phosphorylation were always higher than previously reported, making it hard to see an increase in phosphorylation due to VacA. Differences between the methodology of Nakayama *et al* and our methodology included a different VacA purification procedure and different lysis buffers. These differences may have contributed to the lack of reproducibility between the two experiments. Several independent labs have been able to confirm p38 and Erk 1/2 phosphorylation in both gastric epithelial cells and T cells in response to purified VacA, indicating that the effect is real and would be an interesting area of future study to understand how activation of these proteins is involved in VacA-induced cellular alterations.

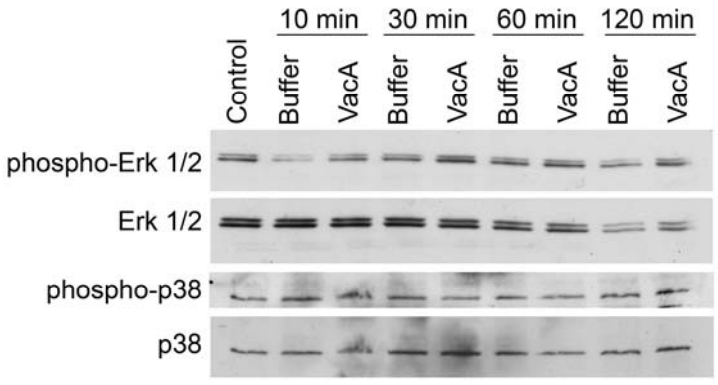

Figure V-1. Effect of purified VacA on Erk 1/2 and p38 phosphorylation. AZ-521 cells were incubated with 10 μg/ml purified, acid-activated VacA or acid-buffer not containing VacA (*Buffer*) for the indicated times. *Control* refers to cells that did not receive any treatment. Cell lysates were prepared and analyzed by western blot using phospho-specific MAPK antibodies and antibodies that detect total levels of endogenous MAPK protein.

Effect of the *cag* PAI on MAPK signaling pathways- Due to our inability to detect Erk 1/2 and p38 phosphorylation in response to purified VacA, we began studying the effects of adding intact *H. pylori* bacteria to epithelial cells. For these studies, wild-type *H. pylori* strain 26695 and an isogenic *cag* PAI knockout mutant were added to HeLa, MKN-28, and AGS cells. *H. pylori* was grown in broth culture for initial experiments; however, we later used *H. pylori* grown on blood agar plates and obtained similar results. $1x10^8$ bacteria/ml were added to cells and incubated for 10 minutes, 1 hour, or 24 hours. Cells were lysed as described above and immunoblots were performed. As shown in Figure V-2, wild-type *H. pylori* caused more p38 phosphorylation than the *cag* PAI knockout mutant did when these strains were added to HeLa, MKN-28, and AGS cells for 1 hour. In HeLa cells, wild-type *H. pylori* caused more Erk 1/2 phosphorylation than the Δ*cag* PAI did; this was not apparent for MKN-28 or AGS cells. Interestingly, the phosphorylation of Erk 1/2 and p38 was still above background levels when epithelial cells were incubated with the Δ*cag* PAI mutant strain. When *H. pylori* was added to cells, we also observed activation of c-fos and c-jun, two transcription factors that are located downstream of Erk 1/2 and p38, but this activation was not dependent on the *cag* PAI (Figure V-2). Combined, these results suggest that at 1 hour, phosphorylation of p38 and Erk 1/2 is dependent on the *cag* PAI, but that there is also a Cag independent factor present that stimulates MAPK activation. At 10 minutes and 24 hours, we observed bacteria-dependent phosphorylation, but this phosphorylation was not dependent on the *cag* PAI (data not shown).

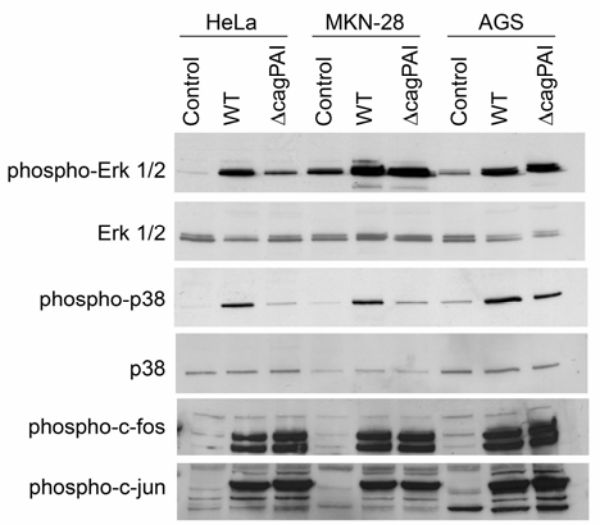

Figure V-2. Effect of the *cag* PAI on MAPK signaling. HeLa, MKN-28, and AGS cells were incubated with wild-type *H. pylori* 26695 (WT) or an isogenic *cag* PAI knockout mutant (Δ*cag* PAI) ($1x10^8$ bacteria/ml) for 1 hour. *Control* refers to cells that did not receive any treatment. Cell lysates were prepared and analyzed by western blot using anti-phospho antibodies (phospho-Erk1/2, phospho-p38, phospho-c-fos, or phospho-c-jun) and antibodies that detect total levels of endogenous MAP kinase protein (Erk 1/2 or p38).

Effect of BabA and VacA on MAPK signaling pathways - Our results described above suggest that the *cag* PAI is not the only factor mediating p38 phosphorylation, so we were next interested in identifying other *H. pylori* factors that played a role in mediating MAPK phosphorylation. We chose to study two *H. pylori* mutant strains: one in which *babA* (an adhesin that binds to Lewis B) had been inactivated, and another in which *vacA* had been inactivated. HeLa, AGS, and MKN-28 cells were incubated with either wild-type *H. pylori* strain J99 or an isogenic *babA* mutant for either 10 or 60 minutes as described above. Cells were lysed and immunoblots performed as described above. At 60 minutes, we observed bacteria-dependent Erk 1/2, p38, c-jun, and c-fos phosphorylation, but this phosphorylation was not dependent on BabA (Figure V-3). Similar results were obtained at the 10 minute time point (data not shown).

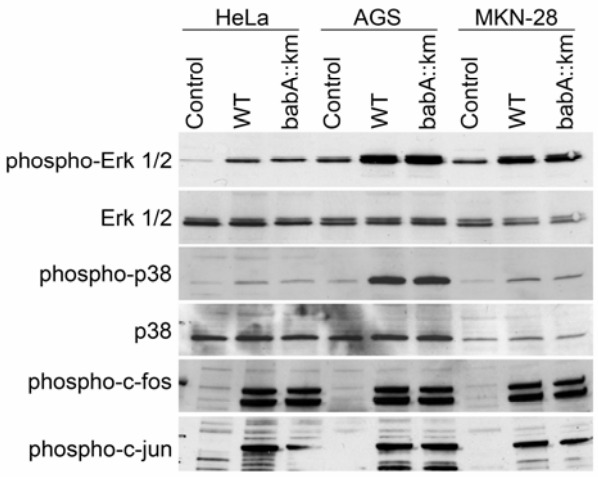

Figure V-3. Effect of BabA on MAPK signaling. HeLa, AGS, and MKN-28 cells were incubated with wild-type *H. pylori* strain J99 (WT) or an isogenic *babA* mutant in which the gene was disrupted by insertion of a kanamycin cassette (babA::km) ($1x10^8$ bacteria/ml) for 1 hour. *Control* refers to cells that did not receive any treatment. Cell lysates were prepared and analyzed by western blot using anti-phospho antibodies (phospho-Erk1/2, phospho-p38, c-fos, or c-jun) and antibodies that detect total levels of endogenous MAP kinase protein (Erk 1/2 or p38).

When wild-type *H. pylori* strain 60190 (VM001) or an isogenic *vacA* mutant in which a kanamycin cassette was inserted (VM022) was incubated with AZ-521 cells, wild-type *H. pylori* caused more Erk 1/2 and p38 phosphorylation than the *vacA* mutant did. This difference was observed at 10, 30, and 60 minutes (Figure V-4). However, when this experiment was repeated with a different *vacA* mutant (A162, freezer stock number 141) in the same parent *H. pylori* strain (freezer stock number 398), there was little or no change in Erk 1/2 or p38 phosphorylation in response to the *vacA* mutant at 10, 30, 60, or 120 minutes (data not shown). This discrepancy could be due to changes in the *H. pylori* strain over time during lab passaging. Further studies would be required to determine which of the above results is the representative result.

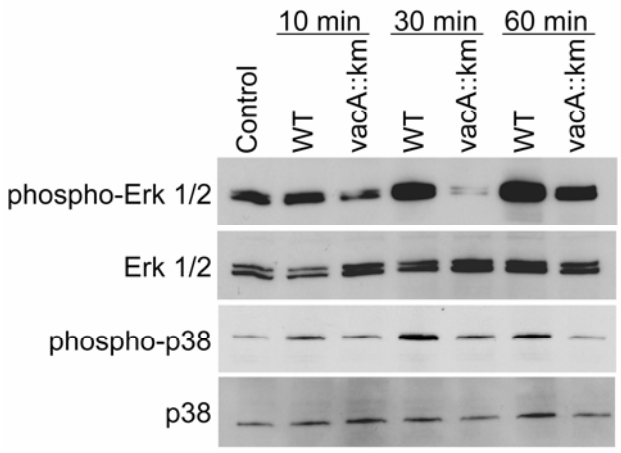

Figure V-4. Effect of a *H. pylori vacA* mutant on phosphorylation of Erk 1/2 and p38. AZ-521 cells were incubated with wild-type *H. pylori* strain 60190 (WT) or an isogenic *vacA* mutant in which a kanamycin cassette was inserted (vacA::km) ($1x10^8$ bacteria/ml) for the indicated times. *Control* refers to cells that did not receive any treatment. Cell lysates were prepared and analyzed by western blot using anti-phospho antibodies (phospho-Erk1/2, phospho-p38) and antibodies that detect total levels of endogenous MAP kinase protein (Erk 1/2, p38).

Conclusions- Overall, we were unable to show an increase in p38 phosphorylation in response to purified VacA, but we detected a small increase in Erk 1/2 phosphorylation due to purified VacA at 10 and 30 minutes. As mentioned above, several labs, including other people in the Cover lab, have been able to detect Erk 1/2 and p38 phosphorylation due to purified VacA. Methods that I used were different than methods from other labs and also different from other people in the Cover lab (for example, in the Cover lab, different lysis buffers and transfer membranes were used). This may have led to the difference in results. We did observe bacteria-dependent phosphorylation, a phenotype that is not completely dependent on *cag* PAI, BabA, or VacA, as p38 and Erk 1/2 were still phosphorylated in the absence of these factors. This highlights the complexity of these signaling pathways and indicates that there are multiple *H. pylori* factors that contribute to the observed effects of *H. pylori* on epithelial cells. These results could be pursued further to understand *H. pylori*-induced activation of Erk 1/2 and p38.

Identification of changes in epithelial cell proteins in response to VacA intoxication

As has been discussed throughout this thesis, one of the most noted effects of VacA on epithelial cells is the formation of large cytoplasmic vacuoles. Although the mechanism by which vacuoles form is becoming more clear, there are still questions regarding whether increased osmotic pressure explains the swelling of VacA-induced vacuoles or whether the process involves fusion of membrane-bound compartments. We also know that VacA can induce cell death, but there is much that remains unknown about this process. Using two-dimensional difference gel electrophoresis (2D-DIGE), we compared VacA treated and untreated AZ-521 cells (a gastric epithelial cell line) with the goals of not only identifying

gastric epithelial cell proteins that were either up- or down-regulated as a result of VacA intoxication, but also potentially identifying VacA-induced post-translational modifications of proteins. For example, we hypothesized that we would be able to detect proteins involved in VacA-induced cell death and cell vacuolation.

Our experimental design involved incubating AZ-521 cells with 10 μg/ml acid-activated VacA plus 5 mM ammonium chloride for five or 20 hours (conditions that would result in cell vacuolation). As a negative control we used cells treated with acidified buffer plus 5 mM ammonium chloride for five or 20 hours. After incubation, the cells were lysed (7M urea, 2M thiourea, 4% CHAPS), the protein concentration determined, and the samples were then analyzed using 2D-DIGE methodology. In brief, this methodology involves differentially labeling proteins from each sample (*i.e.* + VacA, -VacA) with two different cyanine fluorescent dyes (Cy3 and Cy5) prior to gel electrophoresis. The samples are then mixed together, run on the same gel, and imaged individually using dye-specific excitation/emission spectra. Because samples are run on a single gel and imaged individually, this eliminates gel-to-gel variation. Software is then used to directly compare the Cy3- and Cy5-labeled samples. Protein spots are excised and identified using MALDI-TOF MS and tandem TOF/TOF MS/MS.

We performed the experiment in which VacA was incubated with cells for five hours two times; likewise, the 20 hour incubation experiments were also performed twice. The first five hour experiment included three independent replicates and the second five hour experiment included five independent replicates. Each 20 hour experiment included three independent replicates. After both the five hour and 20 hour incubations, we saw the development of large vacuoles in the VacA-treated cells but not in the control cells. At 20

hours, VacA-treated cells were starting to round up, with a few cells floating. Mock-treated cells still looked healthy. Up- and down-regulated gastric epithelial cell proteins that were identified are presented in Table V-1. Several interesting proteins were identified within individual experiments (such as dynein intermediate chain 2, serine/threonine protein kinase PAK2, Grb2 adaptor protein, profilin), but unfortunately, this data was not very reproducible in separate experiments. Differentially regulated proteins that were detected in the five hour and the 20 hour experiment included bovine apolipoprotein and human hnRNP (Table V-1). There were not any differentially regulated proteins that were reproduced between the two 5 hour experiments. Serine threonine PP2A was detected in both of the 20 hour experiments, as was bovine apolipoprotein; however, in the second 20 hour experiment the match was very weak for both proteins. Although not mentioned in the table, bovine serum albumin was upregulated in both 20 hour experiments. In all of our experiments, AZ-521 cells were grown in the presence of fetal bovine serum. Even though the cells were washed before lysis for 2D-DIGE, serum proteins may have stuck to the cells, or were taken up by the cells, potentially explaining our detection of bovine proteins (bovine apolipoprotein and bovine serum albumin).

There are several reasons why we may have had problems identifying many differentially expressed proteins. In general, disadvantages of 2D-electrophoresis include the inability to visualize low-copy number proteins in the presence of highly abundant gene products and the complexity of eukaryotic cell lysates can be difficult to resolve on a 2D gel (61). Additionally, because Cy dyes label lysines, a protein with a high or low lysine content could be labeled more or less efficiently (61). Specific to our experiments, VacA-induced vacuolation may not necessarily be associated with an up- or down-regulation of proteins.

Furthermore, an activation of proteins involved in cell death also may not be associated with a visible change in epithelial cell protein levels. Our experiments were only run at a pH range of 4-7, so using a different pH range might be helpful in identifying other proteins. Additionally, although we looked at two time points, it could be that we did not examine a time point in which changes would be identified.

As mentioned above, there were several differentially regulated proteins that were of interest and could be followed up on. Based on their protein descriptions, it is possible that these proteins could be involved in VacA-induced effects on gastric epithelial cells. Although changes in these particular protein levels were not seen in multiple 2D-DIGE experiments, other methods (such as western blots, RT-PCR) could be used to determine if the changes we observed were real. If any of these changes were real, the role of these proteins could be examined in more detail by knocking down gene expression with siRNA.

Table V-1. Differentially expressed proteins detected by 2D-DIGE/MS analysis.

Protein identified	Accession #	Fold change in response to VacA[a]	p value	Experiment in which change was detected[b]	Protein description
5 hour time point					
Heat shock protein 90 beta	P08238	1.21	0.0069	A	molecular chaperone; has ATPase activity; phosphorylated upon DNA damage
Dynein inter-mediate chain 2	Q13409	1.40	0.05	A	intermediate chains seem to help dynein bind to dynactin
Serine/threonine protein kinase PAK 2	Q13177	1.61	0.0083	A	activated by Cdc42 and Rac; plays a role in regulation of cell shape, motility, cell survival/ death

Heterogeneous ribonuclear proteins C1/C2 (hnRNP)	P07910	1.44	0.015	A	binds pre-mRNA and nucleates the assembly of 40S hnRNP particles
Nucleophosmin	P06748	1.32	0.013	A	involved in diverse cellular processes such as ribosome biogenesis, protein chaperoning, cell proliferation, and regulation of several tumor suppressors
Phospoglycerate mutase 1	P18669	-1.53	0.048	A	interconversion of 3- and 2-phosphoglycerate
Growth factor receptor-bound protein 2 (GRB2 adaptor protein)	P29354	-1.48	0.047	A	associates with activated Tyr-phosphorylated EGF receptors; may interact with RAS in the signaling pathway leading to DNA synthesis; likely represents a regulatory subunit of downstream signaling molecules
Bovine apolipoprotein A-1 precursor	P15497	-1.30	0.0091	A	plays a role in the reverse transport of cholesterol from tissues to the liver
ATP synthase D chain, mitochondrial	O75947	-1.72	0.035	A	mitochondrial membrane ATP synthase produces ATP from ADP in the presence of a proton gradient across the membrane
Eukaryotic translation initiation factor 5A (eIF-5A)	P10159	-1.46	0.025	A	exact role in protein biosynthesis is not known
60S acidic ribo-somal protein P2	P05387	-1.47	0.014	A	plays a role in the elongation step of protein synthesis

Profilin	P35080	-1.38	0.035	A	binds to actin and affects the structure of the cytoskeleton
Galectin-1	P09382	-1.93	0.046	A	may regulate apoptosis, cell proliferation and cell differentiation
Elongation factor 2, isoform 1	P13639	down-regulated	0.0008	B	promotes the GTP-dependent translocation of the growing protein chain from the A-site to the P-site of the ribosome
Elongation factor 2, isoform 2+	P13639	1.29	not provided	B	see above (isoform 1)
20 hour time point					
Serine/threonine PP2A	P30153	1.25 1.28	0.035 0.064	C D	contains two subunits, one of which associates with a variety of regulatory subunits
Bovine apolipoprotein A-1	P15497	2.18 1.30	0.0004 0.035	C D	see description under 5 hour timepoint
Alpha-enolase	P06733	-1.16	0.024	C	roles in glycolysis, growth control, and hypoxia tolerance
26S protease regulatory subunit 7	P35998	-1.10	0.0033	C	involved in the ATP-dependent degradation of ubiquitinated proteins
Heterogeneous ribonuclear proteins C1/C2	P07910	-1.27	0.026	C	see description under 5 hour time point
Cofilin-1 (very weak match)	P23528	-2.09	0.046	D	controls actin polymerization and depolymerization in a pH-sensitive manner

[a] Fold change in response to VacA: Comparing VacA-treated cells with mock-treated cells, positive values represent protein up-regulation and negative values represent protein down-regulation

[b] Experiment in which change was detected: *A* is 5 hour experiment #1, *B* is 5 hour experiment #2, *C* is 20 hour experiment #1, and *D* is 20 hour experiment #2.

Study of VacA and apoptosis

As has been discussed throughout this thesis, VacA is an important pathogenic product of *H. pylori*. It is capable of causing numerous effects on target cells, one of which is apoptosis. There is evidence that in the absence of other *H. pylori* factors, VacA induces epithelial cell apoptosis (12, 28, 50). Other studies have also suggested that VacA has several effects on mitochondria including a decrease in mitochondrial membrane potential (48, 122), release of cytochrome c (28, 123), and a decrease in cellular ATP levels (48); these effects on mitochondria appear to be dependent on VacA channel activity. This is supported by data showing that chemicals that block VacA channels also inhibit VacA-induced reduction of mitochondrial membrane potential and cytochrome c release (123). Two independent labs found that VacA localizes to the mitochondria (28, 123); however, another lab was not able to reproduce this (131). Although it is established that VacA plays a role in apoptosis of several cell types, some unanswered questions include: the mechanism of VacA-induced apoptosis, the role of VacA-mediated apoptosis in *H. pylori* pathogenesis, how cellular intoxication can result in mitochondria membrane permeability, which proapoptotic proteins are involved in VacA-induced apoptosis, if the same regions of the toxin that are required for vacuolation are also required for apoptosis, if VacA does indeed localize to the mitochondria how does internalized VacA travel to that organelle, and how VacA crosses the outer mitochondrial membrane. The preliminary studies in this section were undertaken to further investigate VacA's role in inducing cell death.

The approach we used to study VacA-induced apoptosis was a flow cytometric assay using Annexin V and 7-AAD staining. This assay is based on the principle that loss of plasma membrane is one of the earliest features of apoptosis and when a cell is undergoing

apoptosis, phospholipid phosphatidylserine (PS) is translocated from the inner to the outer leaflet of the plasma membrane. Annexin V can then bind to cells with exposed PS. Because PS translocation can also be evident during necrosis, Annexin V is used in combination with the nucleic acid-binding dye 7-AAD, which can only penetrate the plasma membrane when membrane integrity is lost (later stages of apoptosis or necrosis). Therefore, when analyzing flow cytometry results, three populations can potentially be detected: viable cells (Annexin V and 7-AAD negative), cells undergoing early apoptosis (Annexin V positive, 7-AAD negative), and cells that have undergone late apoptosis or are already dead (Annexin V and 7-AAD positive).

In our first experiments, the gastric epithelial cell lines AGS and AZ-521 were incubated with 10 μg/ml acid-activated VacA plus 5 mM ammonium chloride, ammonium chloride plus acid, or acid alone for 12 or 24 hours. Both of these adherent cell lines were removed from tissue culture plates by scraping using a rubber policeman, stained with Annexin V and 7-AAD, and analyzed by flow cytometry. From these experiments, we concluded that scraping the cells was damaging the cell membrane, leading to high background (data not shown). An experiment to determine the best way to remove adherent cells revealed that Accutase (Innovative Cell Technologies, Inc.), a detachment solution containing proteolytic and collagenolytic enzymes, caused the least amount of cell membrane damage (data not shown), and this product was therefore used in subsequent experiments.

In our next experiments, AZ-521 cells were treated with 10 μg/ml acid-activated VacA plus ammonium chloride, non-activated VacA plus ammonium chloride, or ammonium chloride plus acid for 12, 24, 48, and 72 hours. Acid-activated VacA induced cell death beginning at 24 hours. At 48 and 72 hours, acid-activated and non-activated VacA induced

significantly more cell death than what was observed 24 hours (Figure V-5). There was very little cell death observed when ammonium chloride plus acid was added to cells for 12, 24, and 48 hours; however, by 72 hours the amount of cell death induced by ammonium chloride plus acid had increased compared to the earlier time points. At 72 hours, we began seeing a decrease in late apoptotic cells compared to what was observed at 12, 24, and 48 hours. One reason for this could be that during preparation of the cells for flow cytometry, dead cells were not spun down during centrifugations and were subsequently lost.

Various positive controls used by other groups to induce apoptosis (cisplatin, staurosporine) either did not induce cell death at all in our hands, or did not induce early apoptosis, only late apoptosis/necrosis. Cisplatin has been used to induce early apoptosis at similar concentrations and time periods that we used, but we did not see an induction of early apoptosis. Lack of good controls made results of VacA-induced cell death hard to interpret.

Overall, our results are in agreement with published results that acid-activated VacA is inducing cell death. Our result that non-activated VacA induced cell death does not agree with previously published results (12); however, the previous study used a different gastric epithelial cell line, which may explain the difference in results. The fact that we showed that VacA is killing cells suggests that this project could be studied in more detail, perhaps by delineating the pathway leading to apoptosis and analyzing what proteins are involved in VacA-induced cell death.

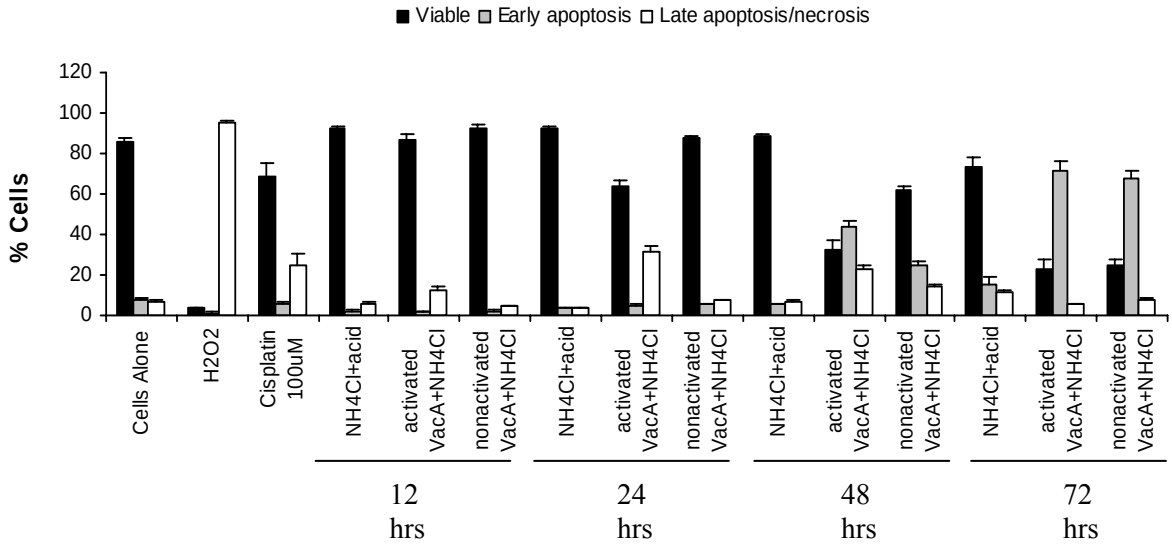

Figure V-5. VacA-induced cell death. AZ-521 cells were treated with acid-activated VacA plus ammonium chloride, non-activated VacA plus ammonium chloride, or ammonium chloride plus acid for 12, 24, 48, and 72 hours. In each case, the VacA concentration used was 10 µg/ml. Positive controls included both H_2O_2 and cisplatin; cells alone were used as a negative control. After treatment, cells were detached with Accutase, stained with Annexin V and 7-AAD, and analyzed by flow cytometry. Viable, early apoptotic, and late apoptotic/necrotic cells are indicated on the graph. Results represent the mean ± the SD from triplicate samples.

Cell fractionation studies

In order to exhibit cellular toxicity, VacA must bind to the plasma membrane of mammalian cells. Upon binding to cell membrane components such as RPTP-α and –β (27, 128, 129), and lipid raft microdomains (85, 96), VacA is subsequently internalized by cells (30, 70, 85, 92). Internalized VacA is known to localize both to endosomal compartments and the mitochondria (28, 58, 93). One study determined that VacA accumulates into GPI-anchored protein-enriched early endosomal compartments (GEECs) within 10 minutes, is enriched in the early endosomes within 30 minutes, and is then transferred to late endosomes within 120 minutes (31). Other than endosomal compartments and mitochondria, it is not well understood which, if any, other intracellular sites VacA interacts with, how VacA may get to these sites, and specifically how VacA can traffic from the cell surface to the mitochondria. We undertook some preliminary cell fractionation experiments with the goal of trying to identify intracellular sites with which VacA may be localizing. Identifying where VacA localizes to within the cell could then lead to studies of VacA sorting and trafficking.

For our experiments, the gastric epithelial cell line AZ-521 was incubated with 10 μg/ml acid-activated VacA plus 5 mM ammonium chloride for 12 hours at 37ºC. As a negative control, we added an acidified buffer not containing VacA plus 5 mM ammonium chloride for the same amount of time. Under these conditions, the cells in which VacA had been added were vacuolated, and no vacuolation was seen for the negative control. The cells were harvested by scraping, centrifuged, and the cell pellet lysed with homogenization medium containing 0.25 M sucrose, 1 mM EDTA, and 10 mM HEPES, pH 7.4. This suspension was subject to successive centrifugations at 3,000g, 16,000g, and 100,000g. The

pellet from the 16,000g centrifugation was resuspended in a solution containing a final concentration of 17.5% iodixanol and centrifuged at 353,000g. Fractions were obtained from the supernatant of the 353,000g spin by puncturing the bottom of the tube and dripping fractions out in 100 µl aliquots. Fractions were analyzed by western blotting with antibodies against endoplasmic reticulum (anti-calnexin), early endosomes (anti-EEA-1), lysosomes (anti-LAMP-1), golgi (anti-golgi 58K), mitochondria (anti-cytochrome c oxidase), and an antibody to detect VacA (anti-958).

At the 12 hour time point, we observed markers for several cellular compartments localizing to different fractions (Figure V-6). Endoplasmic reticulum and golgi were seen in a number of fractions, but with peaks near the top (approximately fractions 12 and 13) and bottom of the gradient (approximately fractions 4-6). Cytochrome c was localized at the bottom of the gradient, mainly in fractions 4-6. Early endosomes were localized in many fractions, but with a peak in fraction 3, and lysosomes were localized near the top of the gradient in fractions 16-19. Upon probing these fractions for VacA, we found that VacA was in all fractions, with peaks in both top and bottom fractions (Figure V-6). This data is in accordance with what has been observed before, suggesting that VacA localizes with lysosomes and mitochondria. However, VacA may also be localizing to several other compartments. We next tried an experiment in which acid-activated VacA was incubated with AZ-521 cells for only 1 and 4 hours at 37ºC to see if there was a different distribution of VacA at these earlier time points. At both 1 and 4 hours, we also observed VacA in almost all fractions (data not shown).

As mentioned above, VacA can presumably traffic to early endosomes within 30 minutes (31), so it may not be unreasonable to see VacA in so many fractions at our 1 hour

time point. Our results that VacA is found in many fractions at 1, 4, and 12 hours are potentially interesting. It would be interesting to follow up on these preliminary cell fractionation studies, first by repeating these experiments with more controls, and then perhaps using confocal microscopy to observe co-localization of VacA with markers for different cellular compartments. One good control would be to incubate VacA with cells at 4ºC for 1 hour to allow for binding, but not internalization. These studies may help us to further understand if VacA is indeed localizing to so many different intracellular sites and may help to decipher what functions VacA may serve at these sites.

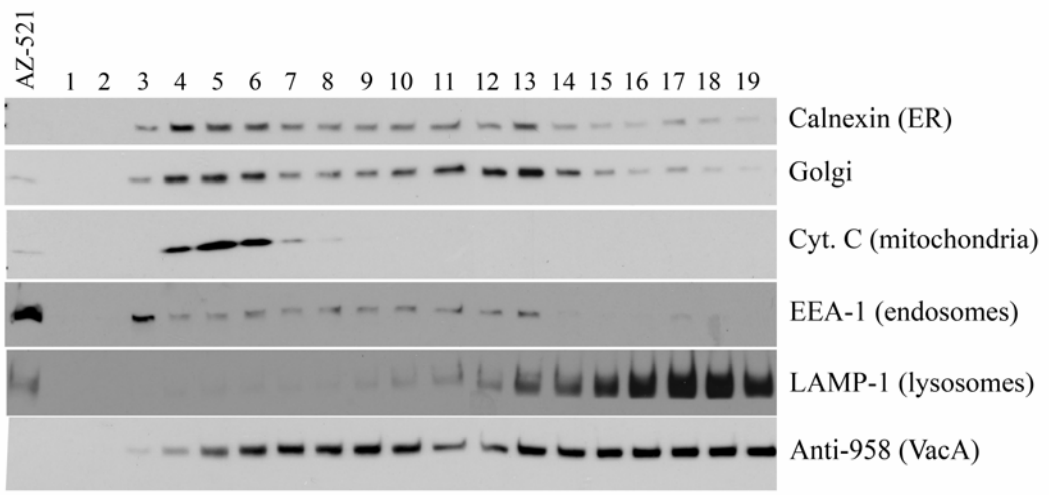

Figure V-6. VacA intracellular localization. AZ-521 cells were treated with 10 µg/ml acid-activated VacA plus ammonium chloride for 12 hours. After treatment, cells were lysed and fractionated as described in the text. Fractions were analyzed by western blotting with antibodies against calnexin (endoplasmic reticulum), golgi, cytochrome c (mitochondria), EEA-1 (early endosomes), LAMP-1 (lysosomes), and anti-958 (VacA). Fraction numbers are shown above the western blot (fractions 1-19), with fraction 1 being the bottom fraction and fraction 19 being the fraction at the top of the gradient.

Studies of GFP-tagged p33 and p55 VacA domains

Flow cytometry- During my rotation in the Cover laboratory, I constructed plasmids that would express a protein with an amino- or carboxy-terminal GFP tag (these plasmids could be used to clone in any protein of interest). These plasmids were later used by others in the lab to clone a GFP tag at the carboxy-terminus of the VacA p33 domain and the amino-terminus of the p55 domain, making these constructs useful tools for fluorescence studies. I used the p33- and p55-GFP-tagged proteins for a preliminary experiment to study binding of these toxins to cells using flow cytometry. From work presented in Chapter II, we know from confocal microscopy and western blotting techniques that p33 and p55 each bind to cells at low levels when added to cells individually, but when mixed and added to cells, binding is greatly increased. We wanted to know if these results could be recapitulated using the GFP-tagged proteins and flow cytometry. A flow cytometric-based binding assay would be an alternative quantitative and high-throughput assay. For preliminary flow cytometry studies of the GFP-tagged proteins, each domain was first recombinantly expressed (112). Each domain contained either a GFP tag or a His_6 tag so that we could detect binding of each domain when added to cells individually or in combination. *E. coli* soluble extracts containing recombinant VacA proteins were either added to cells individually, or mixtures of the recombinant proteins were incubated with HeLa cells for 1 hour at 37ºC. For these experiments, HeLa cells were first detached from tissue culture plates; recombinantly expressed proteins were normalized and then mixed and added to HeLa cells in suspension. Recombinantly expressed proteins that were added to cells included p33GFP+p55His, p33His+p55GFP, p33GFP alone, p55GFP alone, p33His alone, and p55His alone. After incubation, cells were washed with cold PBS, fixed with 2% paraformaldehyde, and analyzed

by flow cytometry (results shown in Figure V-7). Our first conclusion from this experiment was that we are able to successfully detect binding of GFP-tagged proteins using flow cytometry (Figure V-7), potentially making this a useful tool for future studies. As expected, there was little binding of p33 or p55 alone, but binding was increased when p33 and p55 were mixed and added to cells (Figure V-7). This result was seen regardless of whether the GFP tag was on p33 (p33GFP+p55His) or p55 (p33His+p55GFP). A combination of p33GFP+p55GFP results in cell vacuolation when these fragments are recombinantly expressed, mixed, and added to cells (data not shown), suggesting that the GFP tag does not inactivate VacA. Mixtures of p33GFP+p55His or p33His+p55GFP were not tested for vacuolation.

In future experiments, flow cytometry could be used to determine if inactive VacA mutants are defective in binding. In an approach similar to the experiment described above, mutant p33 fragments could be mixed with wild-type p55-GFP, or mutant p55 fragments could be mixed with wild-type p33-GFP to determine residues that are important for binding of the toxin to host cells. It would be expected that if there are residues important for binding, the mixture of mutant and wild-type protein will not yield as high binding as a mixture of wild-type p33 and wild-type p55.

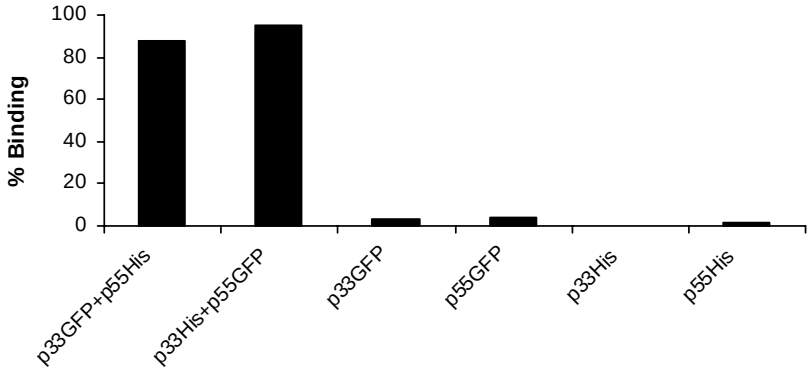

Figure V-7. Binding of p33 and p55 VacA domains detected by flow cytometry. *E. coli* soluble extracts containing similar amounts of the indicated VacA proteins were added to HeLa cells for 1 hour at 37ºC. The ability of the VacA fragments to interact with host cell membranes was assessed by flow cytometry. Background fluorescence of cells alone was subtracted from each sample.

Confocal microscopy- I also used the p33GFP-tagged protein and p55His$_6$-tagged proteins for a preliminary experiment to study internalization of these proteins using confocal microscopy. As described in Chapter II, confocal microscopy was successfully used to study binding and internalization of Myc-His-tagged and His-tagged p33 and p55 domains using indirect labeling methods. By using GFP-tagged proteins, we wanted to study the localization of each domain within mammalian cells by direct detection of GFP fluorescence.

For preliminary microscopy studies of the GFP-tagged proteins, each domain was first recombinantly expressed using the same methods as for p33 and p55 without the GFP tag (112). *E. coli* soluble extracts containing recombinant VacA proteins were either added to cells individually, or mixtures of the recombinant proteins were incubated with HeLa cells (grown on cover glasses) for 1 hour at 37ºC. Recombinantly expressed proteins that were added to cells included p33GFPHis+p55His, p33GFPHis alone, and p55His alone. After 1 hour, unbound proteins were removed, the cell monolayer was washed, and fresh tissue culture medium was added to the cells for an additional 15 hours at 37ºC to allow for internalization. The cells were then washed, fixed with 3.7% formaldehyde, and permeabilized with methanol for 25 minutes at -20ºC. Cells were incubated with an anti-VacA polyclonal antiserum followed by a Cy-3 conjugated secondary antibody. In this way, we would be able to visualize the p55 domain with the VacA polyclonal antiserum, and the GFP tag would be used to visualize p33, allowing us to study the localization of each domain within cells. Cover glasses were washed, mounted on slides, and analyzed by confocal microscopy. For cells in which we were only visualizing GFP, cover glasses were mounted on slides after fixation with 3.7% formaldehyde. After addition of p33GFPHis+p55His to cells, we observed very little co-localization of p33 and p55 (Figure V-8). Using the anti-

VacA antiserum, we were able to visualize p55 (top panels) and p33 was visualized using its GFP tag (middle panels). The merged images (bottom panels) show visualization of p33GFP in green and p55His in red. Controls for this experiment included a negative control in which HeLa cells that did not receive treatment were stained with the anti-VacA antibody (no staining observed), p55His added to cells alone and stained with the anti-VacA antibody (no staining observed), p33GFPHis added to cells alone (no internalization observed), and purified VacA added to cells and stained with the anti-VacA antibody (extensive internalization observed) (data not shown). This experiment was repeated several times, and each time we detected very little co-localization of the p33 and p55 VacA domains. We did not assess internalization of the combination of a p33 protein mixed with a GFP-tagged p55.

Although we did not pursue this observation further, this is a potentially exciting area for future studies. It would be interesting to try to identify intracellular sites with which p33 and p55 are localizing. There is some evidence that when DNA encoding p33GFP is transfected into mammalian cells, it localizes with the mitochondria (28); however, using the transfection system, p55GFP was not found to localize to mitochondria (28). Our system in which VacA is added to the outside of cells and allowed to internalize could be used to investigate trafficking and localization of p33 and p55. Additional markers could be used to identify cellular compartments with which these domains are localizing. GFP tags could be added to various p33 and p55 mutants that are already available in the lab to further study intracellular trafficking and localization.

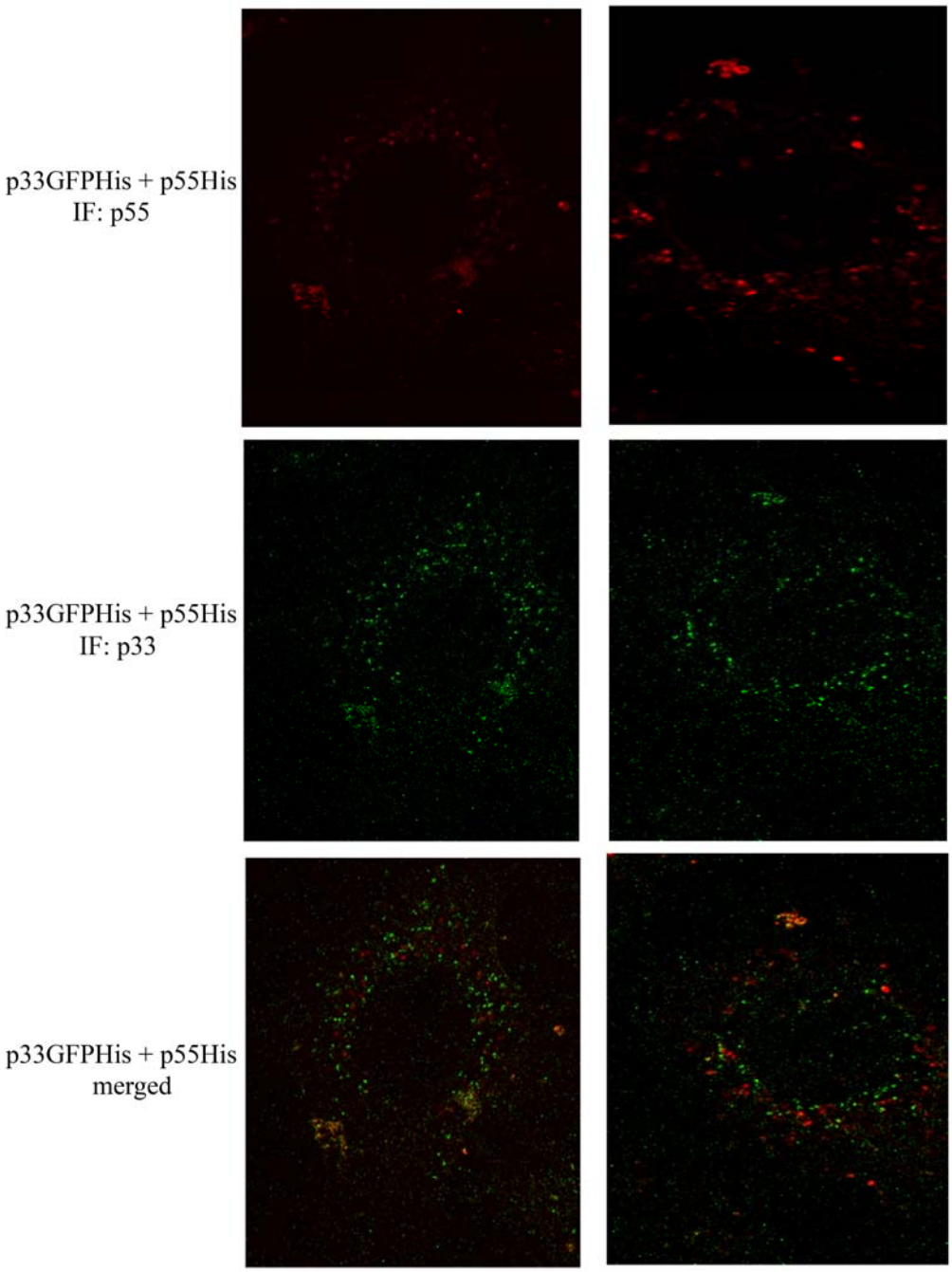

Figure V-8. Internalization of p33GFP and p55His into HeLa cells. *E. coli* soluble extracts containing p33GFPHis or p55His were mixed and added to HeLa cells for 1 hour at 37ºC. Cells were then incubated in fresh medium for an additional 15 hours at 37ºC. The ability of the p33/p55 mixture to enter cells was analyzed using indirect immunofluoresence (*IF*) of permeabilized cells using an anti-VacA antibody to detect the p55 domain (top panels) or GFP fluorescence to detect the p33 domain (center panels). Merged images are shown in the bottom panels. The top and bottom rows represent two different imaged cells.

CHAPTER VI

CONCLUSIONS AND FUTURE DIRECTIONS

Conclusions

One protein that *H. pylori* secretes that has been correlated with the development of gastroduodenal disease is known as the vacuolating cytotoxin, or VacA. Over the years, we have begun to understand more about the toxin itself and steps leading to the intoxication process of host epithelial cells. In a very basic sense, we know that in order to exert effects on host epithelial cells, VacA must first bind to one of several receptors on the cell surface, oligomerize, form anion-selective channels, and be internalized into host cells. Even though we have learned a lot about VacA since its discovery approximately 20 years ago, there are still many unanswered questions. Structure-function studies of VacA will help us to have a greater understanding of how VacA contributes to the pathogenesis of *H. pylori*, and might lead to better treatment and prevention of *H. pylori*-associated disease. Thus, the main goal of my thesis project was to undertake a structure-function analysis of the p55 domain of VacA.

Chapter II of this thesis describes interaction of the p33 and p55 domains with host cells. We show that p33 and p55 each can each bind to the cell surface, and that the interaction is higher when these domains are added to cells together. When added individually, neither p33 nor p55 was detected inside cells; however, when these two domains are mixed and added to cells, both domains are internalized. We also show that when sequentially added to cells, p55 must be added first, followed by p33, in order to result in internalization and vacuolating activity.

Chapter III of this thesis describes the characterization of a p55 subdomain that plays a role in the formation of oligomeric structures. This subdomain may contain a region of the toxin spanning residues 345-415, based on an analysis of six-amino-acid deletion mutations introduced at the amino-terminal end of p55. Mutant proteins in which these amino acids were deleted lacked vacuolating activity when plasmids encoding these proteins were transfected into cells, suggesting this region may have an important functional activity. Our data show that VacA Δ346-347 lacked vacuolating activity when added to the outside of cells, and did not cause membrane depolarization, suggesting that this mutant toxin cannot form membrane channels. Biochemical approaches including gel filtration, BN-PAGE, and a modified SDS gel electrophoresis approach were used to probe the oligomeric state of VacA Δ346-347. Collectively, data from these various techniques showed that this mutant can form a complex larger than a monomer, but smaller than wild-type VacA oligomers. Further analysis by immunoprecipitation demonstrated that not only could p55 Δ346-347 interact with wild-type p33, but a p33-p55 Δ346-347 mixture could interact with wild-type full-length VacA. Additionally, VacA Δ346-347 acts as a dominant-negative inhibitor of wild-type VacA. Our model predicts that even though the Δ346-347 mutation doesn't completely abrogate p33-p55 interactions, it could interfere with VacA oligomerization via disruption of intermolecular interactions (as opposed to an intramolecular interaction).

Little is known about which amino acid sequences in VacA contribute to protein-protein interactions and oligomerization. We clearly demonstrate that the Δ346-347 mutation disrupts VacA oligomerization, making this the smallest mutation known to play a role in the formation of oligomeric structures. Our study provides new insights into properties of VacA that are conferred by an amino-terminal region of p55 required for vacuolating activity, but

that is not known to be required for binding of the toxin. Importantly, assembly of VacA monomers into oligomeric structures is likely to be required for membrane channel formation, and membrane channel formation is very important for many of the cellular effects of VacA.

In Chapter IV, we present data analyzing coils of the p55 β-helix and their role in secretion and vacuolating activity of the toxin. Mutations were designed so that each would result in the deletion of a single coil of the β-helix. We thus made the prediction that the length of the β-helix would change, but there would be very little change in protein folding compared to wild-type VacA. Comparison of the deletion mutants with wild-type VacA demonstrated that several coils within the p55 domain could be deleted without substantially altering expression or secretion of the mutant proteins; however, deletion of coils near the carboxy-terminus drastically altered secretion and exhibited increased susceptibility to trypsin. Additionally, several individual coils could be deleted within the β-helix and the mutant proteins still retain vacuolating activity. Deletion of one specific coil, VacA Δ433-461, resulted in reduction of vacuolating activity in HeLa cells, and no detectable activity in RK13 or AZ-521 cells, suggesting this region contributes to vacuolating activity. Overall, the data demonstrate that there are regions of plasticity within the β-helix that can tolerate changes without substantially altering protein secretion or activity.

It has been predicted that nearly all proteins secreted by type Va autotransporter pathways have a predominantly right-handed parallel β-helical fold (47). In addition to the p55 domain of VacA, structures of two other autotransporter passenger domains have been solved and are found to fold as a β-helix: pertactin from *B. pertussis* and hemoglobin protease (Hbp) from *E. coli* (24, 80). In recent years, labs studying pertactin, Hbp, and BrkA

(another protein from *B. pertussis* secreted by an autotransporter system whose structure has not been solved, but is predicted to fold as a β-helix) have focused their efforts on elucidating the mechanisms by which these proteins are folded and secreted by the bacterium. Approximately 90 residues at the carboxy-terminus of BrkA are important for folding of the BrkA passenger domain (79). The equilibrium unfolding behavior of pertactin and Pet (a homologue of Hbp) reveals a stable core at their carboxy-terminus that might serve as a scaffold that would allow folding of the more amino-terminal portions of the passenger (47, 89). Thus, one common theme that is arising is the importance of the carboxy-terminal portion in folding of the passenger domains.

When I began my project in the lab, the functions of several regions of p33 had been identified. We knew that residues 1-32 within the p33 domain were necessary for channel formation, and we knew that amino acids 1-422 (consisting of the entire p33 domain and 111 amino acids of the p55 domain) were sufficient for intracellular activity. In 2006, Telford *et al* found that amino acids 49-57 in the p33 domain are important for the formation of large oligomers (35). Strikingly, very little was known about regions of the p55 domain important for specific functional activities. Therefore, my project focused on a structure-function analysis of the VacA p55 domain (see Figure VI-1 for a summary of regions we found to be important for functional activities). Our studies focused on the β-helical portion of the p55 domain (and therefore did not include study of the carboxy-terminal globular domain from amino acids 736-811) outside of the region of VacA known to be important for intracellular toxin activity. Our work revealed that amino acids 346 and 347 are important for oligomerization of VacA. Additionally, we found that a single coil of the β-helix from amino acids 433-461 is important for vacuolating toxin activity. Our work also showed that single

coils localized between amino acids 484-544 are dispensable; specifically, mutant proteins with deletion of these coils fold similarly to wild-type VacA, are secreted, and can induce vacuolating toxin activity when single coils within this region are deleted. Finally, we show that deletion of single coils near the carboxy-terminus (amino acids 559-628) resulted in markedly decreased secretion and increased susceptibility to trypsin, suggesting that this region is important for proper folding and secretion of the toxin. In summary, our work has contributed to a greater understanding of specific regions within the p55 domain that are important for specific functional activities.

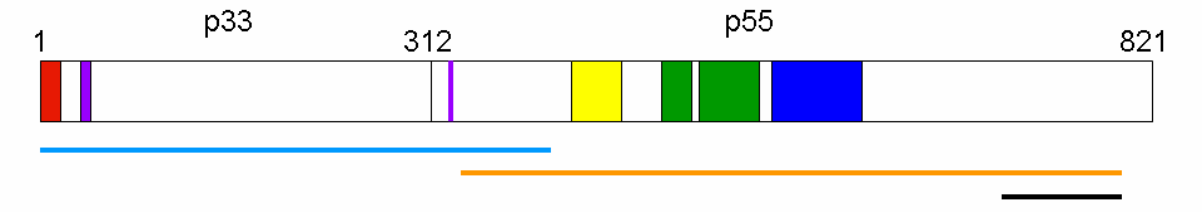

Figure VI-1. Newly identified functional regions of the VacA p55 domain. Prior to our work, the amino-terminus of p33 (shown in red) was found to be important in membrane channel formation, amino acids 49-57 (shown in purple within the p33 domain) were found to be important for oligomerization, and amino acids 1-422 (shown by the light blue line) were found to be important for intracellular activity. Residues that are part of the crystal structure (amino acids 355-811) are shown by the orange line, and the black line demonstrates residues that are part of the globular domain of the p55 crystal structure (amino acids 736-811). Our studies have revealed that amino acids 346 and 347 (shown in purple within the p55 domain) play an important role in oligomerization of VacA. We also found that the single coil comprised of amino acids 433-461 (shown in yellow) is important for vacuolating activity. Single coils between amino acids 484-544 (shown in green) are not required for efficient folding, secretion, or vacuolating activity. Single coils at the carboxy-terminus of the β-helical region are important for secretion and folding of the toxin (amino acids 559-628, shown by the blue box).

Chapter V of this thesis describes preliminary data from several projects in which we studied MAPK activation, investigated changes in epithelial cell proteins, apoptosis, intracellular localization of VacA, and studies of GFP-tagged VacA domains. Each of these projects further investigated effects of VacA on epithelial cells. As described in detail in Chapter V, interesting data were generated from each of these projects. Of particular interest, we found that p33 and p55 domains do not co-localize (Figure V-8) when mixed and allowed to internalize into mammalian cells, suggesting that the trafficking of these domains to different cell organelles could be investigated. We know that within cells, VacA can localize to late endocytic compartments and mitochondria, but it is not known if both the p33 and p55 domains are required for VacA targeting to particular organelles. Much of the data that was obtained in Chapter V could be used for future projects in the lab to better understand the biological role of this multifunctional toxin.

Future Directions

Our studies have expanded our knowledge of residues important for oligomerization of VacA and have begun to probe the role of the β-helical fold in VacA activity. However, there are still numerous questions remaining. A greater understanding of how the toxin can assemble into oligomers would lead to a better understanding of how VacA causes alterations in human cells. It is still unclear if VacA binds to cells as a monomer, as an oligomer, or both, and which of these types of binding are most relevant for toxin activity. In addition, it would be of interest to study further the roles of the p55 and p33 domains in VacA activity. Specifically, p33 and p55 have been shown to interact with each other; neither protein alone

has toxic activity, but a mixture of these proteins is cytotoxic, suggesting that p33 and p55 interactions may be required for cytotoxicity.

There are several broad questions that remain unanswered in regards to the β-helix. It is likely that since most passenger domains secreted by autotransporter pathways fold as a β-helix, the β-helical structure might facilitate protein secretion; however, it is not known how this structure would facilitate protein secretion. Additionally, it is not clear what structural features are responsible for the unique properties of these passenger domains secreted by autotransporter pathways. And finally, the source of the energetic force utilized for efficient outer membrane secretion is not known. To our knowledge, our study is unique in that single coils were deleted down the length of the β-helix rather than studying folding of the wild-type protein or making large deletions at the carboxy-terminus of the protein.

Some of the questions that would be interesting to follow up on are:

- Our results show that amino acids 346 and 347 within the p55 domain are essential for assembly of VacA into functional oligomeric complexes. Using the crystal structure of the VacA p55 domain, can we identify other regions of the toxin that are important for oligomerization? Based on the crystal structure, one region hypothesized to be important for oligomerization is located near the amino-terminus of p55, composed of residues 355-411. This region is highly conserved among VacA sequences, suggesting it may be functionally significant. Residues 345-415 were shown to be essential for vacuolating activity when a series of plasmids encoding these mutant VacA proteins (each mutant containing a six amino acid deletion) were transfected into cells (unpublished data discussed in Chapter III). Because mutant proteins lacking amino acids 345-415 do not exhibit vacuolating activity, and we show that amino acids 346 and 347 are important for

oligomerization, it may be that the entire region from amino acids 345-415 is important for assembly of functional oligomeric complexes. Amino acids 355-411 make up two full coils of the β-helix, with one coil being composed of residues 355-383 and the other of residues 384-411. I have made mutations of each of these single coils in full-length VacA in both *E. coli* (for recombinant expression) and in *H. pylori*, but have not yet studied either mutant in any detail. The 355-383 and 384-411 mutations could also be made in the p55 domain and mixed with wild-type p33. These proteins could then be used for immunoprecipitation studies or yeast two-hybrid studies to investigate whether amino acids 355-411 are important for p33-p55 interactions. Immunoprecipitation studies could also be performed with a mixture of wild-type p33, mutant p55, and wild-type full-length VacA. Immunoprecipitation studies could therefore help us to identify amino acids important in protein-protein interactions.

- Are there similar structural requirements for various VacA activities? VacA is a multifunctional toxin, meaning that it can cause multiple cellular effects. These activities have been highlighted throughout this thesis, but the mechanism underlying each activity has not been completely elucidated. It is thought that some activities, such as vacuolation, mitochondrial membrane permeability, and autophagy, are dependent on the formation of anion-selective channels; however, other activities, such as activation of p38 and intracellular signaling in T cells, are thought to occur through a channel-independent mechanism (9, 107). VacA Δ346-347 does not induce membrane depolarization or form large oligomers, making this a particularly interesting mutant to further study MAPK activation and inhibition of T cell activation. Additionally, this mutant could be used to study channel-dependent activities to further test the hypothesis that mitochondrial

membrane permeability and autophagy are dependent on the formation of anion-selective channels.

A panel of single coil deletions has now been made from amino acids 433 to 628 within the *vacA* gene of the *H. pylori* chromosome. The availability of these mutants makes for a useful tool when probing regions of VacA that mediate specific functional activities. These mutants can be used to investigate whether single coil deletion proteins differ from wild-type VacA in ability to cause alterations in signal transduction pathways, immune cells, and autophagy.

- Can we gain further insight into how VacA contributes to *H. pylori* colonization of the mouse stomach using a VacA mutant defective in oligomerization? Mouse adapted strains of *H. pylori* have been used in animal models to better understand the role of VacA *in vivo*. *vacA*-null strains of *H. pylori* are capable of colonizing the stomachs of mice, as well as gnotobiotic piglets and Mongolian gerbils (22, 78, 125). However, a study by Salama *et al* demonstrated that when mice are co-infected with an *H. pylori* strain producing VacA and an isogenic *vacA*-null mutant, the *vacA*-null mutant did not colonize mice as efficiently as the wild-type *H. pylori* strain (94), suggesting that VacA may play a role in colonization. Very little work has been done to determine whether *in vitro* activities of VacA are also important in an animal model of infection. Because VacA Δ346-347 is secreted, but does not form large oligomers and does not induce membrane depolarization, this mutant would be interesting to further investigate in a mouse model. An important first step would be to investigate the ability of *H. pylori* strains containing either wild-type VacA or a *vacA*-null mutant alone and in combination to colonize mice. Competition experiments could be then be performed in which wild-type mice are co-infected with an *H. pylori* strain that

produces wild-type VacA and a strain that produces the mutant VacA Δ346-347 protein, or co-infection experiments could be performed with an *H. pylori* strain that produces the VacA Δ346-347 mutant protein and a *vacA*-null mutant *H. pylori* strain. For these experiments, an inserted antibiotic cassette would be used to distinguish colonization between the strains used for co-infection. Mice would be sacrificed at different time points post-infection and stomach homogenates plated on antibiotic blood plates. These experiments should help to determine if wild-type strains can out-compete the *H. pylori* strain producing mutant VacA Δ346-347 protein or if the *H. pylori* strain producing mutant VacA Δ346-347 protein can out-compete the *vacA*-null mutant *H. pylori* strain. If the wild-type *H. pylori* strain colonizes better than the strain producing VacA Δ346-347, this would suggest channel formation and oligomerization may be important in colonization. In general, these experiments may expand our current knowledge of VacA's role in colonization.

Experiments could also be performed to study disease progression. In this regard, an *H. pylori* strain producing the VacA Δ346-347 mutant protein could be used to infect INS-GAS mice. These are hypergastrinemic mice, meaning they have an excessive secretion of gastrin. Unlike other mice infected with *H. pylori*, these mice can develop gastric cancer. The INS-GAS mice, therefore, would be advantageous when analyzing the role of VacA in disease. Overall, the animal studies described in this section would help us to understand what properties of VacA (such as oligomerization) may contribute to colonization and disease progression.

- A single coil of the β-helix is made up of three β strands connected by loops; are these loops important for VacA activity? In a recent study designed to locate epitopes of

pertactin that are recognized by human antibodies, loops of the pertactin β-helix were modified by site-directed and deletion mutagenesis (40). This study found that modification of many of the loops resulted in a loss or decrease in binding of monoclonal antibodies (40). In some cases, the modification of loops resulted in an increase in binding of monoclonal antibodies to mutant proteins compared to wild-type pertactin, suggesting exposure of some epitopes that would normally be masked by nearby loops (40). This group did not specifically study effects on activity of the protein after modification of loops. In a similar manner, loops of the VacA p55 β-helix could be modified in several ways to investigate the importance of the loops. One loop usually tends to be longer than the other two loops that connect the three β strands in a single coil; amino acids in the longer loop could be deleted to shorten this loop. Also, amino acids could be substituted (for similar or opposite charges) instead of deleted. These various mutants could be used to investigate if the loops are important for VacA functional activities, or if they are more important for folding and/or secretion of the toxin.

- Amino acids 433-461 appear to be important in vacuolating activity. Can we narrow down this region to specifically determine which amino acids are important and why deletion of these amino acids leads to a reduction in vacuolating activity? Narrowing down this stretch of 28 amino acids would help to map regions of the toxin that are important for vacuolation. Performing random mutagenesis of the p55 domain did not result in the identification of any point mutations that resulted in loss of vacuolating activity (68), suggesting that it might be necessary to modify multiple amino acids to abrogate VacA activity. Because we see a difference in vacuolating activity in different cell types, our

data also suggest that amino acids 433-461 may be important in cell specificity, highlighting the importance of this region.

- Can we learn more about the structure of VacA by introducing the single coil deletions into the p55 domain of VacA and recombinantly expressing each? When I introduced these mutations into full-length VacA, my preliminary data indicate that these mutants were not solubly expressed very well during recombinant expression in *E. coli*; however, these experiments were only performed once, and conditions were not optimized. It might be possible to introduce these mutations into the p55 domain and obtain better soluble expression than I obtained with mutants in full-length VacA. The p55 domain containing the mutations could be recombinantly expressed and mixed with wild-type p33 to study oligomerization and activity.
- We have shown that several single coils can be deleted without substantially altering expression or secretion of mutant proteins; what would happen if single coils were inserted as opposed to deleted? The exact reason as to why the β-helical structure facilitates protein secretion is not known. It has been hypothesized that the right-handed parallel β-helices represent a single superfamily of folds that evolved from a common ancestor, most likely from duplication of coil sequences (44). Two other autotransporter proteins that fold as β-helices, pertactin and Hbp, contain 16 coils and 24 coils, respectively (24, 80), and the VacA p55 domain contains approximately 13 coils (29), highlighting that the length of β-helical passenger domains is not constant. The idea of adding a coil to the VacA p55 β-helix is not far from what may happen in some VacA proteins, specifically m2 VacA. m2 VacA has a 23 amino acid insert, not present in m1 VacA, which is an imperfect repeat of the sequence located just upstream, and is approximately the length of a single coil. VacA

mutants could be made in which coils were duplicated to further understand if specific contacts in the β-helix are required for efficient secretion and folding, and if these contacts are maintained or broken by coil duplication. These studies could be extended by adding the mutant VacA to cells to ask if the addition of coils results in changes to binding and/or internalization of the toxin.

- What is the role of the carboxy-terminal region of the passenger domain of VacA in folding and secretion? Our data suggest that amino acids 559-628 are important for proper secretion and folding of VacA. To further understand this region, we could follow an experimental design similar to DC Oliver *et al*, in which they were able to identify a conserved region of BrkA from *B. pertussis* that is necessary for folding of its passenger domain (79). The goal of the following experiments would be to determine if the carboxy-terminus of VacA promotes folding of VacA and would thus confer stability to the exported protein. A properly folded passenger domain is expected to be stable in the presence of proteases, but a protein not able to fold properly is expected to be unstable and degrade during secretion due to the presence of proteases in the outer membrane. Surface expression of full-length wild-type and mutant VacA would be compared using *E. coli* strains UT5600 and UT2300. *E. coli* UT5600 is deficient in the outer membrane proteases OmpT and OmpP; *E. coli* UT2300 is the wild-type strain that contains both OmpT and OmpP. OmpT and OmpP have intrinsic proteolytic activity and cleave proteins primarily between pairs of basic amino acids. Secretion of VacA from these *E. coli* strains has not been performed before, so the possibility exists that VacA will not be translocated across the outer bacterial membrane; however, *E. coli* UT5600 and UT2300 have successfully been used to study secretion of autotransporters from several bacterial species including

Neisseria and *Shigella* (49, 104). We would compare wild-type VacA with a mutant construct that is lacking amino acids 559-628 (lacking 3 single coils). General steps to probe the importance of the carboxy-terminus include:

1. express full-length, 140 kDa VacA to test whether VacA is surface-expressed in *E. coli*
2. examine surface expression of a mutant VacA protein lacking amino acids 559-628 in *E. coli* UT5600 and UT2300; if amino acids 559-628 are important for folding, the expectation is that surface expression would be detected in strain UT5600, but that in strain UT2300, the passenger would be susceptible to proteolysis and would not be detected on the surface
3. *in vivo trans* complementation of VacA folding in which *E. coli* would be co-transformed with plasmids expressing a mutant that expresses the VacA signal sequence, amino acids 559-628 of the passenger domain, and the translocation unit (the remainder of the passenger domain would be deleted) and a mutant that contains all of VacA except amino acids 559-628; in this set of experiments, if amino acids 559-628 are important for folding, the two mutants could act *in trans* to promote proper folding and the passenger domain be surface exposed
4. if amino acids 559-628 are found to be important for folding in the above experiments, trypsin analysis of VacA expressed on the surface of *E. coli* strain UT5600 could be performed; this would include trypsin susceptibility experiments where the bacteria is exposed to low levels of trypsin over time to monitor stability of the passenger domain

- Does VacA have a carboxy-terminal 'stable core' that is important for secretion and folding *in vivo*? Two other autotransporter proteins, pertactin and plasmid-encoded toxin (Pet, from *E. coli*), have been found to undergo three-state unfolding in which the protein unfolds via two transitions and takes on a partially folded state at intermediate concentrations of denaturant (47, 89). In each case, the partially folded state consists of a protease-resistant core structure located at the carboxy-terminus of the β-helix. It has been hypothesized that the stable core may be important for efficient secretion of autotransporter passenger domains, in that correct folding of the carboxy-terminal core structure could create a scaffold that would allow folding of the remaining β-helix, and would therefore provide the driving force for secretion (89).

To investigate the folding of VacA and to determine if the p55 domain of VacA contains a stable core similar to other autotransporter passenger domains, a series of several experiments could be performed similar to the above referenced studies (47, 89). Both wild-type p55 and single-coil deletion mutants introduced into p55 could be used in these experiments. In the first experiment, we could use tryptophan fluorescence emission to monitor the folding of the p55 domain. The p55 VacA domain has three tryptophans (Trp) located throughout the sequence-one that is buried in the protein, and two that are partially surface exposed (Figure VI-2A). Tryptophan has intrinsic fluorescence properties that are sensitive to the environment and change when a protein folds/unfolds. Thus, Trp fluorescence can be used to monitor protein folding. Changes in Trp fluorescence emission intensity as p55 is denatured in increasing concentrations of guanidine hydrochloride (GdnHCl) would be monitored. The expectation is that as p55 is denatured, the fluorescence intensity will decrease (Figure VI-2B). An unfolding curve could then be

generated by measuring fluorescence emission of VacA in various concentrations of GdnHCl. If p55 unfolds similarly to pertactin and Pet, we would expect to see native VacA p55 (the plateau above transition 1), partially folded VacA p55, and denatured VacA p55 (the plateau below transition 2) (Figure VI-2C).

There are two potential alternative approaches if following changes in tryptophan fluorescence does not work. The first is that tyrosine residues, which also have intrinsic fluorescence, can be used to follow protein folding (the tyrosine residues in p55 are highlighted in Figure VI-1A). The second alternative approach is to use a probe that binds specifically to protein hydrophobic surfaces (i.e. ANS or TNS).

If the above mentioned folding transitions (native, partially folded, and denatured) are observed for p55, proteolytic digestion with proteinase K would be used to show the location of ordered structure within the partially folded state. Both native and partially folded p55 would be exposed to proteinase K over a series of time points and samples resolved by SDS-PAGE to reveal any remaining folded structure. If a smaller fragment is detected over time after partially folded p55 is exposed to proteinase K, this would suggest retention of structure (i.e. "stable core"). The smaller fragment would be eluted from the gel and analyzed by MALDI-TOF. The sequence of this fragment (as determined by complete trypsin digestion) would be mapped onto the sequence of full-length p55. Mapping this fragment to full-length p55 would reveal where this stable core is located within p55. The identification of a stable core at the carboxy-terminus might suggest that these rungs of the β-helix form a template for efficient formation of the native β-helix.

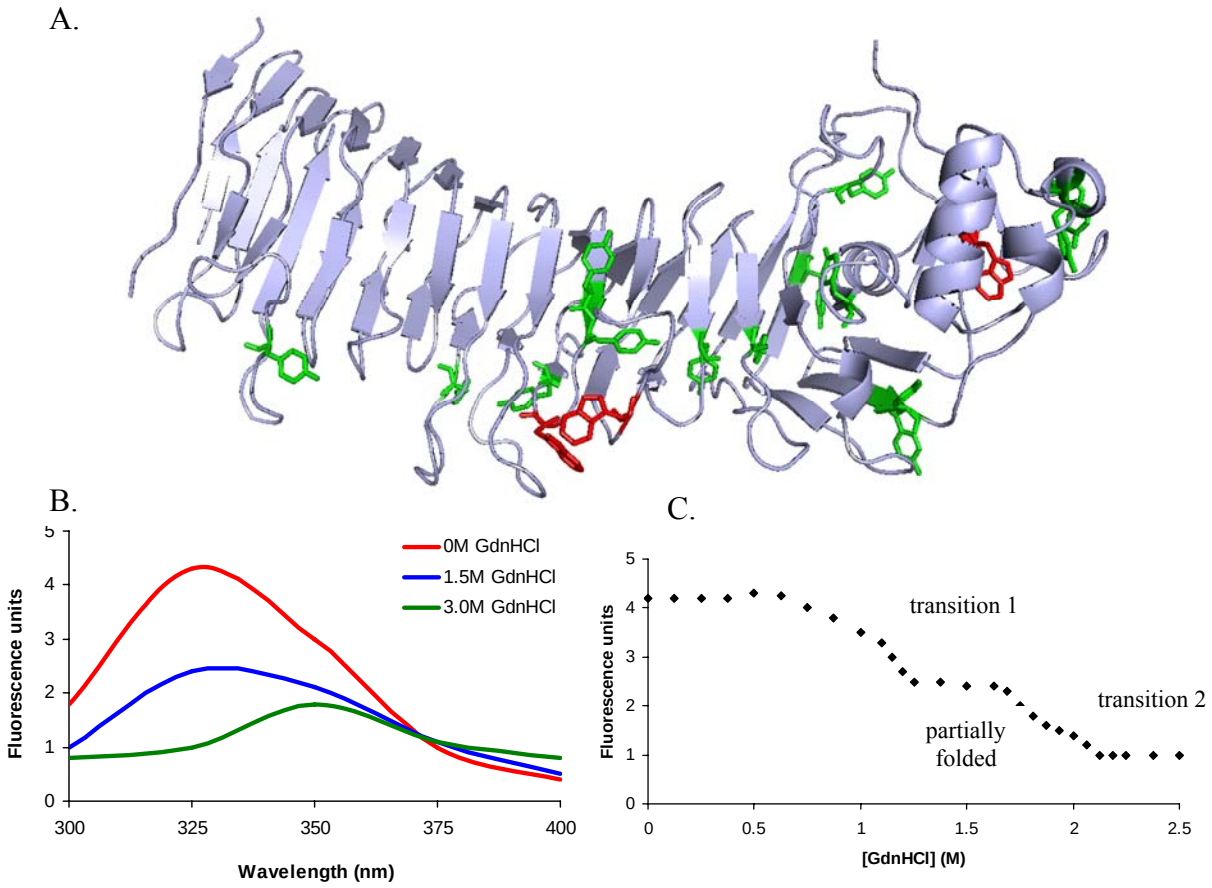

Figure VI-2. Determining if the VacA p55 domain has a C-terminal stable core. (A) VacA p55 domain crystal structure with tryptophan residues highlighted in red (residues 577, 603, 772) and tyrosine residues highlighted in green. (B) Hypothetical graph showing expected emission spectra from GdnHCl-induced unfolding of the p55 domain. The red line represents native p55, and the blue and green lines are showing increased concentrations of GdnHCl and a reduction in folding. (C) Hypothetical graph showing p55 steady-state fluorescence emission at various GdnHCl concentrations. If the p55 domain exhibits three-state unfolding behavior, two distinct transitions and a partially folded structure would be visible.

APPENDIX

List of publications

Ivie, S. E., M. S. McClain, H. M. S. Algood, D. B. Lacy, and T. L. Cover. Structure-function analysis of a β-helical region in the *Helicobacter pylori* VacA p55 domain. Submitted for publication.

Ivie, S. E., M. S. McClain, V. J. Torres, H. M. S. Algood, D. B. Lacy, R. Yang, S. R. Blanke, and T. L. Cover. 2008. *Helicobacter pylori* VacA subdomain required for intracellular toxin activity and assembly of functional oligomeric complexes. Infection and Immunity 76:2843-51.

Torres, V. J., S. E. Ivie, M. S. McClain, and T. L. Cover. 2005. Functional properties of the p33 and p55 domain of the *Helicobacter pylori* vacuolating cytotoxin. J Biol Chem 280:21107-14.

BIBLIOGRAPHY

1. Algood, H. M., V. J. Torres, D. Unutmaz, and T. L. Cover. 2007. Resistance of primary murine CD4+ T cells to *Helicobacter pylori* vacuolating cytotoxin. Infect Immun 75:334-341.

2. Atherton, J. C. 2006. The pathogenesis of *Helicobacter pylori*-induced gastro-duodenal diseases. Annu Rev Pathol 1:63-96.

3. Atherton, J. C., P. Cao, R. M. Peek, Jr., M. K. Tummuru, M. J. Blaser, and T. L. Cover. 1995. Mosaicism in vacuolating cytotoxin alleles of *Helicobacter pylori*. Association of specific vacA types with cytotoxin production and peptic ulceration. J Biol Chem 270:17771-17777.

4. Blaser, M. J. 1992. Hypotheses on the pathogenesis and natural history of *Helicobacter pylori*-induced inflammation. Gastroenterology 102:720-727.

5. Blaser, M. J., and D. E. Berg. 2001. *Helicobacter pylori* genetic diversity and risk of human disease. J Clin Invest 107:767-773.

6. Bumann, D., S. Aksu, M. Wendland, K. Janek, U. Zimny-Arndt, N. Sabarth, T. F. Meyer, and P. R. Jungblut. 2002. Proteome analysis of secreted proteins of the gastric pathogen *Helicobacter pylori*. Infect Immun 70:3396-3403.

7. Cao, P., M. S. McClain, M. H. Forsyth, and T. L. Cover. 1998. Extracellular release of antigenic proteins by *Helicobacter pylori*. Infect Immun 66:2984-2986.

8. Censini, S., C. Lange, Z. Xiang, J. E. Crabtree, P. Ghiara, M. Borodovsky, R. Rappuoli, and A. Covacci. 1996. cag, a pathogenicity island of Helicobacter pylori, encodes type I-specific and disease-associated virulence factors. Proc Natl Acad Sci U S A 93:14648-14653.

9. Cover, T. L., and S. R. Blanke. 2005. *Helicobacter pylori* VacA, a paradigm for toxin multifunctionality. Nat Rev Microbiol 3:320-332.

10. Cover, T. L., and M. J. Blaser. 1992. Purification and characterization of the vacuolating toxin from *Helicobacter pylori*. J Biol Chem 267:10570-10575.

11. Cover, T. L., P. I. Hanson, and J. E. Heuser. 1997. Acid-induced dissociation of VacA, the *Helicobacter pylori* vacuolating cytotoxin, reveals its pattern of assembly. J Cell Biol 138:759-769.

12. Cover, T. L., U. S. Krishna, D. A. Israel, and R. M. Peek, Jr. 2003. Induction of gastric epithelial cell apoptosis by *Helicobacter pylori* vacuolating cytotoxin. Cancer Res 63:951-957.

13. Cover, T. L., W. Puryear, G. I. Perez-Perez, and M. J. Blaser. 1991. Effect of urease on HeLa cell vacuolation induced by *Helicobacter pylori* cytotoxin. Infect Immun 59:1264-1270.

14. Cover, T. L., M. K. Tummuru, P. Cao, S. A. Thompson, and M. J. Blaser. 1994. Divergence of genetic sequences for the vacuolating cytotoxin among *Helicobacter pylori* strains. J Biol Chem 269:10566-10573.

15. Cover, T. L., S. G. Vaughn, P. Cao, and M. J. Blaser. 1992. Potentiation of *Helicobacter pylori* vacuolating toxin activity by nicotine and other weak bases. J Infect Dis 166:1073-1078.

16. Dautin, N., and H. D. Bernstein. 2007. Protein Secretion in Gram-Negative Bacteria via the Autotransporter Pathway. Annu Rev Microbiol 61:89-112.

17. de Bernard, M., D. Burroni, E. Papini, R. Rappuoli, J. Telford, and C. Montecucco. 1998. Identification of the *Helicobacter pylori* VacA toxin domain active in the cell cytosol. Infect Immun 66:6014-6016.

18. de Bernard, M., A. Cappon, G. Del Giudice, R. Rappuoli, and C. Montecucco. 2004. The multiple cellular activities of the VacA cytotoxin of *Helicobacter pylori*. Int J Med Microbiol 293:589-597.

19. de Bernard, M., A. Cappon, L. Pancotto, P. Ruggiero, J. Rivera, G. Del Giudice, and C. Montecucco. 2005. The *Helicobacter pylori* VacA cytotoxin activates RBL-2H3 cells by inducing cytosolic calcium oscillations. Cell Microbiol 7:191-198.

20. de Bernard, M., E. Papini, V. de Filippis, E. Gottardi, J. Telford, R. Manetti, A. Fontana, R. Rappuoli, and C. Montecucco. 1995. Low pH activates the vacuolating toxin of *Helicobacter pylori*, which becomes acid and pepsin resistant. J Biol Chem 270:23937-23940.

21. Dunn, B. E., H. Cohen, and M. J. Blaser. 1997. *Helicobacter pylori*. Clin Microbiol Rev 10:720-741.

22. Eaton, K. A., T. L. Cover, M. K. Tummuru, M. J. Blaser, and S. Krakowka. 1997. Role of vacuolating cytotoxin in gastritis due to *Helicobacter pylori* in gnotobiotic piglets. Infect Immun 65:3462-3464.

23. El-Bez, C., M. Adrian, J. Dubochet, and T. L. Cover. 2005. High resolution structural analysis of *Helicobacter pylori* VacA toxin oligomers by cryo-negative staining electron microscopy. J Struct Biol 151:215-228.

24. Emsley, P., I. G. Charles, N. F. Fairweather, and N. W. Isaacs. 1996. Structure of *Bordetella pertussis* virulence factor P.69 pertactin. Nature 381:90-92.

25. Figueiredo, C., J. C. Machado, P. Pharoah, R. Seruca, S. Sousa, R. Carvalho, A. F. Capelinha, W. Quint, C. Caldas, L. J. van Doorn, F. Carneiro, and M. Sobrinho-Simoes. 2002. *Helicobacter pylori* and interleukin 1 genotyping: an opportunity to identify high-risk individuals for gastric carcinoma. J Natl Cancer Inst 94:1680-1687.

26. Fischer, W., R. Buhrdorf, E. Gerland, and R. Haas. 2001. Outer membrane targeting of passenger proteins by the vacuolating cytotoxin autotransporter of *Helicobacter pylori*. Infect Immun 69:6769-6775.

27. Fujikawa, A., D. Shirasaka, S. Yamamoto, H. Ota, K. Yahiro, M. Fukada, T. Shintani, A. Wada, N. Aoyama, T. Hirayama, H. Fukamachi, and M. Noda. 2003. Mice deficient in protein tyrosine phosphatase receptor type Z are resistant to gastric ulcer induction by VacA of *Helicobacter pylori*. Nat Genet 33:375-381.

28. Galmiche, A., J. Rassow, A. Doye, S. Cagnol, J. C. Chambard, S. Contamin, V. de Thillot, I. Just, V. Ricci, E. Solcia, E. Van Obberghen, and P. Boquet. 2000. The N-terminal 34 kDa fragment of *Helicobacter pylori* vacuolating cytotoxin targets mitochondria and induces cytochrome c release. Embo J 19:6361-6370.

29. Gangwer, K. A., D. J. Mushrush, D. L. Stauff, B. Spiller, M. S. McClain, T. L. Cover, and D. B. Lacy. 2007. Crystal structure of the *Helicobacter pylori* vacuolating toxin p55 domain. Proc Natl Acad Sci U S A 104:16293-16298.

30. Garner, J. A., and T. L. Cover. 1996. Binding and internalization of the *Helicobacter pylori* vacuolating cytotoxin by epithelial cells. Infect Immun 64:4197-4203.

31. Gauthier, N. C., P. Monzo, V. Kaddai, A. Doye, V. Ricci, and P. Boquet. 2005. *Helicobacter pylori* VacA cytotoxin: a probe for a clathrin-independent and Cdc42-dependent pinocytic pathway routed to late endosomes. Mol Biol Cell 16:4852-4866.

32. Gauthier, N. C., V. Ricci, L. Landraud, and P. Boquet. 2006. *Helicobacter pylori* VacA toxin: a tool to study novel early endosomes. Trends Microbiol 14:292-294.

33. Gebert, B., W. Fischer, E. Weiss, R. Hoffmann, and R. Haas. 2003. *Helicobacter pylori* vacuolating cytotoxin inhibits T lymphocyte activation. Science 301:1099-1102.

34. Geisse, N. A., T. L. Cover, R. M. Henderson, and J. M. Edwardson. 2004. Targeting of *Helicobacter pylori* vacuolating toxin to lipid raft membrane domains analysed by atomic force microscopy. Biochem J 381:911-917.

35. Genisset, C., C. L. Galeotti, P. Lupetti, D. Mercati, D. A. Skibinski, S. Barone, R. Battistutta, M. de Bernard, and J. L. Telford. 2006. A *Helicobacter pylori*

Vacuolating Toxin Mutant That Fails To Oligomerize Has a Dominant Negative Phenotype. Infect Immun 74:1786-1794.

36. Go, M. F., V. Kapur, D. Y. Graham, and J. M. Musser. 1996. Population genetic analysis of *Helicobacter pylori* by multilocus enzyme electrophoresis: extensive allelic diversity and recombinational population structure. J Bacteriol 178:3934-3938.

37. Gupta, V. R., H. K. Patel, S. S. Kostolansky, R. A. Ballivian, J. Eichberg, and S. R. Blanke. 2008. Sphingomyelin functions as a novel receptor for *Helicobacter pylori* VacA. PLoS Pathog 4:e1000073.

38. Hawrylik, S. J., D. J. Wasilko, S. L. Haskell, T. D. Gootz, and S. E. Lee. 1994. Bisulfite or sulfite inhibits growth of *Helicobacter pylori*. J Clin Microbiol 32:790-792.

39. Henderson, I. R., F. Navarro-Garcia, and J. P. Nataro. 1998. The great escape: structure and function of the autotransporter proteins. Trends Microbiol 6:370-378.

40. Hijnen, M., R. de Voer, F. R. Mooi, R. Schepp, E. E. Moret, P. van Gageldonk, G. Smits, and G. A. Berbers. 2007. The role of peptide loops of the *Bordetella pertussis* protein P.69 pertactin in antibody recognition. Vaccine 25:5902-5914.

41. Ilver, D., S. Barone, D. Mercati, P. Lupetti, and J. L. Telford. 2004. *Helicobacter pylori* toxin VacA is transferred to host cells via a novel contact-dependent mechanism. Cell Microbiol 6:167-174.

42. Israel, D. A., N. Salama, U. Krishna, U. M. Rieger, J. C. Atherton, S. Falkow, and R. M. Peek, Jr. 2001. *Helicobacter pylori* genetic diversity within the gastric niche of a single human host. Proc Natl Acad Sci U S A 98:14625-14630.

43. Iwamoto, H., D. M. Czajkowsky, T. L. Cover, G. Szabo, and Z. Shao. 1999. VacA from *Helicobacter pylori*: a hexameric chloride channel. FEBS Lett 450:101-104.

44. Jenkins, J., O. Mayans, and R. Pickersgill. 1998. Structure and evolution of parallel beta-helix proteins. J Struct Biol 122:236-246.

45. Ji, X., T. Fernandez, D. Burroni, C. Pagliaccia, J. C. Atherton, J. M. Reyrat, R. Rappuoli, and J. L. Telford. 2000. Cell specificity of *Helicobacter pylori* cytotoxin is determined by a short region in the polymorphic midregion. Infect Immun 68:3754-3757.

46. Junker, M., R. N. Besingi, and P. L. Clark. 2009. Vectorial transport and folding of an autotransporter virulence protein during outer membrane secretion. Mol Microbiol 71:1323-1332.

47. Junker, M., C. C. Schuster, A. V. McDonnell, K. A. Sorg, M. C. Finn, B. Berger, and P. L. Clark. 2006. Pertactin beta-helix folding mechanism suggests common themes for the secretion and folding of autotransporter proteins. Proc Natl Acad Sci U S A 103:4918-4923.

48. Kimura, M., S. Goto, A. Wada, K. Yahiro, T. Niidome, T. Hatakeyama, H. Aoyagi, T. Hirayama, and T. Kondo. 1999. Vacuolating cytotoxin purified from *Helicobacter pylori* causes mitochondrial damage in human gastric cells. Microb Pathog 26:45-52.

49. Klauser, T., J. Kramer, K. Otzelberger, J. Pohlner, and T. F. Meyer. 1993. Characterization of the Neisseria Iga beta-core. The essential unit for outer membrane targeting and extracellular protein secretion. J Mol Biol 234:579-593.

50. Kuck, D., B. Kolmerer, C. Iking-Konert, P. H. Krammer, W. Stremmel, and J. Rudi. 2001. Vacuolating cytotoxin of *Helicobacter pylori* induces apoptosis in the human gastric epithelial cell line AGS. Infect Immun 69:5080-5087.

51. Kuo, C. H., and W. C. Wang. 2003. Binding and internalization of *Helicobacter pylori* VacA via cellular lipid rafts in epithelial cells. Biochem Biophys Res Commun 303:640-644.

52. Kusters, J. G., A. H. van Vliet, and E. J. Kuipers. 2006. Pathogenesis of *Helicobacter pylori* infection. Clin Microbiol Rev 19:449-490.

53. Lanzavecchia, S., P. L. Bellon, P. Lupetti, R. Dallai, R. Rappuoli, and J. L. Telford. 1998. Three-dimensional reconstruction of metal replicas of the *Helicobacter pylori* vacuolating cytotoxin. J Struct Biol 121:9-18.

54. Letley, D. P., and J. C. Atherton. 2000. Natural diversity in the N terminus of the mature vacuolating cytotoxin of *Helicobacter pylori* determines cytotoxin activity. J Bacteriol 182:3278-3280.

55. Letley, D. P., A. Lastovica, J. A. Louw, C. J. Hawkey, and J. C. Atherton. 1999. Allelic diversity of the *Helicobacter pylori* vacuolating cytotoxin gene in South Africa: rarity of the vacA s1a genotype and natural occurrence of an s2/m1 allele. J Clin Microbiol 37:1203-1205.

56. Letley, D. P., J. L. Rhead, K. Bishop, and J. C. Atherton. 2006. Paired cysteine residues are required for high levels of the *Helicobacter pylori* autotransporter VacA. Microbiology 152:1319-1325.

57. Leunk, R. D., P. T. Johnson, B. C. David, W. G. Kraft, and D. R. Morgan. 1988. Cytotoxic activity in broth-culture filtrates of *Campylobacter pylori*. J Med Microbiol 26:93-99.

58. Li, Y., A. Wandinger-Ness, J. R. Goldenring, and T. L. Cover. 2004. Clustering and redistribution of late endocytic compartments in response to *Helicobacter pylori* vacuolating toxin. Mol Biol Cell 15:1946-1959.

59. Lupetti, P., J. E. Heuser, R. Manetti, P. Massari, S. Lanzavecchia, P. L. Bellon, R. Dallai, R. Rappuoli, and J. L. Telford. 1996. Oligomeric and subunit structure of the *Helicobacter pylori* vacuolating cytotoxin. J Cell Biol 133:801-807.

60. Marchetti, M., B. Arico, D. Burroni, N. Figura, R. Rappuoli, and P. Ghiara. 1995. Development of a mouse model of *Helicobacter pylori* infection that mimics human disease. Science 267:1655-1658.

61. Marouga, R., S. David, and E. Hawkins. 2005. The development of the DIGE system: 2D fluorescence difference gel analysis technology. Anal Bioanal Chem 382:669-678.

62. Marshall, B. 2002. *Helicobacter pylori*: 20 years on. Clin Med 2:147-152.

63. Marshall, B. J., and J. R. Warren. 1984. Unidentified curved bacilli in the stomach of patients with gastritis and peptic ulceration. Lancet 1:1311-1315.

64. Massari, P., R. Manetti, D. Burroni, S. Nuti, N. Norais, R. Rappuoli, and J. L. Telford. 1998. Binding of the *Helicobacter pylori* vacuolating cytotoxin to target cells. Infect Immun 66:3981-3984.

65. McClain, M. S., P. Cao, and T. L. Cover. 2001. Amino-terminal hydrophobic region of *Helicobacter pylori* vacuolating cytotoxin (VacA) mediates transmembrane protein dimerization. Infect Immun 69:1181-1184.

66. McClain, M. S., P. Cao, H. Iwamoto, A. D. Vinion-Dubiel, G. Szabo, Z. Shao, and T. L. Cover. 2001. A 12-amino-acid segment, present in type s2 but not type s1 *Helicobacter pylori* VacA proteins, abolishes cytotoxin activity and alters membrane channel formation. J Bacteriol 183:6499-6508.

67. McClain, M. S., and T. L. Cover. 2003. Expression of *Helicobacter pylori* vacuolating toxin in *Escherichia coli*. Infect Immun 71:2266-2271.

68. McClain, M. S., D. M. Czajkowsky, V. J. Torres, G. Szabo, Z. Shao, and T. L. Cover. 2006. Random mutagenesis of *Helicobacter pylori* vacA to identify amino acids essential for vacuolating cytotoxic activity. Infect Immun 74:6188-6195.

69. McClain, M. S., H. Iwamoto, P. Cao, A. D. Vinion-Dubiel, Y. Li, G. Szabo, Z. Shao, and T. L. Cover. 2003. Essential role of a GXXXG motif for membrane channel formation by *Helicobacter pylori* vacuolating toxin. J Biol Chem 278:12101-12108.

70. McClain, M. S., W. Schraw, V. Ricci, P. Boquet, and T. L. Cover. 2000. Acid activation of *Helicobacter pylori* vacuolating cytotoxin (VacA) results in toxin internalization by eukaryotic cells. Mol Microbiol 37:433-442.

71. Mobley, H. L., L. T. Hu, and P. A. Foxal. 1991. *Helicobacter pylori* urease: properties and role in pathogenesis. Scand J Gastroenterol Suppl 187:39-46.

72. Molinari, M., C. Galli, M. de Bernard, N. Norais, J. M. Ruysschaert, R. Rappuoli, and C. Montecucco. 1998. The acid activation of *Helicobacter pylori* toxin VacA: structural and membrane binding studies. Biochem Biophys Res Commun 248:334-340.

73. Molinari, M., C. Galli, N. Norais, J. L. Telford, R. Rappuoli, J. P. Luzio, and C. Montecucco. 1997. Vacuoles induced by *Helicobacter pylori* toxin contain both late endosomal and lysosomal markers. J Biol Chem 272:25339-25344.

74. Montecucco, C., and M. de Bernard. 2003. Immunosuppressive and proinflammatory activities of the VacA toxin of *Helicobacter pylori*. J Exp Med 198:1767-1771.

75. Nakayama, M., M. Kimura, A. Wada, K. Yahiro, K. Ogushi, T. Niidome, A. Fujikawa, D. Shirasaka, N. Aoyama, H. Kurazono, M. Noda, J. Moss, and T. Hirayama. 2004. *Helicobacter pylori* VacA activates the p38/activating transcription factor 2-mediated signal pathway in AZ-521 cells. J Biol Chem 279:7024-7028.

76. Nguyen, V. Q., R. M. Caprioli, and T. L. Cover. 2001. Carboxy-terminal proteolytic processing of *Helicobacter pylori* vacuolating toxin. Infect Immun 69:543-546.

77. O'Toole, P. W., M. C. Lane, and S. Porwollik. 2000. *Helicobacter pylori* motility. Microbes Infect 2:1207-1214.

78. Ogura, K., S. Maeda, M. Nakao, T. Watanabe, M. Tada, T. Kyutoku, H. Yoshida, Y. Shiratori, and M. Omata. 2000. Virulence factors of *Helicobacter pylori* responsible for gastric diseases in Mongolian gerbil. J Exp Med 192:1601-1610.

79. Oliver, D. C., G. Huang, E. Nodel, S. Pleasance, and R. C. Fernandez. 2003. A conserved region within the *Bordetella pertussis* autotransporter BrkA is necessary for folding of its passenger domain. Mol Microbiol 47:1367-1383.

80. Otto, B. R., R. Sijbrandi, J. Luirink, B. Oudega, J. G. Heddle, K. Mizutani, S. Y. Park, and J. R. Tame. 2005. Crystal structure of hemoglobin protease, a heme binding autotransporter protein from pathogenic *Escherichia coli*. J Biol Chem 280:17339-17345.

81. Padilla, P. I., A. Wada, K. Yahiro, M. Kimura, T. Niidome, H. Aoyagi, A. Kumatori, M. Anami, T. Hayashi, J. Fujisawa, H. Saito, J. Moss, and T. Hirayama. 2000. Morphologic differentiation of HL-60 cells is associated with appearance of

RPTPbeta and induction of *Helicobacter pylori* VacA sensitivity. J Biol Chem 275:15200-15206.

82. Pagliaccia, C., M. de Bernard, P. Lupetti, X. Ji, D. Burroni, T. L. Cover, E. Papini, R. Rappuoli, J. L. Telford, and J. M. Reyrat. 1998. The m2 form of the *Helicobacter pylori* cytotoxin has cell type-specific vacuolating activity. Proc Natl Acad Sci U S A 95:10212-10217.

83. Papini, E., M. de Bernard, E. Milia, M. Bugnoli, M. Zerial, R. Rappuoli, and C. Montecucco. 1994. Cellular vacuoles induced by *Helicobacter pylori* originate from late endosomal compartments. Proc Natl Acad Sci U S A 91:9720-9724.

84. Papini, E., E. Gottardi, B. Satin, M. de Bernard, P. Massari, J. Telford, R. Rappuoli, S. B. Sato, and C. Montecucco. 1996. The vacuolar ATPase proton pump is present on intracellular vacuoles induced by *Helicobacter pylori*. J Med Microbiol 45:84-89.

85. Patel, H. K., D. C. Willhite, R. M. Patel, D. Ye, C. L. Williams, E. M. Torres, K. B. Marty, R. A. MacDonald, and S. R. Blanke. 2002. Plasma membrane cholesterol modulates cellular vacuolation induced by the *Helicobacter pylori* vacuolating cytotoxin. Infect Immun 70:4112-4123.

86. Peek, R. M., Jr., and M. J. Blaser. 2002. *Helicobacter pylori* and gastrointestinal tract adenocarcinomas. Nat Rev Cancer 2:28-37.

87. Perez-Perez, G. I., D. Rothenbacher, and H. Brenner. 2004. Epidemiology of *Helicobacter pylori* infection. Helicobacter 9 Suppl 1:1-6.

88. Pohlner, J., R. Halter, K. Beyreuther, and T. F. Meyer. 1987. Gene structure and extracellular secretion of *Neisseria gonorrhoeae* IgA protease. Nature 325:458-462.

89. Renn, J. P., and P. L. Clark. 2008. A conserved stable core structure in the passenger domain beta-helix of autotransporter virulence proteins. Biopolymers 89:420-427.

90. Reyrat, J. M., S. Lanzavecchia, P. Lupetti, M. de Bernard, C. Pagliaccia, V. Pelicic, M. Charrel, C. Ulivieri, N. Norais, X. Ji, V. Cabiaux, E. Papini, R. Rappuoli, and J. L. Telford. 1999. 3D imaging of the 58 kDa cell binding subunit of the *Helicobacter pylori* cytotoxin. J Mol Biol 290:459-470.

91. Rhead, J. L., D. P. Letley, M. Mohammadi, N. Hussein, M. A. Mohagheghi, M. Eshagh Hosseini, and J. C. Atherton. 2007. A new *Helicobacter pylori* vacuolating cytotoxin determinant, the intermediate region, is associated with gastric cancer. Gastroenterology 133:926-936.

92. Ricci, V., A. Galmiche, A. Doye, V. Necchi, E. Solcia, and P. Boquet. 2000. High cell sensitivity to *Helicobacter pylori* VacA toxin depends on a GPI-anchored protein

and is not blocked by inhibition of the clathrin-mediated pathway of endocytosis. Mol Biol Cell 11:3897-3909.

93. Ricci, V., P. Sommi, R. Fiocca, M. Romano, E. Solcia, and U. Ventura. 1997. *Helicobacter pylori* vacuolating toxin accumulates within the endosomal-vacuolar compartment of cultured gastric cells and potentiates the vacuolating activity of ammonia. J Pathol 183:453-459.

94. Salama, N. R., G. Otto, L. Tompkins, and S. Falkow. 2001. Vacuolating cytotoxin of *Helicobacter pylori* plays a role during colonization in a mouse model of infection. Infect Immun 69:730-736.

95. Schmitt, W., and R. Haas. 1994. Genetic analysis of the *Helicobacter pylori* vacuolating cytotoxin: structural similarities with the IgA protease type of exported protein. Mol Microbiol 12:307-319.

96. Schraw, W., Y. Li, M. S. McClain, F. G. van der Goot, and T. L. Cover. 2002. Association of *Helicobacter pylori* vacuolating toxin (VacA) with lipid rafts. J Biol Chem 277:34642-34650.

97. Sellman, B. R., M. Mourez, and R. J. Collier. 2001. Dominant-negative mutants of a toxin subunit: an approach to therapy of anthrax. Science 292:695-697.

98. Seto, K., Y. Hayashi-Kuwabara, T. Yoneta, H. Suda, and H. Tamaki. 1998. Vacuolation induced by cytotoxin from *Helicobacter pylori* is mediated by the EGF receptor in HeLa cells. FEBS Lett 431:347-350.

99. Singh, Y., H. Khanna, A. P. Chopra, and V. Mehra. 2001. A dominant negative mutant of *Bacillus anthracis* protective antigen inhibits anthrax toxin action in vivo. J Biol Chem 276:22090-22094.

100. Strobel, S., S. Bereswill, P. Balig, P. Allgaier, H. G. Sonntag, and M. Kist. 1998. Identification and analysis of a new vacA genotype variant of *Helicobacter pylori* in different patient groups in Germany. J Clin Microbiol 36:1285-1289.

101. Suerbaum, S., and P. Michetti. 2002. *Helicobacter pylori* infection. N Engl J Med 347:1175-1186.

102. Sundrud, M. S., V. J. Torres, D. Unutmaz, and T. L. Cover. 2004. Inhibition of primary human T cell proliferation by *Helicobacter pylori* vacuolating toxin (VacA) is independent of VacA effects on IL-2 secretion. Proc Natl Acad Sci U S A 101:7727-7732.

103. Supajatura, V., H. Ushio, A. Wada, K. Yahiro, K. Okumura, H. Ogawa, T. Hirayama, and C. Ra. 2002. Cutting edge: VacA, a vacuolating cytotoxin of *Helicobacter pylori*,

directly activates mast cells for migration and production of proinflammatory cytokines. J Immunol 168:2603-2607.

104. Suzuki, T., M. C. Lett, and C. Sasakawa. 1995. Extracellular transport of VirG protein in Shigella. J Biol Chem 270:30874-30880.

105. Szabo, I., S. Brutsche, F. Tombola, M. Moschioni, B. Satin, J. L. Telford, R. Rappuoli, C. Montecucco, E. Papini, and M. Zoratti. 1999. Formation of anion-selective channels in the cell plasma membrane by the toxin VacA of *Helicobacter pylori* is required for its biological activity. Embo J 18:5517-5527.

106. Telford, J. L., P. Ghiara, M. Dell'Orco, M. Comanducci, D. Burroni, M. Bugnoli, M. F. Tecce, S. Censini, A. Covacci, Z. Xiang, and et al. 1994. Gene structure of the *Helicobacter pylori* cytotoxin and evidence of its key role in gastric disease. J Exp Med 179:1653-1658.

107. Terebiznik, M. R., D. Raju, C. L. Vazquez, K. Torbricki, R. Kulkarni, S. R. Blanke, T. Yoshimori, M. I. Colombo, and N. L. Jones. 2009. Effect of *Helicobacter pylori*'s vacuolating cytotoxin on the autophagy pathway in gastric epithelial cells. Autophagy 5:370-379.

108. Tombola, F., C. Carlesso, I. Szabo, M. de Bernard, J. M. Reyrat, J. L. Telford, R. Rappuoli, C. Montecucco, E. Papini, and M. Zoratti. 1999. *Helicobacter pylori* vacuolating toxin forms anion-selective channels in planar lipid bilayers: possible implications for the mechanism of cellular vacuolation. Biophys J 76:1401-1409.

109. Tombola, F., L. Morbiato, G. Del Giudice, R. Rappuoli, M. Zoratti, and E. Papini. 2001. The *Helicobacter pylori* VacA toxin is a urea permease that promotes urea diffusion across epithelia. J Clin Invest 108:929-937.

110. Tombola, F., F. Oregna, S. Brutsche, I. Szabo, G. Del Giudice, R. Rappuoli, C. Montecucco, E. Papini, and M. Zoratti. 1999. Inhibition of the vacuolating and anion channel activities of the VacA toxin of *Helicobacter pylori*. FEBS Lett 460:221-225.

111. Tombola, F., C. Pagliaccia, S. Campello, J. L. Telford, C. Montecucco, E. Papini, and M. Zoratti. 2001. How the loop and middle regions influence the properties of *Helicobacter pylori* VacA channels. Biophys J 81:3204-3215.

112. Torres, V. J., S. E. Ivie, M. S. McClain, and T. L. Cover. 2005. Functional properties of the p33 and p55 domains of the *Helicobacter pylori* vacuolating cytotoxin. J Biol Chem 280:21107-21114.

113. Torres, V. J., M. S. McClain, and T. L. Cover. 2004. Interactions between p-33 and p-55 domains of the *Helicobacter pylori* vacuolating cytotoxin (VacA). J Biol Chem 279:2324-2331.

114. Torres, V. J., M. S. McClain, and T. L. Cover. 2006. Mapping of a domain required for protein-protein interactions and inhibitory activity of a *Helicobacter pylori* dominant-negative VacA mutant protein. Infect Immun 74:2093-2101.

115. Utt, M., B. Danielsson, and T. Wadstrom. 2001. *Helicobacter pylori* vacuolating cytotoxin binding to a putative cell surface receptor, heparan sulfate, studied by surface plasmon resonance. FEMS Immunol Med Microbiol 30:109-113.

116. van Doorn, L. J., C. Figueiredo, R. Sanna, S. Pena, P. Midolo, E. K. Ng, J. C. Atherton, M. J. Blaser, and W. G. Quint. 1998. Expanding allelic diversity of *Helicobacter pylori* vacA. J Clin Microbiol 36:2597-2603.

117. Vinion-Dubiel, A. D., M. S. McClain, P. Cao, R. L. Mernaugh, and T. L. Cover. 2001. Antigenic diversity among *Helicobacter pylori* vacuolating toxins. Infect Immun 69:4329-4336.

118. Vinion-Dubiel, A. D., M. S. McClain, D. M. Czajkowsky, H. Iwamoto, D. Ye, P. Cao, W. Schraw, G. Szabo, S. R. Blanke, Z. Shao, and T. L. Cover. 1999. A dominant negative mutant of *Helicobacter pylori* vacuolating toxin (VacA) inhibits VacA-induced cell vacuolation. J Biol Chem 274:37736-37742.

119. Wang, H. J., P. C. Chang, C. H. Kuo, C. S. Tzeng, and W. C. Wang. 1998. Characterization of the C-terminal domain of *Helicobacter pylori* vacuolating toxin and its relationship with extracellular toxin production. Biochem Biophys Res Commun 250:397-402.

120. Wang, H. J., and W. C. Wang. 2000. Expression and binding analysis of GST-VacA fusions reveals that the C-terminal approximately 100-residue segment of exotoxin is crucial for binding in HeLa cells. Biochem Biophys Res Commun 278:449-454.

121. Wang, W. C., H. J. Wang, and C. H. Kuo. 2001. Two distinctive cell binding patterns by vacuolating toxin fused with glutathione S-transferase: one high-affinity m1-specific binding and the other lower-affinity binding for variant m forms. Biochemistry 40:11887-11896.

122. Willhite, D. C., and S. R. Blanke. 2004. *Helicobacter pylori* vacuolating cytotoxin enters cells, localizes to the mitochondria, and induces mitochondrial membrane permeability changes correlated to toxin channel activity. Cell Microbiol 6:143-154.

123. Willhite, D. C., T. L. Cover, and S. R. Blanke. 2003. Cellular vacuolation and mitochondrial cytochrome c release are independent outcomes of *Helicobacter pylori* vacuolating cytotoxin activity that are each dependent on membrane channel formation. J Biol Chem 278:48204-48209.

124. Willhite, D. C., D. Ye, and S. R. Blanke. 2002. Fluorescence resonance energy transfer microscopy of the *Helicobacter pylori* vacuolating cytotoxin within mammalian cells. Infect Immun 70:3824-3832.

125. Wirth, H. P., M. H. Beins, M. Yang, K. T. Tham, and M. J. Blaser. 1998. Experimental infection of Mongolian gerbils with wild-type and mutant *Helicobacter pylori* strains. Infect Immun 66:4856-4866.

126. Wittig, I., H. P. Braun, and H. Schagger. 2006. Blue native PAGE. Nat Protoc 1:418-428.

127. Wren, B. W., J. Henderson, and J. M. Ketley. 1994. A PCR-based strategy for the rapid construction of defined bacterial deletion mutants. Biotechniques 16:994-996.

128. Yahiro, K., T. Niidome, M. Kimura, T. Hatakeyama, H. Aoyagi, H. Kurazono, K. Imagawa, A. Wada, J. Moss, and T. Hirayama. 1999. Activation of *Helicobacter pylori* VacA toxin by alkaline or acid conditions increases its binding to a 250-kDa receptor protein-tyrosine phosphatase beta. J Biol Chem 274:36693-36699.

129. Yahiro, K., A. Wada, M. Nakayama, T. Kimura, K. Ogushi, T. Niidome, H. Aoyagi, K. Yoshino, K. Yonezawa, J. Moss, and T. Hirayama. 2003. Protein-tyrosine phosphatase alpha, RPTP alpha, is a *Helicobacter pylori* VacA receptor. J Biol Chem 278:19183-19189.

130. Yahiro, K., A. Wada, E. Yamasaki, M. Nakayama, Y. Nishi, J. Hisatsune, N. Morinaga, J. Sap, M. Noda, J. Moss, and T. Hirayama. 2004. Essential domain of receptor tyrosine phosphatase beta (RPTPbeta) for interaction with *Helicobacter pylori* vacuolating cytotoxin. J Biol Chem 279:51013-51021.

131. Yamasaki, E., A. Wada, A. Kumatori, I. Nakagawa, J. Funao, M. Nakayama, J. Hisatsune, M. Kimura, J. Moss, and T. Hirayama. 2006. *Helicobacter pylori* vacuolating cytotoxin induces activation of the proapoptotic proteins Bax and Bak, leading to cytochrome c release and cell death, independent of vacuolation. J Biol Chem 281:11250-11259.

132. Ye, D., and S. R. Blanke. 2002. Functional complementation reveals the importance of intermolecular monomer interactions for *Helicobacter pylori* VacA vacuolating activity. Mol Microbiol 43:1243-1253.

133. Ye, D., D. C. Willhite, and S. R. Blanke. 1999. Identification of the minimal intracellular vacuolating domain of the *Helicobacter pylori* vacuolating toxin. J Biol Chem 274:9277-9282.